Polymeric Chemisorbents for Organic Acid Recovery from Aqueous Solution

By

Alexandre Tremblay

A thesis submitted to the Department of Chemical Engineering

In conformity with the requirements for the degree of Master of Applied Science

Queen's University

Kingston, Ontario, Canada

May, 2025

Copyright © Alexandre Xavier Joseph Tremblay, 2025

Abstract

The high cost of recovering succinic acid (SA) from fermentation media during bioproduction makes it difficult for bioproduced SA to compete with petrochemically-derived SA. Two new polymeric sorbents and multiple recovery methods that have the potential to reduce bioproduction costs are examined. The first sorbent is a polyionic liquid (PIL) with a bicarbonate salt of poly(1-vinyl-3-dodecylimidazolium bicarbonate). The second sorbent is a smart hydrogel consisting of N,N-dimethylaminoethylacrylamide (DMEA) and tris[2-(acryloylamino)ethyl]amine (TAAEA). Both sorbents successfully chemisorb succinic acid from dilute aqueous solution with efficiencies that are competitive to polymeric chemisorbents that are reported in literature. Novel recovery methods that are more environmentally conscious than traditional methods are tested, such as the use of saturated $NaHCO_3$ or saturated H_2CO_3 solutions on the PIL, or the use of a strain-sensitive smart recovery on the hydrogel. The saturated $NaHCO_3$ recovery and the smart recovery are both effective at concentrating succinic acid from dilute aqueous solution with high recovery yields. These recovery methods simultaneously desorb succinic acid and regenerate the basic PIL. These recovery methods are competitive to traditional organic acid recoveries such as recovery by alkaline salt and other recoveries that are reported in literature.

Acknowledgments

I'd like to thank Arash for being a great person. I'd like to thank Queen's University for supporting me as I have done my degree. I'd like to thank my mother and little brother for giving me inspiration throughout my degree. I'd like thank to thank God for giving me strength as I did my degree. I'd like to thank Dr. Barz for allowing me to use the resources of his lab to do my experiments. I'd like to thank Dr. Escobedo for allowing me to use his 3D printer while designing and iterating my piston. I'd like to thank Dr. Scott Parent for collaborating with me on these projects. Thank you degree! I'm now starting my next chapter!

Table of Contents

Abstract i

Acknowledgments ii

List of Figures vii

List of Tables viii

List of Schemes xi

Abbreviations xiii

Chapter 1 Introduction 1

1.1 Succinic Acid Bioproduction 1

1.2 Polyionic Liquids 3

1.3 Poly(acrylamide) Hydrogels 8

1.4 Chemisorption and Physisorption 12

1.5 Succinic Acid Recovery 13

1.5.1 Traditional Succinic Acid Recovery 13

1.5.2 Researched Succinic Acid Sorption 14

1.5.3 Researched Succinic Acid Desorption 16

1.6 Summary of Hypotheses 17

References 18

Copyrights 21

Chapter 2 A Bicarbonate Functionalized Polyionic Liquid for Organic Acid Recovery 23

2.1 Experimental 23
2.1.1 Materials 23
2.1.2 ($VC_{12}Im$)(Cl) and P[($VC_{12}Im$)(Cl)] Synthesis 23
2.1.3 P[($VC_{12}Im$)(Cl)] Bead Processing 24
2.1.4 Ion Exchange with $NaHCO_3$ (aq) 24
2.1.5 Physisorption Capacities 25
2.1.6 Chemisorption Capacities 25
2.1.7 Organic Acid Titrations 25
2.1.8 PIL Water Absorption 25
2.1.9 Ion Exchange of P[($VC_{12}Im$)(Cl)] with a Saturated H_2CO_3 Solution 26
2.1.10 SA Desorption with Dilute HCl (aq) 26
2.1.11 SA Desorption with Saturated H_2CO_3 (aq) 26
2.1.12 SA Desorption with Saturated $NaHCO_3$ (aq) 27
2.1.13 Analytical Methods 27
2.1.14 Error 27
2.2 Results and Discussion 28
2.2.1 P[($VC_{12}Im$)(Cl)] Synthesis and Organic Acid Sorption Capacities 28
2.2.2 Synthesis of P[($VC_{12}Im$)$(Cl)_x(HCO_3)_y$] 30
2.2.3 Acid Chemisorption Capacities of P[($VC_{12}Im$)$(Cl)_{0.40}(HCO_3)_{0.60}$] 33
2.2.4 Succinic Acid Recovery and PIL Regeneration 35

2.3 Conclusions 37

References 38

Chapter 3 The Strain-Sensitivity of Amine Functionalized Hydrogel Basicity and Its Application for the Recovery of Succinic Acid from Dilute Aqueous Solution 40

3.1 Experimental 40

3.1.1 Materials 40

3.1.2 DMEA, DMEP and TAAEA Synthesis 40

3.1.3 PDMEA and Hydrogel Synthesis 41

3.1.4 Hydrogel Swelling Ratios 41

3.1.5 Titrations of Organic Acid Solution 42

3.1.6 Hydrogel Sorption Capacities 42

3.1.7 Analytical Methods 44

3.1.8 Error 45

3.2 Results and Discussion 46

3.2.1 Hydrogel Synthesis and Physical Characterization 46

3.2.2 Crosslink Density and Basicity 50

3.2.3 Strain Sensitivity of Hydrogel Basicity 53

3.3 Conclusions 60

References 61

Chapter 4 Comparison of the Researched Recoveries to Literature Recoveries 63

4.1 Comparing PIL-HCO_3 with the 4% Hydrogel 63

4.2 Comparison of the SA Recovery Methods to Traditional Organic Acid Recovery Methods 67

4.3 Comparison of the Researched Recoveries to the Recoveries of the Failed Ventures 70

4.3.1 Descriptions of the Venture Recoveries 70

4.3.2 Advantages and Disadvantages of the Researched Recoveries 71

References 75

Copyrights 75

Chapter 5 Thesis Conclusions 76

5.1 Assessing Hypotheses 76

5.1.1 Confirmed Hypotheses 76

5.1.2 Unconfirmed Hypotheses 76

5.2 Final Conclusions and Future Work 77

Appendices 78

Appendix A Literature Information 78

Appendix B Figures 80

Appendix C Data 84

List of Figures

Figure 2.1. Physisorption of BA with P[(VC_{12}Im)(Cl)] in pH 3.1 Solution (2.5 g·BA/L, 20 °C). 29

Figure 2.2. Anion Exchange of P[(VC_{12}Im)(Cl)] to P[(VC_{12}Im)$(Cl)_x(HCO_3)_y$] at Various Bicarbonate Ion Concentrations (20°C; F = 0.01; $[NaHCO_3]_0$ = 0.05 M – saturated*; Moles·HCO_3^-/Moles·Cl^- = 1.5 – sat.*). 31

Figure 2.3. Titration Curves of SA and BA Using PIL-HCO_3 (2.5 g·acid/L, 20 °C). 33

Figure 3.1. 30% Hydrogel Synthesized Using Different Solvents: a) Toluene; b) Water. 46

Figure 3.2. Hydrogels After Synthesis: a) 3.5%; b) 4%; c) 5%; d) 10%; e) 30%; f) 50%. 47

Figure 3.3 Swelling Ratio of the Hydrogels of Varying TAAEA Weight Fractions at a F = 0.01 in Water (pH 7.0), 2.5 g·SA/L Solution (pH 3.0) and HCl Solution (pH 3.0) (25 °C). 49

Figure 3.4. Hydrogels of Various TAAEA Weight Fractions (wt%) Swelled at Equilibrium in Water (pH 7.0) at a F = 0.01 (25 °C): a) 3.5%; b) 4% c) 5% d) 10%; e) 30%; f) 50%. 50

Figure 3.5. Chemisorption Dynamics of Benzoic Acid Using PDMEA and the 3.5% and 30% Hydrogels at Approximately 1.0 mole·amine/1.0 mole·BA (2.5 g·BA/L, 25 °C). 51

Figure 3.6. BA Solution Titrations with Various 3° Amine Containing Materials (2.5 g·BA/L, 25 °C).......... 52

Figure 3.7. Swelling Ratio of the 4% Hydrogel at Various Strains (25 °C)... 56

Figure 3.8. Succinic Acid Capacity of the 4% Hydrogel at Various Strains (25 °C). 57

Figure 3.9. The Relation of Swelling Ratio to SA Capacity for the 4% Hydrogel (25 °C). 58

Figure A.1. CO_2 Equilibrium in Water at RT (© Mohammad Ghobadi, reprinted with permission) [1]. 78

Figure B.1 UV-Vis Calibration of Benzoic Acid (λ = 225 nm) Between 0 – 0.1 mM at 20 °C (Slope = 8.2275). 80

Figure B.2 The Degradation of Linear PDMEA During Dynamic Scanning Calorimetry Scans Between 0 – 200 °C (3rd cycle). 81

Figure B.3 Dynamic Scanning Calorimetry Plots of the Various Hydrogels Between 0 - 180 °C (3rd cycle). 82

List of Tables

Table 1.1 Summary of the Industrial Ventures of the Bioproduction of SA in the 2010s (© Mickel Jansen, adapted with permission) [8].. 3

Table 1.2 Properties of a Sample of ILs (© Kun Dong, adapted with permission) [9]................................ 4

Table 2.1 Desorption of Succinic Acid Using Various Recovery Methods. 36

Table 3.1 Hydrogel Formulations.. 47

Table 3.2 Sorption Capacities of Hydrogels of Various TAAEA Weight Fractions at 3.0 moles·amine/1.0 mole·SA (F = 0.01) in 2.5 g·SA/L Solution (25 °C). 53

Table 3.3 Succinic Acid Desorption Solution Concentrations Between Various Strains (25 °C)................ 60

Table 4.1 Succinic Acid Capacities of Base Functionalized Polymers. 64

Table 4.2 Comparison of PIL-HCO_3 with the 4% Hydrogel for the Recovery of SA.................................... 65

Table A.1 SA Producing Bacteria [2]..78

Table C.1 Absorption of SA and BA using PIL-Cl: BA Measured Using UV-Vis at a λ = 225 nm; SA Measured with ^{1}H NMR with a Citric Acid Reference of 41 mg (20 °C).. 84

Table C.2 Raw Data of the Ion Exchange Equilibrium of Cl^- to HCO_3^- in PIL-Cl that is Suspended in $NaHCO_3$ (aq) at Various Concentrations (0.05 M – Saturated; F = 0.01; 20 °C).. 85

Table C.3 Summary of the Ion Exchange Equilibrium of Cl^- to HCO_3^- in PIL-Cl that is Suspended in 5 ml of $NaHCO_3$ (aq) at Various Concentrations (0.05 M – Saturated; F = 0.01; 20 °C)... 86

Table C.4 Ion Exchange of Cl^- to HCO_3^- in PIL-Cl that is Suspended in 150 ml of $NaHCO_3$ (aq) for 48 h (0.50 M; F = 0.007; 20 °C).. 86

Table C.5 Ion Exchange of Cl^- to HCO_3^- in PIL-Cl that is Suspended in CO_2 Saturated Aqueous Solution for 24 h (P = 59 bar; F = 0.007; 20 °C)... 87

Table C.6 Raw Data of the Equilibrium Water Uptake (%) by the Various PIL Salts (F = 0.01, 20 °C)......... 87

Table C.7 Raw Data of the Titrations of SA and BA to 2.5 moles·HCO_3^-/1.0 mole·SA and 1.5 moles·HCO_3^-/1.0 mole·BA by PIL-HCO_3 (2.5 g·acid/L, 20 °C). 88

Table C.8 Raw Data of the Recovery of SA by Various Recovery Technologies; Measured with ^1H NMR with a Citric Acid Reference (41 mg) (20 °C). 89

Table C.9 Raw Data of the Equilibrium Swelling Ratio (g·water/g·hydrogel) of the 3.5% Hydrogel in DI Water (pH 7.0), Aqueous 2.5 g·SA/L Solution (pH 3.0) and Aqueous HCl Solution (pH 3.0) (F = 0.01, 25 °C). 90

Table C.10 Raw Data of the Equilibrium Swelling Ratio (g·water/g·hydrogel) of the 5% Hydrogel in DI Water (pH 7.0), Aqueous 2.5 g·SA/L Solution (pH 3.0) and Aqueous HCl Solution (pH 3.0) (F = 0.01, 25 °C). 91

Table C.11 Raw Data of the Equilibrium Swelling Ratio (g·water/g·hydrogel) of the 10% Hydrogel in DI Water (pH 7.0), Aqueous 2.5 g·SA/L Solution (pH 3.0) and Aqueous HCl Solution (pH 3.0) (F = 0.01, 25 °C). 92

Table C.12 Raw Data of the Equilibrium Swelling Ratio (g·water/g·hydrogel) of the 30% Hydrogel in DI Water (pH 7.0), Aqueous 2.5 g·SA/L Solution (pH 3.0) and Aqueous HCl Solution (pH 3.0) (F = 0.01, 25 °C). 93

Table C.13 Raw Data of the Equilibrium Swelling Ratio (g·water/g·hydrogel) of the 50% Hydrogel in DI Water (pH 7.0), Aqueous 2.5 g·SA/L Solution (pH 3.0) and Aqueous HCl Solution (pH 3.0) (F = 0.01, 25 °C). 94

Table C.14 Summary of the Equilibrium Swelling Ratios (g·water/g·hydrogel) of the Various Hydrogels in DI Water (pH 7.0), Aqueous 2.5 g·SA/L Solution (pH 3.0) and Aqueous HCl Solution (pH 3.0) (F = 0.01, 25 °C). 95

Table C.15 Chemisorption Dynamics of BA by PDMEA and the 3.5% and 30% Hydrogels at Approximately 1 mole·amine/1 mole·BA (2.5 g·acid/L, 25 °C). 96

Table C.16 Raw Data of the Titrations of BA with DMEP to 1.5 moles·amine/1.0 mole·BA (2.5 g·BA/L, 25 °C). 97

Table C.17 Raw Data of the Titrations of BA with PDMEA to 1.5 moles·amine/1.0 mole·BA (2.5 g·BA/L, 25 °C). 98

Table C.18 Raw Data of the Titrations of BA with the 3.5% Hydrogel to Approximately 1.5 moles·amine/1.0 mole·BA (2.5 g·BA/L, 25 °C). 99

Table C.19 Raw Data of the Titrations of BA with the 30% Hydrogel to Approximately 1.5 moles·amine/1.0 mole·BA (2.5 g·BA/L, 25 °C). 100

Table C.20 Succinic Acid Capacities of the Various Hydrogels at 3.0 moles·amine/1.0 mole·SA (2.5 g·SA/L; F = 0.01; 25 °C); Measured with ^{1}H NMR with a Citric Acid Reference (41 mg). 101

Table C.21 Swelling Ratios of the Fully Swollen 3.5% and 4% Hydrogels within the 25 ml Experiments at Approximately 3.0 moles·amine/1.0 mole·SA (F = 0.01, 25°C). 102

Table C.22 Back Titrations of the Fully Swollen 3.5% and 4% Hydrogels within the 25 ml Experiments at Approximately 3.0 moles·amine/1.0 mole·SA (F = 0.01), using 15 mM NaOH in 15 mM HCl (25 °C). 102

Table C.23 Strain measurements of the 4% Hydrogel. 103

Table C.24 Back Titrations of the Strained 4% Hydrogel After Sorption with 3.0 moles·amine/1.0 mole·SA in 2.5 g·SA/L (F = 0.01), using 15 mM NaOH in 15 mM HCl (25 °C). 104

List of Schemes

Scheme 1.1. Chemicals Derived from Succinic Acid (© Tanja Kurzrock, reprinted with permission) [3]. ... 1

Scheme 1.2. Common Cations and Anions of ILs (© Kun Dong, adapted with permission) [9]: **1)** 1,3-Dialkylimidazolium; **2)** N-alkylpyridinium; 6); **3)** 1,1-Dialkylpyrrolidinium; **4)** 1,2,3-Trialkylsulfonium; **5)** Tetraalkylammonium; **6)** 1,1,3,3-Tetramethylguanidinium; **7)** Halides; **8)** Tetrafluoroborate; **9)** Bis(trifluoromethylsulfonyl)imide; **10)** Benzenesulfonate; **11)** Thiocyanate; **12)** Organic Acid. 5

Scheme 1.3. Polyionic Liquid Cationic Backbones (© David Mecerreyes, reprinted with permission) [10]. 6

Scheme 1.4. Destruction of the Imidazolium Ring by Hydroxide (© Yuesheng Ye, adapted with permission) [13]. 7

Scheme 1.5. Synthesis of the Hydrogel. 9

Scheme 1.6. Smart Material Properties of Hydrogels (© Abdulraheim Hasan, reprinted with permission) [22]. 11

Scheme 1.7. Traditional Recovery of Succinic Acid using Alkaline Salt (© Tanja Kurzrock, reprinted with permission) [3]. 13

Scheme 1.8. Weak Acid/Weak Base Equilibrium of the Chemisorption of Organic Acids by the Bicarbonate Salt: a) Succinic Acid; b) Benzoic Acid... 15

Scheme 1.9. Weak Acid/Weak Base Equilibrium of the Chemisorption of Organic Acids by the Hydrogel: a) Succinic Acid; b) Benzoic Acid. 16

Scheme 2.1. Synthesis of $P[(VC_{12}Im)(Cl)_x(HCO_3)_y]$.. 30

Scheme 2.2. Desorption of SA from PIL-SA using CO_2-Saturated Water. 36

Scheme 2.3. Equilibrium of CO_2 in Water [13]. 37

Scheme 3.1. Schematic of Syringe: a) L_{Ref}; b) L_0. 44

Scheme 4.1 Comparison of Traditional Acid Extraction with the Proposed Industrial SA Recovery Processes of PIL-HCO_3 with Saturated $NaHCO_3$ and the 4% Hydrogel with its Smart Recovery: a) Traditional Acid Recovery (© Tanja Kurzrock, reprinted with permission); b) 4% Hydrogel Smart Recovery; c) PIL-HCO_3 Saturated $NaHCO_3$ Recovery. 69

Scheme 4.2 Processes of the Venture Technologies: a) $Mg(OH)_2$ Precipitation; b) Ammonia Precipitation. 73

Scheme 4.3 Processes of the Venture Technologies: a) Low pH Fermentation; b) Electrodialysis. 74

Scheme B.1 Recoveries of Succinic Acid with PIL-HCO_3. 83

Abbreviations

AIBN – Azobisisobutyronitrile

BA – Benzoic Acid

BF_4 - Tetrafluoroborate

CD – Crosslink Density

C_n – Alkyl chain with n number of carbons

DI – Deionized

DSC – Differential Scanning Calorimetry

DMEA – N,N-Dimethylaminoethylacrylamide

DMEP – N,N-Dimethylaminoethylpropanamide

F – Phase Fraction (m_{PIL}/m_{aq})

IL – Ionic Liquid

Im – Imidazolium

ISPR – *In-Situ* Product Removal

kt - Kiloton

M - Mass

NMR – Nuclear Magnetic Resonance

NTf_2 - Bistriflimide

PBS – Poly(butlyene succinate)

PC – Partition Coefficient

$\mathbf{P_{CO_2}}$ – Partial Pressure of CO_2

PDMEA – Poly(N,N-Dimethylaminoethylacrylamide)

pH – Power of Hydrogen

PIL – Polyionic Liquid

PIL-Cl - P[(VC_{12}Im)(Cl)]

PIL-HCO_3 - P[(VC_{12}Im)$(Cl)_{0.40}(HCO_3)_{0.60}$]

PIL-OH – P[(VC_{12}Im)$(Br)_{0.42}(OH)_{0.58}$]

P[(VC_{12}Im)$(Br)_{0.42}(OH)_{0.58}$] - Poly(1-vinyl-3-dodecylimidizolium hydroxide)

P[(VC_{12}Im)(Cl)] – Poly(1-vinyl-3-dodecylimidizolium chloride)

P[(VC_{12}Im)$(Cl)_{0.40}(HCO_3)_{0.60}$] - Poly(1-vinyl-3-dodecylimidizolium bicarbonate)

Pyr – Pyridine

Rt – Room Temperature

SA – Succinic Acid

SATP – Standard Ambient Temperature and Pressure

TAAEA – Tris[2-(acryloylamino)ethyl]amine

TAC – Tricarboxylic Acid Cycle

TBAB – Tetrabutylammonium Bromide

T_g – Glass Transition Temperature

UV-Vis – Ultraviolet-Visible

V - Vinyl

(VC_{12}Im)(Cl) – 1-vinyl-3-dodecylimidizolium hydroxide

V50 – Azobis(2-methylpropionamidine)dihydrochloride

w_b^a **–** Weight fraction of material b in material a.

Chapter 1

Introduction

1.1 Succinic Acid Bioproduction

The bioproduction of organic acids is a potentially effective route to commodity chemicals such as succinic acid [1], [2]. Succinic acid is a precursor to many chemicals (Scheme 1.1) and is used in many industries such as the food industry [3]. SA can be converted into polymers such as biodegradable poly(butylene succinate) (PBS). PBS is made by converting SA to 1,4-Butanediol, and copolymerizing SA with 1,4-Butanediol [4].

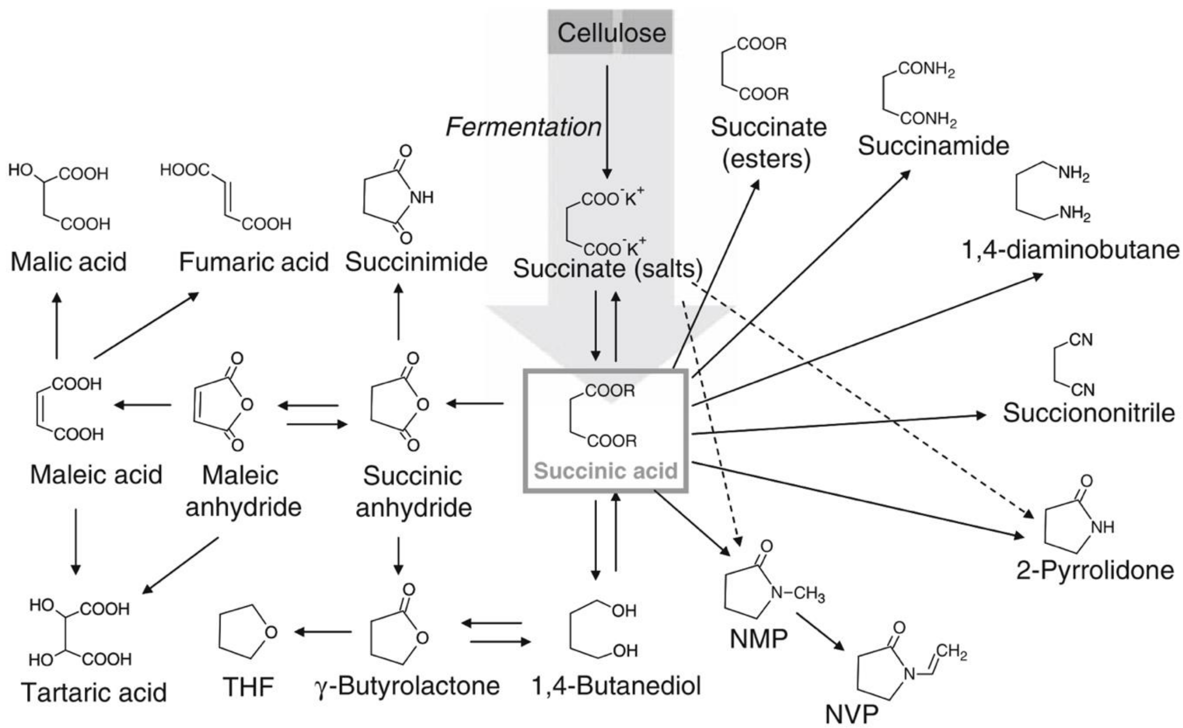

Scheme 1.1. Chemicals Derived from Succinic Acid (© Tanja Kurzrock, reprinted with permission) [3].

The pH of optimal SA production during fermentation varies amongst bacteria, but generally requires maintenance between 6.0 - 7.2 for stable production [5]. One bacterium, *Actinobacillus succinogenes* CGMCC1593 (Table A.1), has its optimal SA production at pH 6.7 and does not metabolize SA at pH < 5.5. The technique of *in-situ* product recovery (ISPR) removes succinic acid from fermentation broth during bioproduction. This is a useful method to stabilize the broth pH and succinic acid concentration during fermentation, and also provides increased yields, productivity rates and enrichments of succinic acid [5], [6].

The bioproduction of succinic acid was thought to be a profitable venture during the 2010s. This technology was a green substitute to SA that was traditionally produced from the hydrogenation of petrochemically sourced maleic anhydride. The company, BioAmber, implemented a plant that produced 30 kt·SA/annum in 2015 in Sarnia, Canada. This plant quickly went into bankruptcy in 2018 due to an inability to financially compete with petrochemically produced SA. Other companies, including Myriant and a joint venture of BASF and Corbion, also started and closed their bioproduction plants in that decade. It became evident that the implemented bioproduction processes were not economically competitive [7], [8]. A summary of the ventures that are reported in [8] is provided in Table 1.1.

The technology that was used for SA recovery varied between the ventures. Methods such as ammonium salt precipitation and fermenting at low pH created barriers to efficient SA production by having complex recoveries and low SA yields [8]. Green and simple recovery methods that are based upon the polymeric chemisorbents that are developed in this thesis have the potential to overcome these issues. Although the chemicals that are used to synthesize these polymers are petrochemically derived, the total sourcing from petrochemical sources for the bioproduction of SA is minimal compared to SA that is directly made from petrochemical sources. Although fermentations are not conducted in this work, the SA concentration that is studied in this work (2.5 g·SA/L aqueous solution) is commonly used to assess the recovery of SA from dilute aqueous solution.

Table 1.1 Summary of the Industrial Ventures of the Bioproduction of SA in the 2010s (© Mickel Jansen, adapted with permission) [8].

Company	SA Production (kton/year)	Year started	City	Recovery Technology
Myriant	14	2013	Lake Providence, Louisiana, USA	Ammonia precipitation
BioAmber	30	2014	Sarnia, Ontario, Canada	Electrodialysis, Low pH fermentation
Succinity (BASF/Corbion-Purac)	10	2013	Barcelona, Spain	Mg process
Reverdia (DSM/Roquette)	10	2012	Cassano Spinola, Italy	Low pH fermentation

1.2 Polyionic Liquids

Ionic liquids (ILs) are salts that have a melting point < 100 ^{o}C. Most ILs remain in the liquid phase at 1 atm up to 200 – 300 ^{o}C. ILs have many pragmatic properties, including negligible vapor pressure and tunable cations and anions. The tunable anions allow engineers to adjust properties such as the glass transition temperature, solubility, viscosity and conductivity by exchanging the anion. A list of a few properties of a few common ILs is presented (Table 1.2) [9].

Table 1.2 Properties of a Sample of ILs (© Kun Dong, adapted with permission) [9].

IL/Property	Melting Temperature (K)	Density (g/ml)	Viscosity (cP)	Conductivity (mS/cm)
$(C_2C_1Im)(Cl)$	361.8	1.12	48.3	0.3
$(C_4C_1Im)(Cl)$	314.1	1.08	30.0	1.0
$(C_4C_1Im)(BF_4)$	190.15	1.20	100.0	3.5
$(C_4C_1Im)(NTf_2)$	270.2	1.44	49.0	3.9
$(C_4Pyr)(BF_4)$	288.5	1.21	163.0	2.5
$(C_4Pyr)(NTf_2)$	299.0	1.44	61.0	3.1

Ionic liquids have been studied for a range of applications, including catalysis, plastics, CO_2 capture and electrochemical energy storage. Common IL cations and bridged anions are presented (Scheme 1.2) [9]. IL nomenclature is written with the following format: the main IL structure is abbreviated, such as Im for imidazolium; any saturated alkyl chains are written as C_n and are assumed to be on the heteroatom (e.g. nitrogen); the individually charged species are written in parentheses. The IL that is used in this thesis is 1-vinyl-3-dodecylimidazolium chloride ($(VC_{12}Im)(Cl)$).

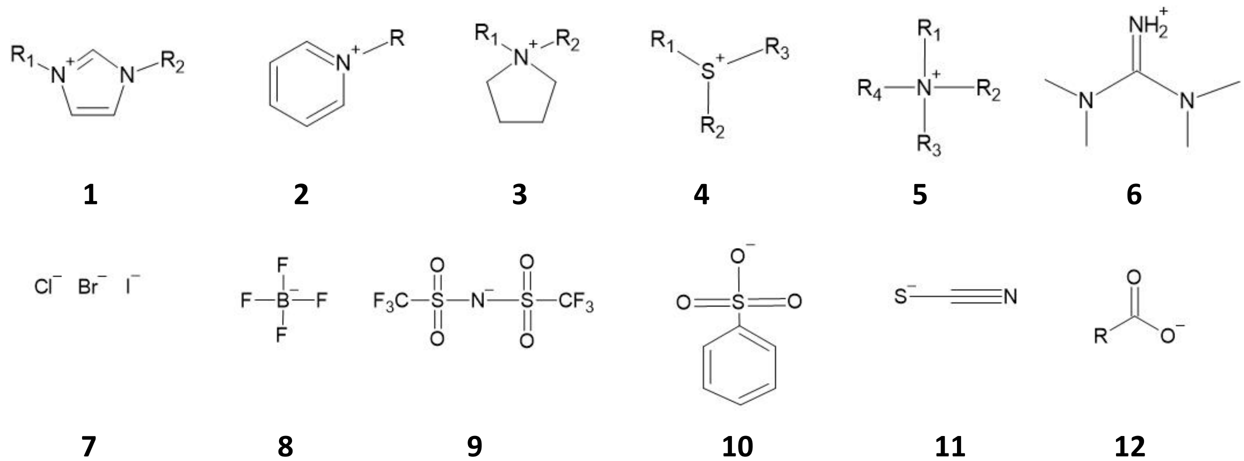

Scheme 1.2. Common Cations and Anions of ILs (© Kun Dong, adapted with permission) [9]: **1)** 1,3-Dialkylimidazolium; **2)** N-alkylpyridinium; 6); **3)** 1,1-Dialkylpyrrolidinium; **4)** 1,2,3-Trialkylsulfonium; **5)** Tetraalkylammonium; **6)** 1,1,3,3-Tetramethylguanidinium; **7)** Halides; **8)** Tetrafluoroborate; **9)** Bis(trifluoromethylsulfonyl)imide; **10)** Benzenesulfonate; **11)** Thiocyanate; **12)** Organic Acid.

Polyionic liquids are polymers that are made from ILs that have polymerizable groups. PILs have similar characteristics to ILs, while also having polymer properties [10]. An article published by Marcilla et al. explains that poly[(VBuIm)(Cl)] is soluble in water; however, the article also describes that changing the counter ion to make poly[(VEtIm)(BF_4)] or poly[(VEtIm)(PF_6)] makes the PIL hydrophobic [11]. All of the PIL salts in this work are not soluble in water and are hydrated by less than their dry mass. This insolubility is useful for bioproducing SA, since it makes the PIL non-bioavailable.

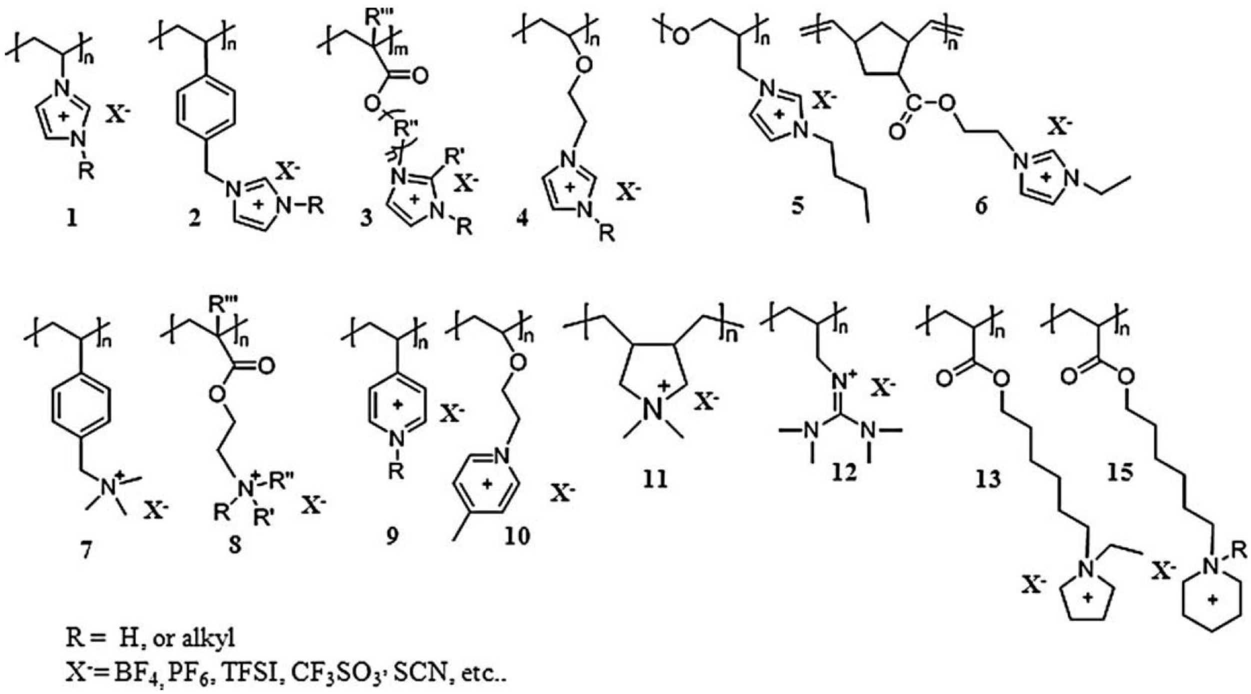

Scheme 1.3. Polyionic Liquid Cationic Backbones (© David Mecerreyes, reprinted with permission) [10].

Common PIL backbones are presented (Scheme 1.3). Imidazolium is the most implemented charged species in PILs as of 2011 (**1-6**). Others including tetraalkyl ammonium (**7, 8**), pyridinium (**9,10)**, pyrrolidonium (**11, 13)**, guanidinium (**12**) and piperidinium (**15**) were also commonly implemented [10]. The imidazolium ring is implemented in this thesis. Free radical polymerization was the most reported polymerization method of ILs, although other methods such as atom transfer radical polymerization, reversible fragmentation transfer polymerization and ring-opening polymerization were also used [10]. Free radical polymerization is used to make poly(1-vinyl-3-dodecylimidazolium chloride) (P[(VC_{12}Im)(Cl)]) from (VC_{12}Im)(Cl) in this thesis. David Mecerreyes, reprinted with permission

Within our research group's previous work, a polyionic liquid of poly(1-vinyl-3-dodecylimidizolium hydroxide) (P[(VC_{12}Im)$(Br)_{0.42}(OH)_{0.58}$]) is used to recover SA from dilute aqueous solution (2.5 g·SA/L) [12]. Although the PIL has a competitive SA capacity to polymeric chemisorbents that are published in literature, the potential for OH^- to destroy the imidazolium ring by nucleophilic attack at C(2) is a concern for the PIL's industrial application (Scheme 1.4). The destruction of Im in Scheme 1.4 is adapted from the reported destruction of poly(1-[(2-methacryl-oyloxy)ethyl]-3-butylimidazolium hydroxide). Ye and Elabd also reported that a hydroxide-imidazolium PIL can be fully destroyed in 3 months [13].

The anion of $P[(VC_{12}Im)(Br)_{0.42}(OH)_{0.58}]$ (PIL-OH) is also unstable. The anion is well-reported to react with water to form CO_2 [14]. Another group reports the complete destruction of the hydroxide anion in ammonium-based poly(estersulfone) in 4 days [15]. The instabilities of the cation and anion of our research group's previous PIL warrants the research of a more stable analog.

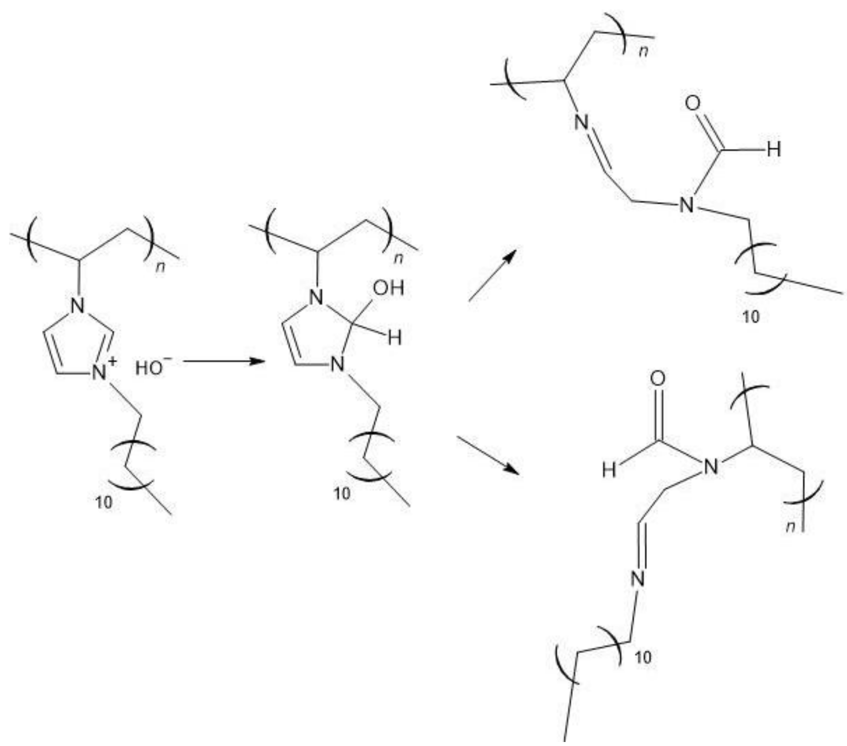

Scheme 1.4. Destruction of the Imidazolium Ring by Hydroxide (© Yuesheng Ye, adapted with permission) [13].

To improve the stability of the PIL salt, a bicarbonate salt is assessed in this thesis. Bicarbonate is reported to be stable in air at room temperature; however, it decomposes above approximately 80 ^oC [16]. This degradation forms the weak base of carbonate, which has the same stoichiometry for organic acid extraction in the PIL as bicarbonate. Therefore, any degradation in mild temperatures should have a limited effect on the extraction efficiency of the PIL. The basicity of the PIL should even be preserved at extreme temperatures, since carbonate only degrades to an oxide at approximately 500 ^oC [17]. In future works, the PIL of $P[(VC_{12}Im)(Cl)_x(CO_3)_y])$ could be synthesized to create a PIL that has higher temperature stability than $P[(VC_{12}Im)(Cl)_x(HCO_3)_y])$.

1.3 Poly(acrylamide) Hydrogels

Hydrogels are cross-linked polymers that absorb an extensive mass of water due to their hydrophilicity. This hydrophilicity is produced by hydrophilic functional groups that are integrated into the hydrogel network such as carboxylic acids, sulfonic acids, amines and hydroxides [18]. Within hydrogels that have ionizable functional groups, the generated electrostatic repulsions between the functional groups can also greatly increase the swelling of water [19], [20]. The structure and mechanical properties of hydrogels are similar to that of biological tissue. Therefore, hydrogels are often implemented in biomedical engineering [18].

Acrylamide-based polymers are amongst the most studied hydrogel materials [18]. In this thesis, the acrylamide-based monomer of N,N-dimethylaminoethylacrylamide (DMEA) is copolymerized by free radical initiation with tris[2-(acryloylamino)ethyl]amine (TAAEA) to form a hydrogel (Scheme 1.5). The formed hydrogel has amine functionalization from the 3^o amines in DMEA and TAAEA. These amines make the hydrogel basic, which is essential for recovering SA from dilute aqueous solution.

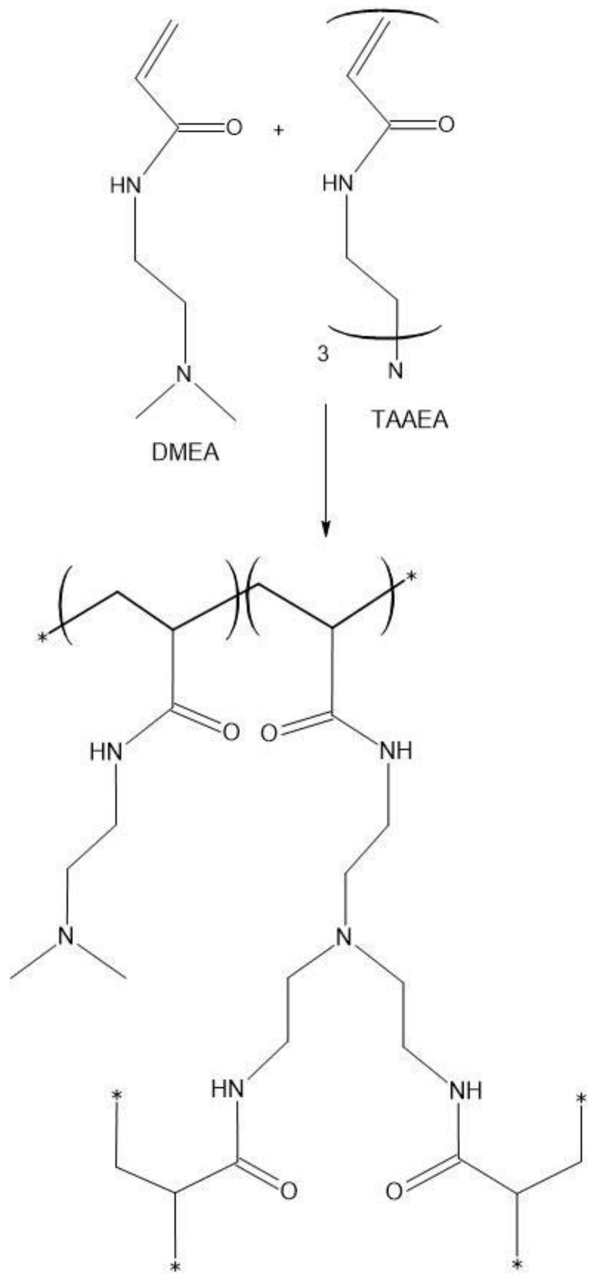

Scheme 1.5. Synthesis of the Hydrogel.

The basicity of the weakly basic amine in the hydrogel is affected by its activity in any given equilibrium reaction. In this thesis, the amine reacts with weak organic acid. Polymerizing the amine prevents its equidistant dispersal through aqueous solution. This increases the activity coefficient of the amine in an equilibrium reaction relative to free amine in solution. Crosslinking the amine raises its activity coefficient relative to dissolved polymer; the elongation of the polymer chains is restricted. A higher activity coefficient of the amine increases its free energy of organic acid chemisorption. This lowers the quantity of amines that convert to the ammonium carboxylate salt. Therefore, hydrogels with higher crosslink densities (CDs) have higher activities and lower chemisorption capacities. Gustafson et al. support this theory, and report that increasing the CD of a hydrogel lowers its basicity [21]. **It is hypothesized that increasing the crosslink density of our hydrogel lowers its basicity.** Although we do not directly measure the crosslink density in terms of moles of crosslinks per volume of hydrogel in this thesis, we create various crosslink densities by changing the weight fraction of the comonomer of TAAEA relative to DMEA. Higher weight fractions of TAAEA increases the crosslinking and lowers the volume of water that the hydrogel can absorb. Therefore, changing the weight fraction of TAAEA increases the crosslink density of our hydrogel through two methods.

The concept that we can change the basicity of the amine in the hydrogel by increasing the hydrogel's CD is used to desorb succinic acid from the hydrogel. We attempt to change the activity of the ammonium salts after they have reached equilibrium in acid solution by adding strain to the hydrogel with mechanical pressure. Instead of increasing activities by increasing the weight fraction of TAAEA relative to DMEA, we are attempting to increase activities by imposing strain. **It is hypothesized that this strain increases the activity of the ammonium salt, which causes the equilibrium reaction to reverse and succinic acid to desorb.**

The hypothesized strain sensitivity of our amine-functionalized hydrogel is only one of many smart material properties of hydrogels (Scheme 1.6) [22]. The pH sensitivity of hydrogels is well-reported. Our hydrogel is placed in aqueous solutions of pH 7.0 and pH 3.0 (SA and HCl) to assess the variation of swelling with solution pH. The solution pH that collapses our hydrogel is also assessed. The well-studied smart material property of temperature is not investigated in this thesis. However, an important study that uses the stimulus of temperature in a manner that is similar to our hypothesized use of pressure to release weak acid from a hydrogel is reported by Caykara et al. This group uses temperature to release adsorbed solutes from a hydrogel. The group synthesizes a hydrogel that is similar to ours; it is made with the comonomers of N-[3-dimethylaminopropylmethacrylamide] and acrylamide, and is crosslinked with N,N-methylenebisacrylamide. When the hydrogel increases in temperature and collapses, the surfactants are reported to release with the displaced solution [23]. Similar to this finding by Caykara et al., it is suspected that our use of pressure to collapse our hydrogel releases sorbed SA.

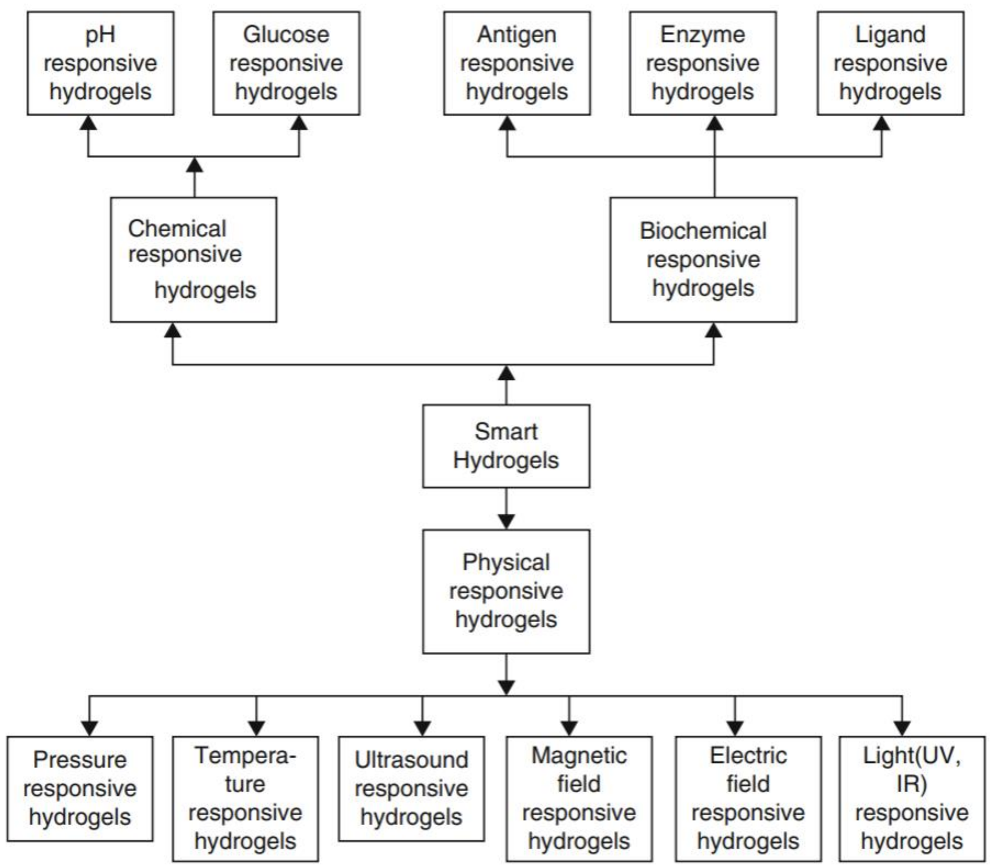

Scheme 1.6. Smart Material Properties of Hydrogels (© Abdulraheim Hasan, reprinted with permission) [22].

1.4 Chemisorption and Physisorption

The sorption of weak organic acid is achieved through chemisorption or physisorption. Chemisorption is the sorption of solute from solution due to a chemical reaction. Physisorption is the sorption of solute by a sorbent without a change of the sorbent's chemical structure [24]. In this thesis, succinic acid and benzoic acid (BA) are chemisorbed from solution by both sorbents through the formation of ammonium carboxylate salts. Both acids also physisorb to both sorbent structures.

The proposed mechanisms of physisorption are different between the two sorbents. In the PIL, the physisorption of weak acid is proposed to occur by the attraction of the hydrophobic component of the weak acid to the hydrophobic dodecyl tail. This is facilitated by Van der Waals forces [25]. Within the hydrogel, the presence of amide and amine functional groups generates the proposal that hydrogen bonding interactions are responsible for the majority of the physisorption. The physisorptions of the reactive polymer salts of both sorbents cannot be isolated for measurement since the chemisorptions are simultaneous.

The non-reactive analog of $P[(VC_{12}Im)(Cl)]$ is used to assess the physisorption of both acids with the PIL. Although this physisorption does not measure the physisorption of the PIL's succinate salt, it does give an indicator of the PIL's physisorption efficiency. Quantitative assessments of the hydrogel's physisorption are not performed since a non-reactive analog is not made.

The total sorptions of SA with the bicarbonate salt and the hydrogels are measured. pH can be used to identify whether the majority of a sorption is chemisorption or physisorption. A high pH measurement (pH 7.0) after extraction in a solution of pH 3.0 (2.5 g·SA/L) indicates that all but a negligible quantity of acid is chemisorbed from the solution. A high measured sorption with a low pH after extraction indicates that protons do not react with the sorbent; the majority of the sorption is physisorption.

1.5 Succinic Acid Recovery

1.5.1 Traditional Succinic Acid Recovery

Methods for isolating organic acids from aqueous solution include precipitation with alkaline salt and various electrodialysis techniques [1], [3], [26]. Processes involving alkaline salts generally provide low SA yields with byproducts that cannot be recycled without additional processing. An example of a generated by-product that requires additional processing is gypsum, which is produced from the acidification of CaSA with H_2SO_4 (Scheme 1.7). Due in large part to these issues, 60% of SA bioproduction costs are associated with the purification of SA from fermentation broth [3]. These high costs associated with the traditional isolating technique have sparked research into alternative recovery technologies.

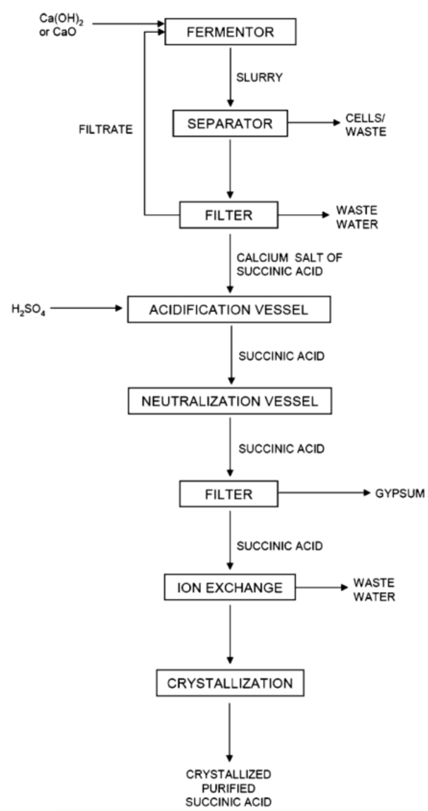

Scheme 1.7. Traditional Recovery of Succinic Acid using Alkaline Salt (© Tanja Kurzrock, reprinted with permission) [3].

1.5.2 Researched Succinic Acid Sorption

As mentioned previously, SA is removed from dilute aqueous solution using the weakly basic chemisorbents of the bicarbonate salt and the hydrogel. Benzoic acid is also extracted to assess the sorption of monocarboxylic acids with the sorbents. The identical first pKas of SA and BA (pKa_{BA} = 4.20, $pKa_{1,SA}$ = 4.21) allows for a fairly direct comparison of the sorbents' recovery efficiencies of monocarboxylic and dicarboxylic acids. This result is important, since it gives insight into the potential sorption efficiencies of common monocarboxylic acids that are produced from fermentation, such as lactic acid (pKa = 3.85) [27]. The use of BA is also useful to confirm assessed trends. Its high UV-Vis activity allows for UV-Vis to be used as an additional analytical technique to NMR.

The reaction of the bicarbonate salt or the hydrogel with a weak organic acid are weak acid/weak base equilibrium reactions. The equilibrium reactions of BA and SA with both sorbents are presented in Scheme 1.8 and Scheme 1.9. To show the full neutralization of both acids, the equilibrium with SA with both sorbents considers the chemisorption of both carboxylic acid groups.

The mechanism of acid chemisorption is different between the sorbents. The ammonium bicarbonate salt can only be changed through an ion exchange or from a chemical reaction. The chemical reaction with SA in solution yields ammonium succinate + CO_2 + water (Scheme 1.8). The reaction of the by-product of CO_2 with water produces H_2CO_3, which forms an equilibrium with HCO_3^- and CO_3^{2-}. These ions can exchange with succinate and form the bicarbonate or carbonate salts. This potential ion exchange would lower the sorbent's chemisorption efficiency. To efficiently chemisorb weak acid and prevent equilibrium formation, the system is sparged with air to strip the formed CO_2. This technique creates a pseudo-irreversible reaction. **This reaction is hypothesized to make the bicarbonate salt act as a strong base for the recovery of SA, while possessing the weakly nucleophilic properties that preserve its polymer backbone.**

An amine-functionalized hydrogel is capable of chemisorbing organic acids through a reversible acid/base equilibrium reaction that yields no by-products (Scheme 1.9). The chemical reaction of Scheme 1.9 uses the base of DMEA (NMe_2R) to show the chemisorption of organic acid by the hydrogel. **It is hypothesized that the sorption of SA with both sorbents are competitive with polymeric chemisorbents that are documented in literature.**

a)

b)

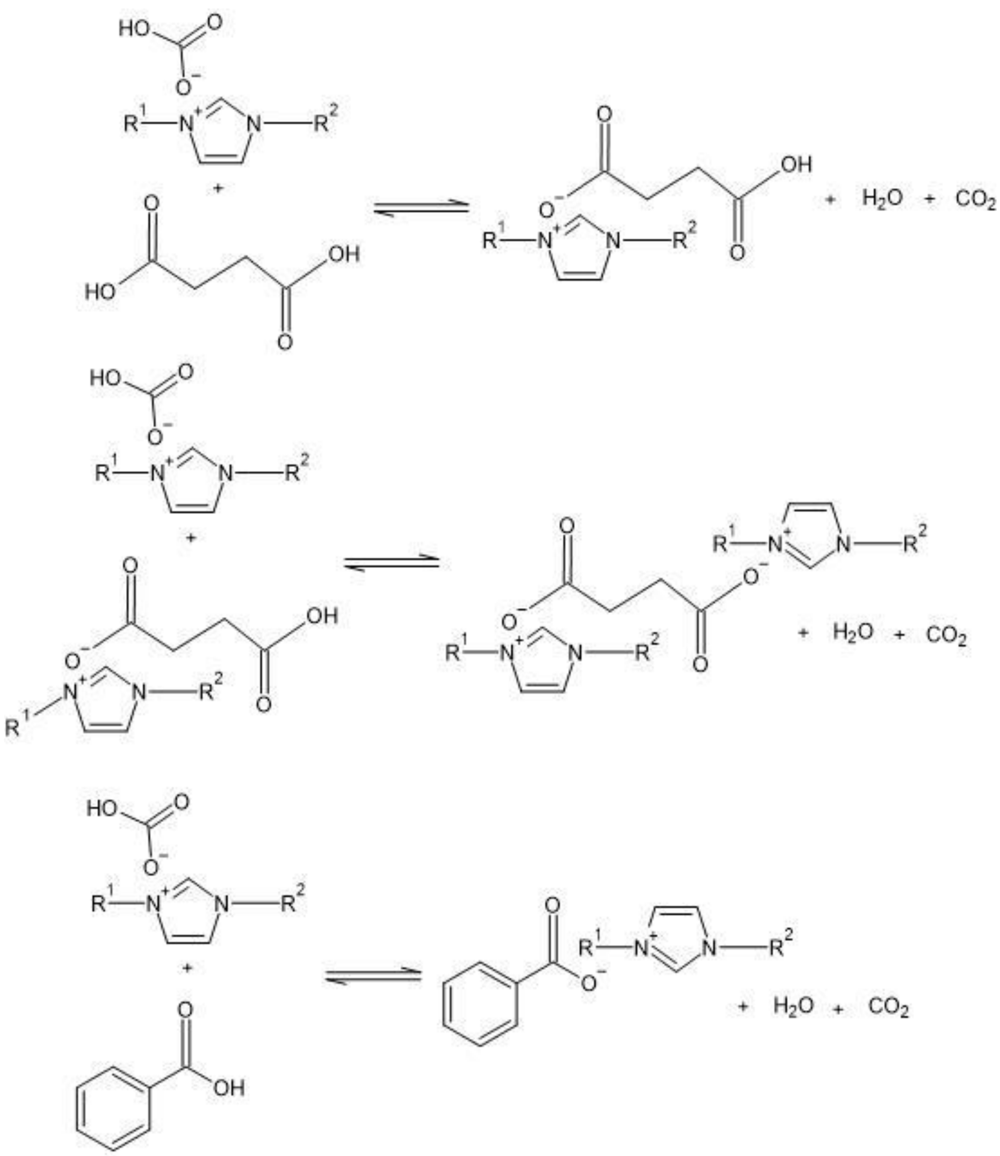

Scheme 1.8. Weak Acid/Weak Base Equilibrium of the Chemisorption of Organic Acids by the Bicarbonate Salt: a) Succinic Acid; b) Benzoic Acid.

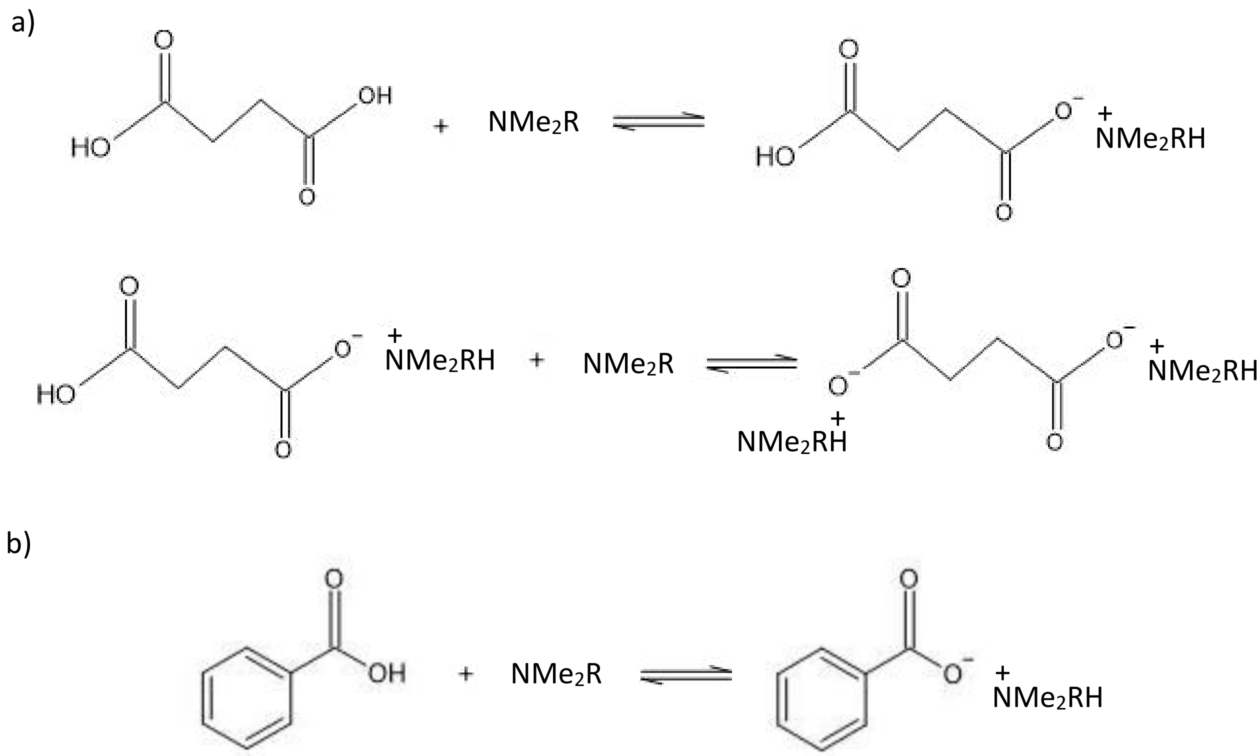

Scheme 1.9. Weak Acid/Weak Base Equilibrium of the Chemisorption of Organic Acids by the Hydrogel: a) Succinic Acid; b) Benzoic Acid.

1.5.3 Researched Succinic Acid Desorption

The full recovery of SA from aqueous solution with both sorbents requires its desorption. The desorption of SA from polymeric sorbents is commonly accomplished with strong acid/base [3]. In amine-functionalized hydrogel systems, regeneration can be done by treatment with NaOH (aq), which collapses the hydrogel and releases sodium succinate into solution. The PIL-succinate salt can be regenerated through acidification with HCl, which yields free SA and the chloride salt of the PIL. The PIL can be regenerated back to its bicarbonate salt through the exchange of Cl^- with HCO_3^- in $NaHCO_3$ (aq). This recovery generates NaCl as an undesirable by product.

In theory, the $P[(VC_{12}Im)(Cl)_x(HCO_3)_y]$ system may also support alternate recovery methods. The first proposed method aims to simultaneously desorb succinate and regenerate PIL-bicarbonate by treatment with saturated $NaHCO_3$ (aq) solution. This desorption avoids acidification, and forms sodium succinate + sodium chloride. The second proposed method aims to desorb SA using a CO_2-saturated aqueous solution at high partial pressure. This method seeks to protonate succinate with weakly acidic H_2CO_3 to form free organic acid and the bicarbonate salt. **It is hypothesized that these two green recovery methods are effective at recovering SA.**

The response of functionalized hydrogels to shifts in pH and other stimuli are widely reported, and may prove useful in the context of acid recovery. **It is hypothesized that the previously described potential strain-sensitive basicity can support an organic acid recovery process. It is also hypothesized that all of the researched recovery methods are competitive with the traditional SA recovery with alkaline salts.**

1.6 Summary of Hypotheses

The hypotheses that are tested in this thesis include:

- the PIL-bicarbonate salt has a competitive SA capacity compared to the hydroxide salt.
- the recovery of SA from the PIL with saturated H_2CO_3 and $NaHCO_3$ is effective.
- the basicity of the hydrogel is sensitive to crosslink density.
- the basicity of the hydrogel is sensitive to strain.
- the strain sensitivity of the hydrogel can be applied to effectively recover SA.
- the PIL-bicarbonate and the hydrogel provide SA capacities that are competitive with chemisorbents that are documented in literature.
- the researched SA recovery methods provide advantages in comparison to traditional organic acid recovery processes involving alkaline salts.

References

[1] T. A. Ewing, N. Nouse, M. van Lint, J. van Haveren, J. Hugenholtz, and D. S. van Es, “Fermentation for the production of biobased chemicals in a circular economy: a perspective for the period 2022–2050,” *Green Chemistry*, vol. 24, no. 17, pp. 6373–6405, Aug. 2022, doi: 10.1039/D1GC04758B.

[2] S. Punia Bangar, S. Suri, M. Trif, and F. Ozogul, “Organic acids production from lactic acid bacteria: A preservation approach,” *Food Biosci*, vol. 46, p. 101615, Apr. 2022, doi: 10.1016/J.FBIO.2022.101615.

[3] T. Kurzrock and D. Weuster-Botz, “Recovery of succinic acid from fermentation broth,” *Biotechnol Lett*, vol. 32, no. 3, pp. 331–339, Feb. 2010, doi: 10.1007/S10529-009-0163-6.

[4] M. Barletta *et al.*, “Poly(butylene succinate) (PBS): Materials, processing, and industrial applications,” *Prog Polym Sci*, vol. 132, p. 101579, Sep. 2022, doi: 10.1016/J.PROGPOLYMSCI.2022.101579.

[5] Y. P. Liu, P. Zheng, Z. H. Sun, Y. Ni, J. J. Dong, and P. Wei, “Strategies of pH control and glucose-fed batch fermentation for production of succinic acid by Actinobacillus succinogenes CGMCC1593,” *Journal of Chemical Technology & Biotechnology*, vol. 83, no. 5, pp. 722–729, May 2008, doi: 10.1002/JCTB.1862.

[6] A. G. Santos, T. L. de Albuquerque, B. D. Ribeiro, and M. A. Z. Coelho, “In situ product recovery techniques aiming to obtain biotechnological products: A glance to current knowledge,” *Biotechnol Appl Biochem*, vol. 68, no. 5, pp. 1044–1057, Oct. 2021, doi: 10.1002/BAB.2024.

[7] X. Li and E. Mupondwa, “Empirical analysis of large-scale bio-succinic acid commercialization from a technoeconomic and innovation value chain perspective: BioAmber biorefinery case study in Canada,” *Renewable and Sustainable Energy Reviews*, vol. 137, p. 110587, Mar. 2021, doi: 10.1016/J.RSER.2020.110587.

[8] M. L. A. Jansen and W. M. van Gulik, "Towards large scale fermentative production of succinic acid," *Curr Opin Biotechnol*, vol. 30, pp. 190–197, Dec. 2014, doi: 10.1016/J.COPBIO.2014.07.003.

[9] K. Dong, X. Liu, H. Dong, X. Zhang, and S. Zhang, "Multiscale Studies on Ionic Liquids," *Chem Rev*, vol. 117, no. 10, pp. 6636–6695, May 2017, doi: 10.1021/acs.chemrev.6b00776.

[10] D. Mecerreyes, "Polymeric ionic liquids: Broadening the properties and applications of polyelectrolytes," *Prog Polym Sci*, vol. 36, no. 12, pp. 1629–1648, Dec. 2011, doi: 10.1016/J.PROGPOLYMSCI.2011.05.007.

[11] R. Marcilla, J. A. Blazquez, J. Rodriguez, J. A. Pomposo, and D. Mecerreyes, "Tuning the solubility of polymerized ionic liquids by simple anion-exchange reactions," *J Polym Sci A Polym Chem*, vol. 42, no. 1, pp. 208–212, Jan. 2004, doi: 10.1002/POLA.11015.

[12] J. Alexiou, R. Biro, A. Tremblay, A. Daugulis, and J. S. Parent, "Base-functionalized polymeric chemisorbents for succinic acid recovery from aqueous solution," *React Funct Polym*, vol. 181, p. 105412, Dec. 2022, doi: 10.1016/J.REACTFUNCTPOLYM.2022.105412.

[13] Y. Ye and Y. A. Elabd, "Relative chemical stability of imidazolium-based alkaline anion exchange polymerized ionic liquids," *Macromolecules*, vol. 44, no. 21, pp. 8494–8503, Nov. 2011, doi: 10.1021/ma201864u.

[14] J. G. Shim, D. W. Lee, J. H. Lee, and N. S. Kwak, "Experimental study on capture of carbon dioxide and production of sodium bicarbonate from sodium hydroxide," *Environmental Engineering Research*, vol. 21, no. 3, pp. 297–303, Sep. 2016, doi: 10.4491/EER.2016.042.

[15] J. Yan and M. A. Hickner, "Anion exchange membranes by bromination of benzylmethyl-containing poly(sulfone)s," *Macromolecules*, vol. 43, no. 5, pp. 2349–2356, Mar. 2010, doi: 10.1021/MA902430Y.

[16] M. Hartman, K. Svoboda, M. Pohořelý, and M. Šyc, "Thermal decomposition of sodium hydrogen carbonate and textural features of its calcines," *Ind Eng Chem Res*, vol. 52, no. 31, pp. 10619–10626, Aug. 2013, doi: 10.1021/IE400896C.

[17] P. K. Gallagher and D. W. Johnson, "The effects of sample size and heating rate on the kinetics of the thermal decomposition of CaCO3," *Thermochim Acta*, vol. 6, no. 1, pp. 67–83, Mar. 1973, doi: 10.1016/0040-6031(73)80007-3.

[18] G. Sennakesavan, M. Mostakhdemin, L. K. Dkhar, A. Seyfoddin, and S. J. Fatihhi, "Acrylic acid/acrylamide based hydrogels and its properties - A review," *Polym Degrad Stab*, vol. 180, p. 109308, Oct. 2020, doi: 10.1016/J.POLYMDEGRADSTAB.2020.109308.

[19] S. Bashir *et al.*, "Fundamental Concepts of Hydrogels: Synthesis, Properties, and Their Applications", doi: 10.3390/polym12112702.

[20] S. G. Roy and P. De, "Swelling properties of amino acid containing cross-linked polymeric organogels and their respective polyelectrolytic hydrogels with pH and salt responsive property," *Polymer (Guildf)*, vol. 55, no. 21, pp. 5425–5434, Oct. 2014, doi: 10.1016/J.POLYMER.2014.08.072.

[21] R. L. Gustafson, H. F. Fillius, and R. Kunin, "Basicities of Weak Base Ion Exchange Resins," *Industrial and Engineering Chemistry Fundamentals*, vol. 9, no. 2, pp. 221–229, 1970, doi: 10.1021/I160034A006.

[22] A. M. A. Hasan and M. E.-S. Abdel-Raouf, *Cellulose-Based Superabsorbent Hydrogels*. 2018. doi: 10.1007/978-3-319-76573-0_11-1.

[23] T. Çaykara, M. Demiray, and O. Güven, "Swelling behavior of poly{N-[3-(dimethylaminopropyl)] methacrylamide-co- acrylamide} hydrogels in aqueous solutions of surfactants," *J Polym Sci B Polym Phys*, vol. 44, no. 12, pp. 1645–1652, Jun. 2006, doi: 10.1002/POLB.20835.

[24] X. Qi, X. Tong, W. Pan, Q. Zeng, S. You, and J. Shen, “Recent advances in polysaccharide-based adsorbents for wastewater treatment,” *J Clean Prod*, vol. 315, p. 128221, Sep. 2021, doi: 10.1016/J.JCLEPRO.2021.128221.

[25] C. J. van Oss, D. R. Absolom, and A. W. Neumann, “The ‘hydrophobic effect’: Essentially a van der Waals interaction,” *Colloid and Polymer Science Kolloid Zeitschrift & Zeitschrift für Polymere*, vol. 258, no. 4, pp. 424–427, Apr. 1980, doi: 10.1007/BF01480835.

[26] L. A. Tung, “Recovery of carboxylic acids at pH greater than pKa,” University of California at Berkeley, 1993.

[27] C. Wang, T. Chang, H. Yang, and M. Cui, “Surface physiological changes induced by lactic acid on pathogens in consideration of pKa and pH,” *Food Control*, vol. 46, pp. 525–531, Dec. 2014, doi: 10.1016/J.FOODCONT.2014.06.024.

Copyrights

Scheme 1.1 reprinted with permission from T. Kurzrock and D. Weuster-Botz, “Recovery of succinic acid from fermentation broth,” *Biotechnol Lett*, vol. 32, no. 3, pp. 331–339, Feb. 2010, doi: 10.1007/S10529-009-0163-6. Copyright 2010 Springer.

Scheme 1.2 adapted with permission from K. Dong, X. Liu, H. Dong, X. Zhang, and S. Zhang, “Multiscale Studies on Ionic Liquids,” *Chem Rev*, vol. 117, no. 10, pp. 6636–6695, May 2017, doi: 10.1021/acs.chemrev.6b00776. Copyright 2017 American Chemical Society.

Scheme 1.3 reprinted with permission from D. Mecerreyes, “Polymeric ionic liquids: Broadening the properties and applications of polyelectrolytes,” *Prog Polym Sci*, vol. 36, no. 12, pp. 1629–1648, Dec. 2011, doi: 10.1016/J.PROGPOLYMSCI.2011.05.007. Copyright 2011 Elsevier.

Scheme 1.4 adapted with permission from Y. Ye and Y. A. Elabd, “Relative chemical stability of imidazolium-based alkaline anion exchange polymerized ionic liquids,” *Macromolecules*, vol. 44, no. 21, pp. 8494–8503, Nov. 2011, doi: 10.1021/ma201864u. Copyright 2011 American Chemical Society.

Scheme 1.6 reprinted with permission from A. M. A. Hasan and M. E.-S. Abdel-Raouf, *Cellulose-Based Superabsorbent Hydrogels*. 2018. doi: 10.1007/978-3-319-76573-0_11-1. Copyright 2018 Springer.

Scheme 1.7 reprinted with permission from T. Kurzrock and D. Weuster-Botz, “Recovery of succinic acid from fermentation broth,” *Biotechnol Lett*, vol. 32, no. 3, pp. 331–339, Feb. 2010, doi: 10.1007/S10529-009-0163-6. Copyright 2010 Springer.

Table 1.1 adapted with permission from T. Kurzrock and D. Weuster-Botz, “Recovery of succinic acid from fermentation broth,” *Biotechnol Lett*, vol. 32, no. 3, pp. 331–339, Feb. 2010, doi: 10.1007/S10529-009-0163-6. Copyright 2010 Springer.

Table 1.2 adapted with permission from K. Dong, X. Liu, H. Dong, X. Zhang, and S. Zhang, “Multiscale Studies on Ionic Liquids,” *Chem Rev*, vol. 117, no. 10, pp. 6636–6695, May 2017, doi: 10.1021/acs.chemrev.6b00776. Copyright 2017 American Chemical Society.

Chapter 2

A Bicarbonate Functionalized Polyionic Liquid for Organic Acid Recovery

2.1 Experimental

2.1.1 Materials

1-vinylimidazole (≥99%), 1-chlorododecane (≥97%), sodium hydroxide (≥97%), sodium bicarbonate (99%), hydrochloric acid (37%), benzoic acid (≥99.5%), citric acid (≥99.5%), phenolphthalein, chloroform-d (99.8 atom % D), methanol-d_4 (≥99.8 atom % D) and 2,2'-azobis(2-methylpropionitirile) (AIBN) (98%) were used as received from Sigma-Aldrich (Canada). All organic solvents and succinic acid (≥99.5%) were used as received from Fisher Scientific (Canada). Carbon dioxide and nitrogen were supplied by Linde Canada, Ltd.

2.1.2 (VC_{12}Im)(Cl) and P[(VC_{12}Im)(Cl)] Synthesis

The (VC_{12}Im)(Cl) monomer was prepared by adding 1-vinylimidazole (10.03 g, 107 mmoles) and 1-chlorododecane (24.30 g, 119 mmoles) into toluene (25 ml) at 100 ^oC under N_2 for 48 h. Cooling the resulting solution to room temperature produced two phases. The bottom phase was washed with hexanes (4 x 20 ml) and was dried *in vacuo* (18.92 g, 59% yield). ^1H NMR ($CDCl_3$): ∂ 0.88 ppm (3 H), 1.25 ppm (18 H), 1.95 ppm (2 H), 4.39 ppm (2 H), 5.36 ppm (1 H), 5.95 ppm (1 H), 7.44 ppm (1 H), 7.60 ppm (1 H), 7.78 ppm (1 H), 11.26 ppm (1 H).

P[(VC_{12}Im)(Cl)] was prepared by the radical polymerization of (VC_{12}Im)(Cl) (13.84 g, 46 mmoles) with 1 mole·AIBN/33 moles·(VC_{12}Im)(Cl) (0.23 g) in a 9:1 toluene:ethanol solution (50 ml). The mixture was stirred at 90 ^oC for 5 h under N_2, and was then cooled to rt. The polymer was recovered by precipitation from acetone (500 ml). The PIL was washed with acetone (500 ml) for 24 h, filtered and dried *in vacuo* (13.13 g, 95% yield). ^1H NMR ($CDCl_3$): ∂ 0.91 ppm (3 H), 1.29 ppm (18 H), 1.93 ppm (2 H), 2.29 ppm (2 H), 4.19 ppm (2 H), 4.88 ppm (1 H), 7.57 ppm (1 H), 8.37 ppm (1 H), 10.11 ppm (1 H).

2.1.3 P[(VC_{12}Im)(Cl)] Bead Processing

The glassy polymer was processed into workable particle sizes by dissolving P[(VC_{12}Im)(Cl)] (9.57 g) in a 9:1 ethanol:water solution (1.5 ml·solvent/1.0 g·polymer). The formed cement was extruded through a syringe in straight lines onto a teflon surface. The shaped polymer product was dried *in vacuo* and was broken into pieces. These pieces were washed twice with excess water, and were dried *in vacuo* (6.71 g, 70% yield).

2.1.4 Ion Exchange with $NaHCO_3$ (aq)

The bicarbonate salt was formed by the ion exchange of Cl^- for HCO_3^- between P[(VC_{12}Im)(Cl)] and $NaHCO_3$. The P[(VC_{12}Im)$(Cl)_x(HCO_3)_y$] equilibrium compositions at various moles·HCO_3^-/moles·Cl^- and various $[NaHCO_3]_0$ (M) were assessed by adding P[(VC_{12}Im)(Cl)] (0.10 g) at a phase fraction of 0.01 to $NaHCO_3$ (aq) for 24 h. The polymer was removed from the solution by vacuum filtration, was washed with water to remove residual base, and was dried *in vacuo*. The resulting P[(VC_{12}Im)$(Cl)_x(HCO_3)_y$] was immersed in 15 mM aqueous HCl solution (1.5 moles·HCl/1.0 mole·monomer) for 24 h. A few drops of phenolphthalein were added and the solution was titrated with 5 mM NaOH until it appeared a light pink. Reference solutions of equal quantities of 15 mM HCl solution were titrated with 5 mM NaOH solution until the solutions appeared a light pink. The references were used to measure the actual [NaOH] of the titrant. The average composition of three trials was reported for each tested $[NaHCO_3]$.

A large-scale ion exchange process was completed to synthesize the PIL that was used for acid chemisorptions throughout this thesis. P[(VC_{12}Im)(Cl)] (1.12 g, 4 mmoles Cl^-) was added to an aqueous solution of 0.50 M $NaHCO_3$ (6.30 g $NaHCO_3$; 75 mmoles $NaHCO_3$; F = 0.007). The mixture was lightly stirred for 48 h. The polymer was then removed from solution by vacuum filtration and was washed with water to remove residual base. The polymer was then dried *in vacuo*. A sample of material (0.20 g) was put into 15 mM aqueous HCl solution (1.5 moles·HCl/1.0·mole polymer) for 24 h. The remaining experiment was completed following the procedure of the equilibrium ion exchange experiments. One exchange was performed, and three titrations of the product of this exchange were completed. The average HCO_3^- composition of these three titrations was reported.

2.1.5 Physisorption Capacities

The physisorption capacities of PIL-Cl for SA (pH 3.0) and BA (pH 3.1) were measured at cumulative phase fractions in 2.5 g·acid/L solutions at 20 °C. The concentration at each phase fraction was measured after 24 h by ^{1}H NMR with a reference of citric acid (41 mg) for SA, and with UV-Vis spectroscopy (λ = 225 nm) for BA.

2.1.6 Chemisorption Capacities

The acid chemisorption capacities of $P[(VC_{12}Im)(Cl)_{0.40}(HCO_3)_{0.60}]$ (PIL-HCO_3) for SA and BA were measured by adding the PIL at 1 mole·HCO_3^-/1 mole·acid to 100 ml of 2.5 g·acid/L solution (20 °C). The solutions were then sparged with humid air for 48 h. The SA capacity was measured by integration of a ^{1}H NMR of the solution. The BA capacity was measured by UV-Vis spectroscopy. Three trials were completed for each acid. The average capacity was reported.

2.1.7 Organic Acid Titrations

Titrations of SA and BA solutions were done by adding cumulative phase fractions of PIL-HCO_3 to 100 ml of 2.5 g·acid/L solution (20 °C). The chemisorptions at each phase fraction were completed to equilibrium, whereupon the aqueous solution pH was measured. An initial assessment determined that the time to reach equilibrium with 1 mole·HCO_3^-/1 mole·acid (F = 0.01) in 2.5 g·acid/L solution was 8 h for SA and 12 h for BA. Two independent titrations were performed for each acid. The data from both titrations were overlayed to generate one titration curve for each acid.

2.1.8 PIL Water Absorption

The equilibrium water absorptions of $P[(VC_{12}Im)(Cl)]$, $P[(VC_{12}Im)(Cl)_{0.40}(HCO_3)_{0.60}]$ and $P[(VC_{12}Im)(Cl)_{0.40}(SA_1)_{0.53}(SA_2)_{0.07}]$ (PIL-SA) were measured by adding PIL (0.10 g) to DI water at a F = 0.01

for 24 h. The polymer was separated from the solution, and was blotted lightly to remove all residual surface water. The wet mass of the polymer was then measured. The reported data of each polymer is the average of three independent trials.

2.1.9 Ion Exchange of P[($VC_{12}Im$)(Cl)] with a Saturated H_2CO_3 Solution

A mixture of PIL-Cl (1.00 g) in DI water at a F = 0.007 was sealed in an autoclave and pressurized with 59 bar of CO_2 at 20 °C. After agitating the mixture gently for 24 h, the polymer was: a) isolated by vacuum filtration; b) washed with water; c) dried *in vacuo*. A sample of the material (0.20 g) was immersed into 15 mM aqueous HCl solution (1.5 mole·HCl/1.0 mole·polymer) for 24 h. The resulting solution was back-titrated with 5 mM NaOH to determine the residual HCO_3^- content of the PIL. The reported result is the average of three titrations that used polymer that had been obtained from two independent pressurization experiments.

2.1.10 SA Desorption with Dilute HCl (aq)

Succinic acid was extracted from dilute aqueous solution using the procedure that was described in Section 2.1.6. The resulting PIL was rinsed with water. The material was first immersed at a F = 0.019 in 0.6 M HCl for 24 h. After the desorption, there was very little unabsorbed water for measurement. A second experiment was conducted using a F = 0.01 in 0.3 M HCl (1.5 moles·HCl/1.0 mole·SA). These conditions provided two phases of a PIL and an aqueous phase. The concentration of SA in the solution was measured by ^1H NMR spectrum integration. One trial was completed for each set of conditions.

2.1.11 SA Desorption with Saturated H_2CO_3 (aq)

To recover SA using saturated H_2CO_3 (aq), PIL + DI water (F = 0.19) were added to an autoclave after SA was initially chemisorbed from 2.5 g·SA/L solution using the method that was described in Section 2.1.6. This recovery method attempted a one-step SA recovery and bicarbonate salt regeneration. The autoclave was pressurized with CO_2 to 59 bar and was agitated lightly for 24 h. After pressurization, the PIL was immediately removed from the solution. The concentration of SA in the aqueous phase was measured by ^{1}H NMR. The average result of three independent experiments was reported.

2.1.12 SA Desorption with Saturated $NaHCO_3$ (aq)

The one-step formation of sodium succinate and regeneration of the basic PIL was assessed by first extracting SA with the PIL with the procedure of Section 2.1.6. The resulting PIL was then washed with water and was charged directly to a saturated $NaHCO_3$ solution at a F = 0.19 for 24 h. The concentration of SA that was liberated into the aqueous phase was measured with ^{1}H NMR. The average concentration of three independent experiments was reported.

2.1.13 Analytical Methods

^{1}H NMR spectra of aqueous solutions that contained SA were acquired in MeOD with a 300 MHz Bruker Avance NMR spectrometer. ^{1}H NMR samples were prepared by adding 1 ml of reaction solution and an internal reference of citric acid (41 mg) to MeOD. Benzoic acid concentrations were measured with Ultraviolet-visible spectroscopy (Uv-vis). A Thermo Scientific Evolution 300 spectrometer was used to measure all Uv-vis spectra. The spectrometer was equipped with a Xenon lamp that operated between 190 - 400 nm. To measure the concentration of BA in a solution, one millilitre of the solution was added to 500 ml of DI water. The average absorbance at a λ = 225 nm of different samples of the 500 ml solution was used to calculate the concentration of BA with a calibration standard (Figure B.1). All of the pH values were measured with a Broadley James Fermprobe that was attached to an Expandable ionAnalyzer 920. The pH probe was calibrated with Metler Toledo calibration standards (pH 4.01, pH 10.01).

2.1.14 Error

All reported error was the population standard deviation of a triplicate data set. No error propagation was done. No instrumental error was included in the calculation of error.

2.2 Results and Discussion

2.2.1 P[(VC_{12}Im)(Cl)] Synthesis and Organic Acid Sorption Capacities

An imidazolium chloride-based PIL bearing saturated C_{12} side chains (P[(VC_{12}Im)(Cl)]) was prepared by radical polymerization of the vinyl monomer ((VC_{12}Im)(Cl)) according to the method of Alexiou et al. [1]. This procedure yields a linear chain architecture, with molecular weights exceeding the critical entanglement threshold. Since the pure PIL material is glassy at room temperature, the polymer was shaped into pellets for experiments. This required: a) dissolving the PIL in ethanol/water; b) extruding the formed cement through a syringe; c) drying the extruded strands under vacuum; d) breaking the resulting rods into pieces that had an average mass of 7.2 $\pm$ 0.7 mg.

Although P[(VC_{12}Im)(Cl)] is not a Bronsted base, it is capable of sequestering organic acids through physisorption [2], [3]. The equilibrium concentration of BA within an aqueous solution at various suspended phase fractions of P[(VC_{12}Im)(Cl)] is presented in Figure 2.1. A polymer phase fraction as small as 0.01 sorbed greater than 80% of the BA from the 2.5 g·BA/L solution. The partition coefficient values (PC = w^{PIL}_{BA} / w^{aq}_{BA}) varied from 274 to 623 over the studied range of phase fractions (0.002 - 0.01). It should be noted that the PC values of organic acids are generally pH-dependent. Therefore, there are marked differences between the activity coefficients of the conjugate acid and base forms of organic acids. In the experiments that were described in Figure 2.1, the aqueous solution pH observed was less than the pKa of BA, which resulted in a high proportion of conjugate acid [4].

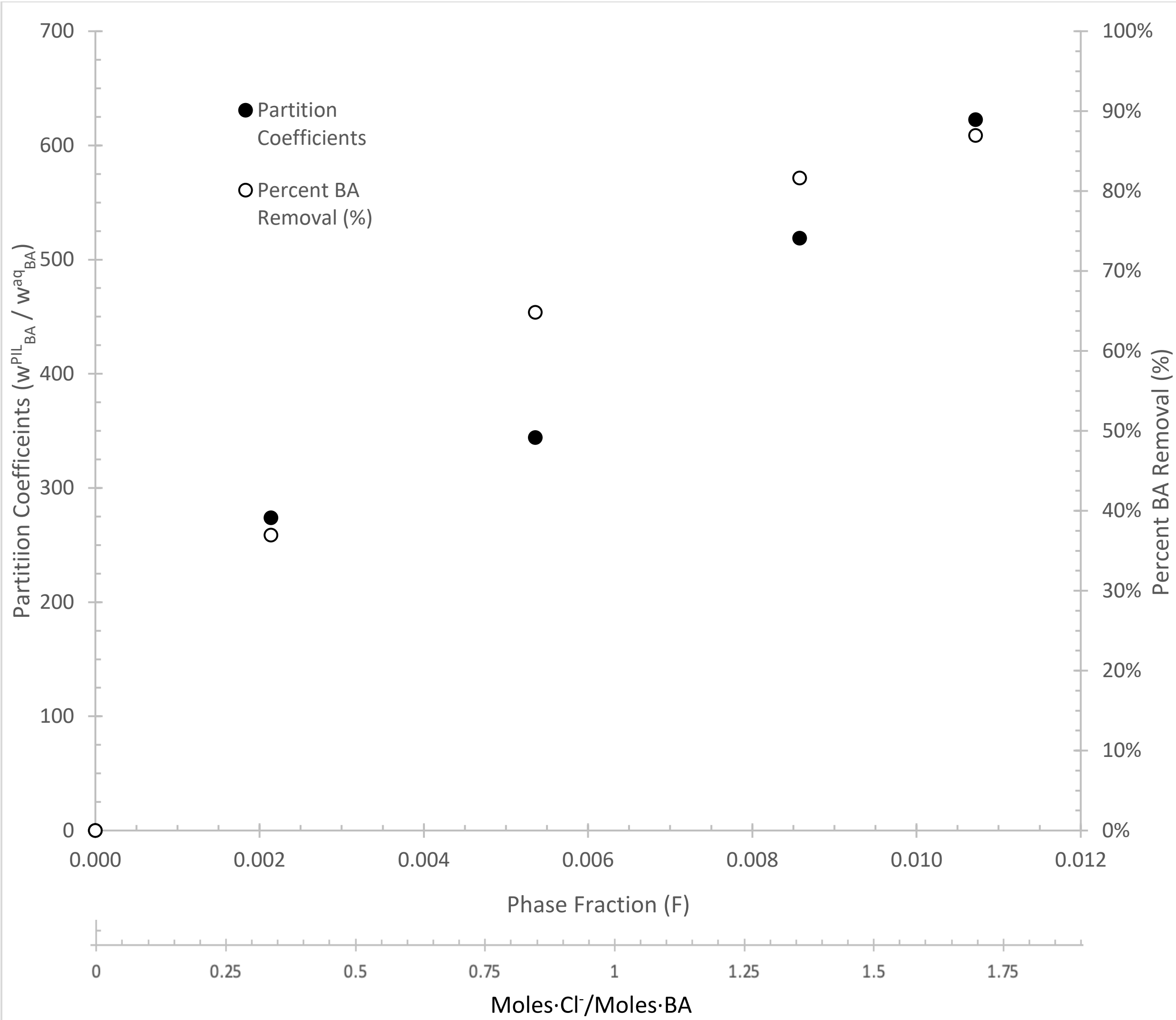

Figure 2.1. Physisorption of BA with P[(VC_{12}Im)(Cl)] in pH 3.1 Solution (2.5 g·BA/L, 20 °C).

The equilibrium distribution of BA between the polymer and aqueous phases of the described system is dictated by the thermodynamic activities within the respective phases [5]. The high PC values observed for P[(VC_{12}Im)(Cl)] + BA is consistent with the PC of n-octanol + BA ($PC_{octanol}$ = 74), and the relatively low solubility of BA in water (3.0 g/L at 20 °C) [6]. It is likely that interactions between the phenyl substituent of BA and the alkyl C_{12} of the PIL are responsible for this affinity. Regardless of the underlying cause, this degree of physisorption brings into question the need for a base-functionalized PIL to recover BA and potentially other hydrophobic organic acids from aqueous solution.

Succinic acid is more hydrophilic than BA (80 g/L in water at rt) [7]. This hydrophilicity is reflected by the relatively low partition coefficients recorded for the P[(VC_{12}Im)(Cl)] + SA system in 2.5 g·SA/L: PC = 35 at a F = 0.01, PC = 44 at a F = 0.04. At the phase fraction of 0.01, the PIL only removes 28% of the SA. This physisorption of SA with P[(VC_{12}Im)(Cl)] is less than a third of that of BA under identical conditions. The weak physisorption of P[(VC_{12}Im)(Cl)] for succinic acid warrants a basic PIL that can efficiently recover succinic acid from dilute aqueous solution.

2.2.2 Synthesis of P[(VC_{12}Im)$(Cl)_x$$(HCO_3)_y$]

The bicarbonate salt of P[(VC_{12}Im)$(Cl)_x$$(HCO_3)_y$] was formed by exchanging Cl^- from P[VC_{12}Im)(Cl)] for HCO_3^- from $NaHCO_3$ (aq) solution (Scheme 2.1). The synthesis and polymerization of (VC_{12}Im)$(Cl)_x$$(HCO_3)_y$ is an alternative synthetic route to form P[(VC_{12}Im)$(Cl)_x$$(HCO_3)_y$], however, the risk of bicarbonate decomposition at typical radical polymerization temperatures motivated the ion exchange of the PIL-chloride salt.

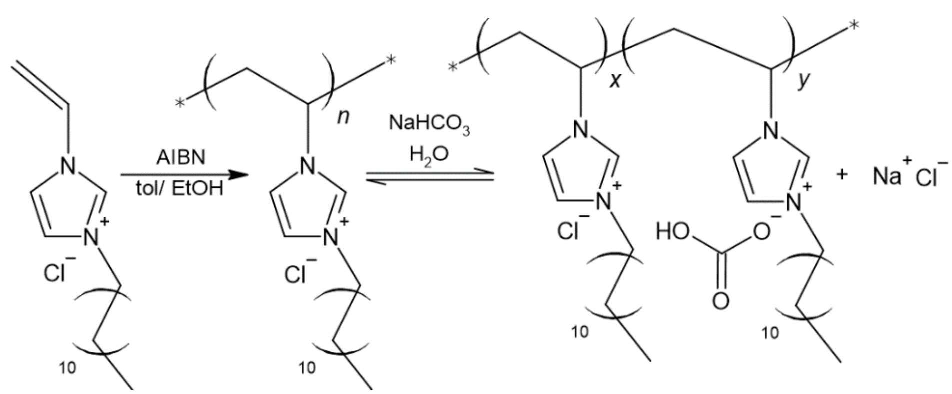

Scheme 2.1. Synthesis of P[(VC_{12}Im)$(Cl)_x$$(HCO_3)_y$].

Suspending P[(VC_{12}Im)(Cl)] at a polymer phase fraction of F = 0.01 in aqueous solutions of various [$NaHCO_3$] (M) produced P[(VC_{12}Im)$(Cl)_x$$(HCO_3)_y$] of varying compositions (Figure 2.2). The use of P[(VC_{12}Im)(Cl)] provided a consistent starting material for careful studies of phase equilibrium behaviour.

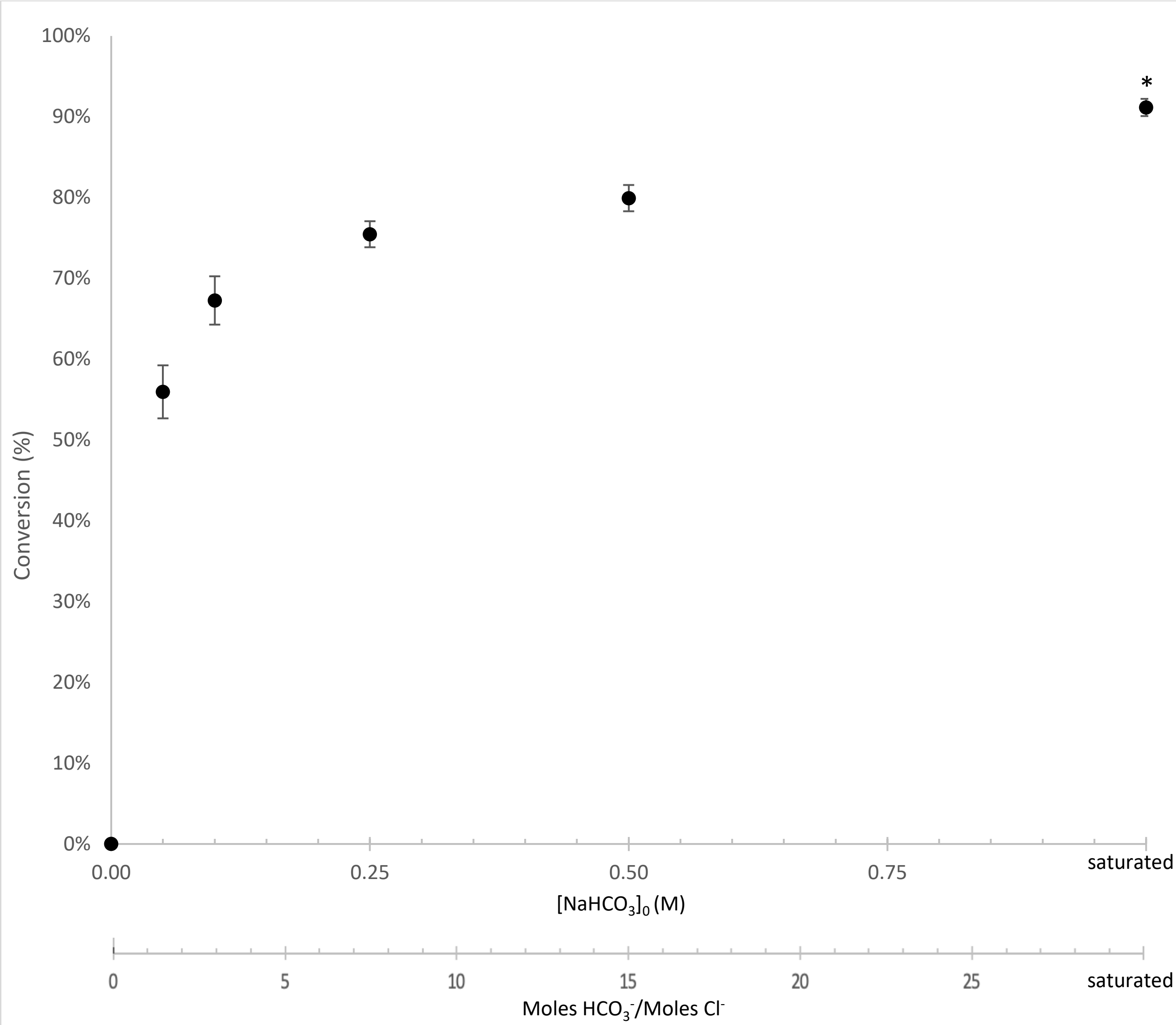

Figure 2.2. Anion Exchange of P[(VC_{12}Im)(Cl)] to P[(VC_{12}Im)$(Cl)_x(HCO_3)_y$] at Various Bicarbonate Ion Concentrations (20°C; F = 0.01; $[NaHCO_3]_0$ = 0.05 M – saturated*; Moles·HCO_3^-/Moles·Cl^- = 1.5 – sat.*).

The data plotted in Figure 2.2 shows that the complete displacement of chloride from the PIL is not achievable under the studied conditions. The highest conversion to HCO_3^- was 91 ± 1% in saturated $NaHCO_3$ solution (> 1 M). During this experiment, 30 moles·HCO_3^-/1 mole·Cl^- were consistently maintained in the aqueous phase. The equilibrium pH of the $NaHCO_3$ solution remained below 8.9 during all of the exchanges. This ensured that HCO_3^- was the predominate anion in the PIL in all of the exchanges over alternatives such as carbonate (Figure A.1) [8].

Ion exchanges at a F = 0.007 and at a F = 0.015 in 0.50 M $NaHCO_3$ (20 moles·HCO_3^-/1 mole·Cl^-; 10 moles·HCO_3^-/1 mole·Cl^-) gave HCO_3^- equilibrium compositions of 80 $\pm$ 1% and 63 $\pm$ 3%, respectively. These results show that increasing the F at a constant $[NaHCO_3]_0$ in the designed system lowers the HCO_3^- equilibrium composition of the PIL. The negligible increase of the HCO_3^- equilibrium composition of the PIL from a lowering of the F was likely a result of the lowered conversion efficiency at high moles·HCO_3^-/mole·Cl^-.

Large quantities of $P[(VC_{12}Im)(Cl)_{0.40}(HCO_3)_{0.60}]$ were produced with an exchange that ran for 48 hours at a F = 0.007. The final solution pH was less than 8.9. The synthesized $P[(VC_{12}Im)(Cl)_{0.40}(HCO_3)_{0.60}]$ product had 1.91 mmoles·HCO_3^-/1.00 g·polymer, and was used for all of the organic acid extraction studies in this work. The functional group content of $P[(VC_{12}Im)(Cl)_{0.40}(HCO_3)_{0.60}]$ was similar to that of our research group's previously developed $P[(VC_{12}Im)(Br)_{0.42}(OH)_{0.58}]$, which had 1.89 mmoles·$OH^-$/g·polymer [1].

The synthesis of the bicarbonate salt was also tested by adding $P[(VC_{12}Im)(Cl)]$ to water (F = 0.007), and pressurizing the system with a partial pressure of CO_2 of 59 bar. HCO_3^- was formed in solution as the conjugate base of H_2CO_3. The final PIL had a low HCO_3^- composition of 11 $\pm$ 2%. This low composition was expected, since the pKa_1 of H_2CO_3 in water is high at 6.36 [9], resulting in a low $[HCO_3^-]$ in solution. While higher P_{CO_2} could increase the extent of HCO_3^- exchange, equipment limitations precluded the testing of this hypothesis.

Although none of the various PIL salts in this thesis are water soluble, they do swell when placed in aqueous solutions. PIL-Cl absorbed 90 $\pm$ 5% of its mass when immersed in DI water at a F = 0.01. PIL-HCO_3 swelled by 76 $\pm$ 4% under these conditions. The sensitivity of swelling to counter ion structure is also observed when PIL-HCO_3 is equilibrated in 2.5 g·SA/L solution at a F = 0.01. The polymer mass increased by 100 $\pm$ 2% in this solution, with a shift of the anion composition in the polymer phase to a mixture of chloride, bicarbonate and succinate.

2.2.3 Acid Chemisorption Capacities of P[($VC_{12}Im$)(Cl)$_{0.40}$(HCO_3)$_{0.60}$]

The chemisorption of organic acids with P[($VC_{12}Im$)(Cl)$_{0.40}$(HCO_3)$_{0.60}$] are weak base/weak acid reactions that liberate CO_2 gas from the PIL phase. To assess the neutralization capacity of our PIL under typical extractive fermentation conditions, aqueous solutions containing 2.5 g/L of BA or SA were titrated with PIL-HCO_3 at rt. During the titrations, the solutions were continuously sparged with water-saturated air. The titration of BA was carried out to 1.5 moles·HCO_3^-/1.0 mole·BA, because BA is monoprotic. The diprotic nature of SA required its titrations to be carried out to 2.5 moles·HCO_3^-/1.0 mole·SA. The titrations of both acids are presented in Figure 2.3.

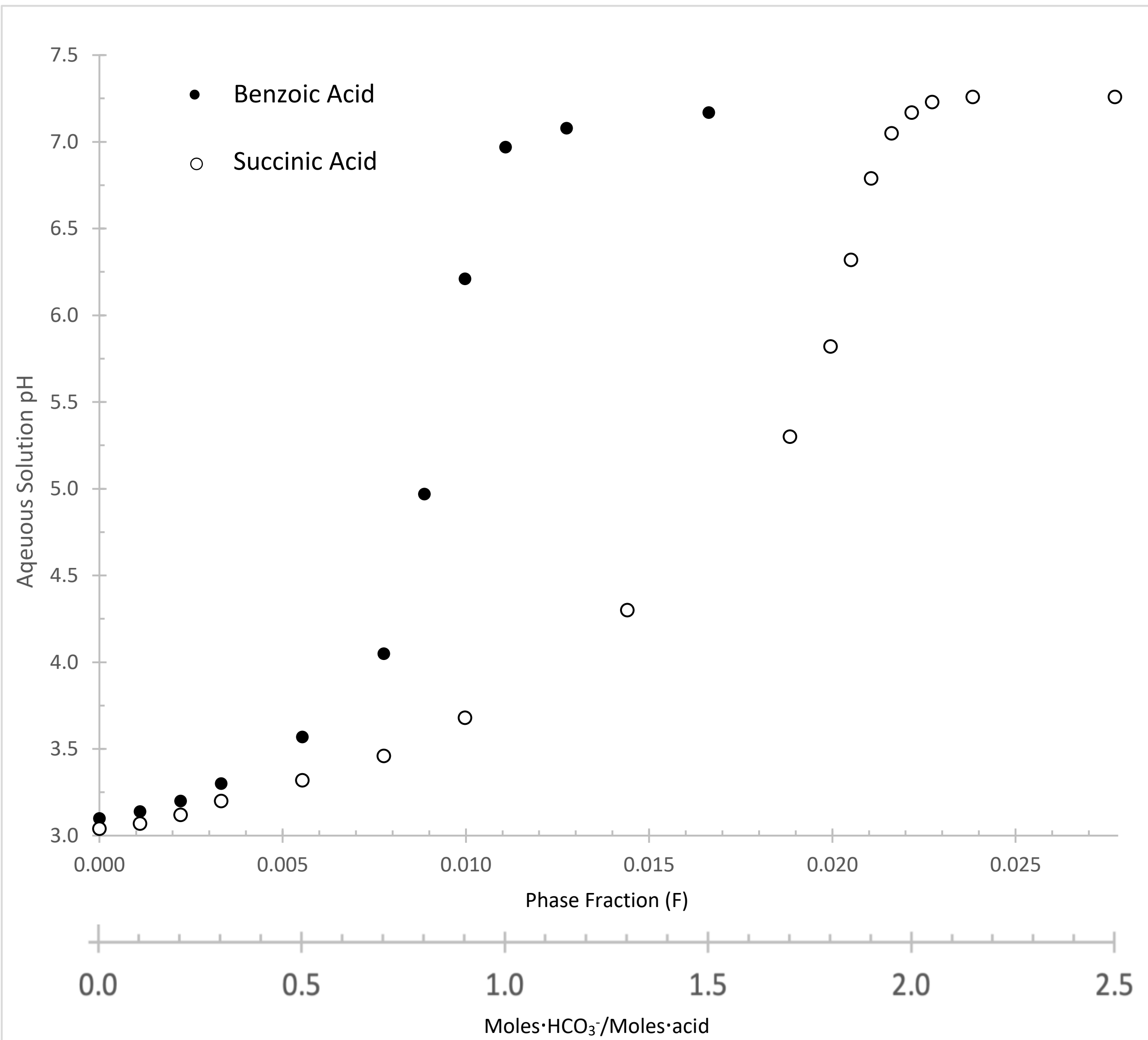

Figure 2.3. Titration Curves of SA and BA Using PIL-HCO_3 (2.5 g·acid/L, 20 °C).

The titration data of Figure 2.3 confirms that both organic acids are neutralized to pH 7.0 upon reaching a stoichiometric amount of base:acidic protons. The weak acid/weak base reactions proceed to completion due to the sparging of the system with air, which strips CO_2 from the system and drives the neutralization process forward.

The upper pH 7.2 boundary that is achieved with PIL-HCO_3 might help support an *in-situ* product removal fermentation process. This is because SA producing bacteria, such as *A. succinogenes* CGMCC1593, have stable SA production in the pH range of 6.0 – 7.2 [10]. The upper pH boundary, therefore, prevents excess bicarbonate from increasing the solution pH to cytotoxic levels. The strongly basic PIL-OH that was assessed in our group's previous work raised the acidic 2.5 g·SA/L solution pH past 8 with excess base. This created a cytotoxic solution, which would lower SA yields during fermentation [10]. This case reveals another advantage of the assessed PIL-HCO_3 over the previously studied PIL-OH.

The chemisorption capacity of PIL-HCO_3 at a standard system composition (F = 0.01, [SA] = 2.5 g/L) was measured for comparison with polymeric sorbents that are reported in literature. A SA capacity of 0.20 g·SA/g·polymer was achieved under these conditions. This PIL-HCO_3 sorbent is as potent as our group's previous PIL-OH sorbent (0.20 g·SA/g·polymer) [1], despite the relatively low basicity of the bicarbonate anion. **The hypothesis that PIL-HCO_3 is a competitive sorbent to the previously assessed PIL-OH is proven.**

The chemisorption efficiencies of PIL-HCO_3 in 2.5 g·acid/L solution at a F = 0.01 are 89% $\pm$ 2% for SA and approximately 100% (101% $\pm$ 1%) for BA. The $P[(VC_{12}Im)(Cl)_{0.40}(SA_1)_{0.53}(SA_2)_{0.07}]$ (PIL-SA) and $P[(VC_{12}Im)(Cl)_{0.40}(BA)_{0.60}]$ salts form from during these chemisorptions, respectively. The lower sorption efficiency for SA in comparison to BA is due to the partial neutralization of the second carboxylic acid group of SA. The similar pKas of the first deprotonation of SA and BA (4.2) allows for this estimation of the loss of efficiency [11], [12].

2.2.4 Succinic Acid Recovery and PIL Regeneration

Designing an SA recovery process with a polymeric sorbent requires the consideration of the sorption of the acid from fermentation broth, the desorption of the acid from the polymer, and the regeneration of the sorbent for subsequent reuse. Three methods of processing our polymer after the sorption of SA were examined from the perspective of a material balance (Scheme B.1).

2.2.4.1 Desorption by Acidification with Dilute HCl (aq)

One method of releasing succinate from PIL-SA involves acidifying the saturated polymer with HCl (aq) to produce aqueous SA solution + PIL-Cl. The latter is subsequently converted to PIL-HCO_3 through the anion exchange process described in Section 2.2.2. The volume of water should be minimized during desorption to produce high SA concentrations. Two volumes and concentrations of HCl were tested to assess an optimal desorption design.

The first experiment involves the use of a relatively high PIL-HCO_3 phase fraction of F = 0.19 in 0.6 M HCl (aq), which provides 1.5 moles·HCl/1.0 mole·SA. Unfortunately, the PIL completely absorbs the aqueous phase under these conditions. This absorption prevents the potential isolation of the organic acid from a fermentation broth. Lowering the phase fraction to 0.1 and adjusting the SA solution concentration to 0.3 M recovers SA more effectively. This second experiment produces an aqueous solution with an SA concentration of 10.8 g·SA/L, and releases 55% of the succinate ions from the PIL (Table 2.1).

Table 2.1 Desorption of Succinic Acid Using Various Recovery Methods.

Technology	Phase Fraction (F)	Recovered [SA] (g/L)	Acid Desorbed (%)
0.3 M HCl	0.11	10.8	55%
0.6 M HCl	0.19	No Separation	No Separation
Saturated $NaHCO_3$	0.19	23.5 ± 3.1	$66\% \pm 9\%$
Saturated H_2CO_3 (P_{CO_2}= 860 psi)	0.19	2.0 ± 0.4	$6\% \pm 1\%$

2.2.4.2 Desorption by Acidification with Saturated H_2CO_3 (aq)

The chemisorption of SA with PIL-HCO_3 (Section 2.2.3) was proven to be driven forward through the stripping of CO_2. Considering the aim of reversing this chemisorption, the deliberate pressurization of the system with CO_2 gas should drive the equilibrium in the reverse direction and desorb SA from the polymer. This approach combines SA recovery with sorbent regeneration (Scheme 2.2).

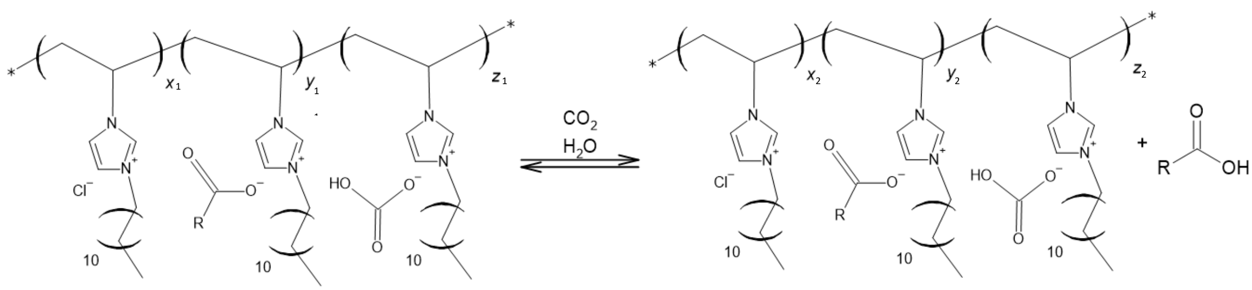

Scheme 2.2. Desorption of SA from PIL-SA using CO_2-Saturated Water.

The efficacy of this recovery was tested by immersing PIL-SA in water at a F = 0.19, and pressurizing the system with 59 bar of CO_2 gas. These conditions produce an aqueous phase with a [SA] = 2.0 ± 0.4 g·SA/L (Table 2.1). This translates to 6% of the maximum theoretical yield. Given that the solution pH is pressure dependent (Scheme 2.3) [13], [14], and that our system was limited to the vapour pressure of

CO_2 at rt, it is suspected that the performance would improve by operating the system at higher partial pressures.

$$CO_2\ (g) \rightleftharpoons CO_2\ (aq)$$

$$CO_2\ (aq) + H_2O\ (l) \rightleftharpoons H_2CO_3\ (aq)$$

$$H_2CO_3\ (aq) \rightleftharpoons H^+\ (aq) + HCO_3^-\ (aq)$$

$$HCO_3^-\ (aq) \rightleftharpoons H^+\ (aq) + {CO_3}^{2-}\ (aq)$$

Scheme 2.3. Equilibrium of CO_2 in Water [13].

2.2.4.3 Desorption with Saturated $NaHCO_3$ (aq)

The third SA recovery process tested in this study involved the direct exchange of succinate within PIL-SA with bicarbonate. Immersing PIL-SA in saturated $NaHCO_3$ (aq) solution at a F = 0.19 (2.6 moles·HCO_3^-/1 mole·SA) produced an aqueous phase with a succinate concentration of 23.5 $\pm$ 3.1 g/L (Table 2.1}. This recovery released 66% of the succinate ions from PIL-SA, and concentrated the initial 2.5 g·SA/L solution by a factor of 9.4. **The hypothesis that the regeneration of the PIL with saturated $NaHCO_3$ (aq) is effective is confirmed. Regeneration by pressurized CO_2 is not effective under the tested conditions.**

2.3 Conclusions

The potency of the assessed bicarbonate salt matches that of the previously researched hydroxide analogue, without suffering from the latter's chemical instability. The recovery of SA from the PIL by acidification with HCl suffers from excessive polymer swelling and modest desorption yields. The recovery of SA with CO_2 pressurization is inefficient at the pressures that are accessed in this study. Treatment of the chemisorbed polymer with saturated $NaHCO_3$ (aq) at the tested conditions is a relatively efficient isolation process that concentrates the target molecule by a factor of 9.4 from the initial dilute solution. There is the potential to optimize the recovery to further concentrate SA.

References

[1] J. Alexiou, R. Biro, A. Tremblay, A. Daugulis, and J. S. Parent, “Base-functionalized polymeric chemisorbents for succinic acid recovery from aqueous solution,” *React Funct Polym*, vol. 181, p. 105412, Dec. 2022, doi: 10.1016/J.REACTFUNCTPOLYM.2022.105412.

[2] K. R. Chaturvedi and T. Sharma, “Carbonated nanofluids for EOR and improved carbon storage,” *Nanotechnology for CO2 Utilization in Oilfield Applications*, pp. 71–84, Jan. 2022, doi: 10.1016/B978-0-323-90540-4.00011-9.

[3] H. Lin, S. Zhang, J. K. Sun, M. Antonietti, and J. Yuan, “Poly(ionic liquid)s with engineered nanopores for energy and environmental applications,” *Polymer (Guildf)*, vol. 202, p. 122640, Aug. 2020, doi: 10.1016/J.POLYMER.2020.122640.

[4] N. R. Ronco, L. G. Gagliardi, and C. B. Castells, “Aqueous-Organic Biphasic Systems: Extraction of Organic Compounds,” *Liquid-Phase Extraction*, pp. 91–119, Jan. 2020, doi: 10.1016/B978-0-12-816911-7.00003-7.

[5] D. H. Everett, “Reporting data on adsorption from solution at the solid/solution interface (Recommendations 1986),” *Pure and Applied Chemistry*, vol. 58, no. 7, pp. 967–984, Jan. 1986, doi: 10.1351/PAC198658070967.

[6] K. Jorge, “SOFT DRINKS | Chemical Composition,” *Encyclopedia of Food Sciences and Nutrition*, pp. 5346–5352, Jan. 2003, doi: 10.1016/B0-12-227055-X/01101-9.

[7] P. López-Porfiri, P. Gorgojo, and M. González-Miquel, “Solubility study and thermodynamic modelling of succinic acid and fumaric acid in bio-based solvents,” *J Mol Liq*, vol. 369, p. 120836, Jan. 2023, doi: 10.1016/J.MOLLIQ.2022.120836.

[8] M. H. Ghobadi, M. Firuzi, and E. Asghari-Kaljahi, “Relationships between geological formations and groundwater chemistry and their effects on the concrete lining of tunnels (case study: Tabriz metro line 2),” *Environ Earth Sci*, vol. 75, no. 12, pp. 1–14, Jun. 2016, doi: 10.1007/S12665-016-5785-0.

[9] X.-X. Wang *et al.*, “The comparison of pKa determination between carbonic acid and formic acid and its application to prediction of the hydration numbers,” 2008, doi: 10.1016/j.cplett.2008.05.074.

[10] Y. P. Liu, P. Zheng, Z. H. Sun, Y. Ni, J. J. Dong, and P. Wei, “Strategies of pH control and glucose-fed batch fermentation for production of succinic acid by Actinobacillus succinogenes CGMCC1593,” *Journal of Chemical Technology & Biotechnology*, vol. 83, no. 5, pp. 722–729, May 2008, doi: 10.1002/JCTB.1862.

[11] Z. Wang, H. Deng, X. Li, P. Ji, and J. P. Cheng, “Standard and absolute pKa scales of substituted benzoic acids in room temperature ionic liquids,” *Journal of Organic Chemistry*, vol. 78, no. 24, pp. 12487–12493, Dec. 2013, doi: 10.1021/JO4021858,

[12] P. Comuzzo and F. Battistutta, “Acidification and pH Control in Red Wines,” *Red Wine Technology*, pp. 17–34, Jan. 2019, doi: 10.1016/B978-0-12-814399-5.00002-5.

[13] M. J. Mitchell, O. E. Jensen, K. A. Cliffe, and M. M. Maroto-Valer, “A model of carbon dioxide dissolution and mineral carbonation kinetics,” *Proceedings of the Royal Society A: Mathematical, Physical and Engineering Sciences*, vol. 466, no. 2117, pp. 1265–1290, May 2010, doi: 10.1098/RSPA.2009.0349.

[14] R. K. Haghi, A. Chapoy, L. M. C. Peirera, J. Yang, and B. Tohidi, “pH of CO2 saturated water and CO2 saturated brines: Experimental measurements and modelling,” *International Journal of Greenhouse Gas Control*, vol. 66, pp. 190–203, Nov. 2017, doi: 10.1016/J.IJGGC.2017.10.001.

Chapter 3

The Strain-Sensitivity of Amine Functionalized Hydrogel Basicity and Its Application for the Recovery of Succinic Acid from Dilute Aqueous Solution

3.1 Experimental

3.1.1 Materials

N,N'-Dimethylethylenediamine (98%), tris(2-aminoethyl)amine (96%), acryloyl chloride (≥97%), propionyl chloride (98%), sodium hydroxide (≥97%), hydrochloric acid (37%), phenolphthalein, benzoic acid (≥99.5%), citric acid (≥99.5%), chloroform-D_3, methanol-D_4 (≥99.8 atom % D), 2,2'-azobis(2-methylpropionitirile) (AIBN) (98%), and 2,2'-azobis(2-methylpropionamidine)dihydrochloride (V50) (%) were used as received from Sigma-Aldrich (Canada). All organic solvents and succinic acid (≥99.5%) were used as received from Fisher Scientific (Canada).

3.1.2 DMEA, DMEP and TAAEA Synthesis

N,N-dimethylaminoethylacrylamide was prepared according to a method that was developed by Chang and McCormick [1]. This method was described in our research group's previous work [2]. The resulting yellow-orange oil of this method was further purified with normal-phase chromatography. Ethyl acetate was used as the eluent through the silica column; the final product was a yellow oil with an overall yield of 77%. ^{1}H NMR ($CDCl_3$): ∂ 2.19 ppm (1 H), ∂ 2.24 ppm (6 H), ∂ 2.45 ppm (2 H), ∂ 3.41 ppm (2 H), ∂ 5.62 ppm (1 H), ∂ 6.12 ppm (1 H), ∂ 6.29 ppm (1 H).

N,N-dimethylaminoethylpropanamide (DMEP) was prepared with the same procedure of DMEA, with a substitution of acryloyl chloride with 11.6 ml of propionyl chloride. This synthesis gave an overall yield of 74%. Tris[2-(acryloylamino)ethyl]amine was prepared by a method that was developed by Patras et al. [3]. This method was described in our research group's previous work (98% yield) [2]. **[DMEP]**: ^{1}H NMR ($CDCl_3$): ∂ 1.15 ppm (3 H), ∂ 2.04 ppm (1 H), ∂ 2.22 ppm (6 H), ∂ 2.41 ppm (2 H), ∂ 3.31 ppm (2 H),

∂ 6.08 ppm (1 H). **[TAAEA]**: ^{1}H NMR: ($CDCl_3$): ∂ 2.34 ppm (1 H), ∂ 2.59 ppm (6 H), ∂ 3.34 ppm (6H), ∂ 5.58 ppm (3 H), ∂ 6.24 ppm (6 H).

3.1.3 PDMEA and Hydrogel Synthesis

Poly(N,N-dimethylaminoethylacrylamide) (PDMEA) with a linear chain architecture was prepared in 95% yield using a method that was described in our group's previous work [2]. Crosslinked hydrogels containing 3.5%, 4%, 5%, 10%, 30% and 50% (wt%) of TAAEA content relative to DMEA provided a range of crosslink densities. All of the hydrogels were made in 1 g batches. The polymerization conditions of the hydrogels were: 80 ^oC, 1 mole·V50/20 moles·DMEA, 5 h. After synthesis, the hydrogels were swelled in DI water for 3 h, vacuum filtered, washed with water, and dried *in vacuo*. [PDMEA]: ^{1}H NMR ($CDCl_3$): 1.53 ppm (2 H), 1.80 ppm (1 H), 2.19 ppm (6 H), 2.76 ppm (2 H), 3.30 ppm (2 H), 3.97 ppm (1 H), 8.32 ppm (1 H).

To determine the conversion of DMEA to the polymer within the hydrogels, the initial mass of DMEA and TAAEA were assumed to remain in the system throughout the synthesis. Any additional measured mass was assumed to be from absorbed water. The mass of the swelled hydrogel after synthesis was measured. The composition of solid hydrogel was calculated. A sample of hydrogel (0.10 g DMEA) was added with 1 mole·tetrabutylammonium bromide (TBAB)/20 moles·DMEA to 1 ml water. The system was equilibrated for 3 h. MeOD was added. The solution was equilibrated for another 2 h, and the quantity of DMEA that was dissolved in the solution that surrounded the hydrogel was measured by ^{1}H NMR.

3.1.4 Hydrogel Swelling Ratios

The swelling ratios of fully swollen 3.5%, 5%, 10%, 30% and 50% hydrogels were measured at a F = 0.01 in three solutions: water (pH 7.0), an aqueous solution containing 2.5 g·SA/L (pH 3.0), and an aqueous solution containing HCl (pH 3.0). In each experiment, dry hydrogel (0.05 g) was immersed in 5 ml of solution for 24 h at 25 ^oC. The swollen hydrogel was isolated and the excess surface moisture was removed by light blotting with paper towel. Measurements of the swelling ratio = (swollen mass – dry mass)/dry mass are reported as the average of triplicate experiments.

3.1.5 Titrations of Organic Acid Solution

The titrations of 2.5 g·BA/L solution were performed by adding incremental quantities of DMEP, PDMEA or hydrogel to an approximate ratio of 1.5 moles·amine/1.0 mole·BA. The system was allowed to equilibrate after each addition, prior to measuring the pH of the solution. DMEP reached equilibrium instantaneously upon its addition to solution. PDMEA took up to 45 minutes to fully dissolve into the aqueous solution. Dry hydrogel took 12 h to reach equilibrium. Two independent titrations were completed for each material. The resulting data was overlayed to produce one titration curve for each material.

3.1.6 Hydrogel Sorption Capacities

3.1.6.1 Unconfined SA Sorption Capacity

The SA sorption capacities of the 5%, 10%, 30% and 50% hydrogels were measured at a polymer phase fraction of F = 0.01 in 5 ml of a 2.5 g·SA/L solution (3.0 moles·amine/1.0 mole·SA) for 24 h. An aliquot of the solution was analyzed by ^{1}H-NMR to determine each material's sorption capacity. The sorption capacities were reported as the average of three independent trials.

Back titrations were completed to measure the chemisorption capacities of the 3.5% and 4.0% hydrogels. The titrations were completed by adding hydrogel at a F = 0.01 (3.0 moles·amine/1.0 mole·SA) to 25 ml of a 2.5 g·SA/L solution for 24 h (25 ^oC). Swelled hydrogel was then added at masses of 2 g (3.5 %) or 1 g (4%) to 15 mM HCl solution (pH 2.2) at 5.0 moles·Cl^-/1.0 mole·amine. After 24 h, the pH of the aqueous solution was measured. The solution was titrated with 15 mM NaOH until the hydrogel collapsed (pH 10.0 or 10.5). Reference solutions of equal quantities of 15 mM HCl solution were also titrated with 15 mM NaOH solution. The reference titrations were done by titrating the HCl solutions to pH 7.0, and then to pH 10.0 or pH 10.5. The titration to pH 7.0 was done to calculate the actual [NaOH] of the titrant. One back titration of each of the 3.5% and 4% hydrogels was done.

3.1.6.2 Strained SA Sorption Capacity

Swollen hydrogels were subjected to mechanical strain by a custom-made aluminum syringe. The engineering strain is defined as the change cylinder length/original cylinder length throughout this work. To apply strain to the hydrogels, the syringe was pressed with sufficient pressure to displace liquid from the hydrogels through a polymer membrane. Unfortunately, the expelled liquid could not be recovered reliably due to its adhesion with the metal and absorption by the membranes. To assess the mass of water and SA that had displaced, a material balance was performed on the hydrogel before and after the application of strain. To measure the quantity of acid that was remaining in the hydrogel after the imposition of strain, back titrations were used. The quantity of water that had been displaced from the hydrogel after the application of strain was assessed by measuring the mass of the hydrogel. The measurements of the mass of released SA and water were used to calculate the concentrations of SA in the released solutions.

The SA sorption capacities of the 4% hydrogel at various strains were measured by loading 1 g of swelled hydrogel from the 25 ml experiment of Section 3.1.6.1 into the syringe. An apparatus of the syringe is provided in this section to aid the understanding of the strain experiments. Within the syringe, the cylinder length with the membranes + metal sieve is referred to as L_{Ref} (Scheme 3.1a). The length of the fully swollen hydrogel + membranes + metal sieve is referred to as L_0 (Scheme 3.1b). These two variables are used to calculate the initial length of the hydrogel in the syringe (Equation 1). The length in the cylinder that the hydrogel needs to reach to achieve the designed strain (L_ε) is calculated from Equation 2. The hydrogel was pressed manually to all of the designed strains within one hour. The pressure that was required to displace solution from the hydrogel increased with strain. After the syringe reached L_ε, the hydrogel was removed from the device. The thin layer of hydrogel between the metal sieve and the membranes was discarded. The sorption capacities were measured with back titrations, with the procedure that was outlined in Section 3.1.6.1. The swelling ratio of strained hydrogel was measured by directly measuring its mass after its removal from the syringe. Two experiments were done for each tested strain and the average values of the sorption capacities and swelling ratios were reported.

$$L_{FullySwollen} = L_0 - L_{Ref} \tag{1}$$

$$L_{\varepsilon} = L_{Ref} + (1 - \varepsilon) * L_{FullySwollen} \tag{2}$$

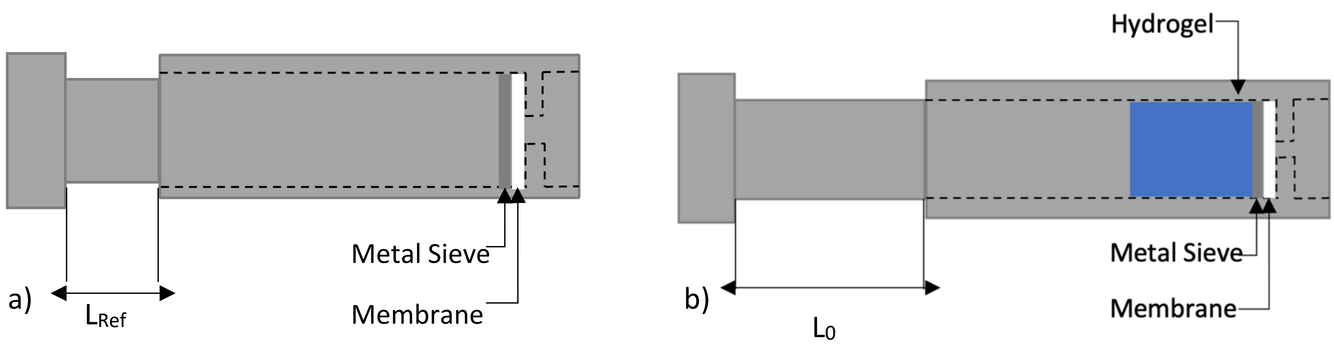

Scheme 3.1. Schematic of Syringe: a) L_{Ref}; b) L_0.

It was necessary for the hydrogel to collapse for chemisorbed succinic acid to release into solution. The collapse of the hydrogel occurred at a solution pH of either 10.0 or 10.5. The pH to collapse lowered when the mechanical strength of the hydrogel lowered; the mechanical strength lowered at higher strains.

3.1.7 Analytical Methods

^{1}H-NMR spectra of SA solutions were acquired in MeOD with a 300 MHz Bruker Avance NMR spectrometer. Citric acid (41 mg) was used as an internal reference for spectrum peak integrations. Differential scanning calorimetry (DSC) measurements were conducted using a TA instruments Q100 differential scanning calorimeter that was equipped with a RCS-90 cooling unit. A known mass of dried hydrogel (5-15 mg) was hermetically sealed in an aluminum pan. The measurements were carried out with 3 cycles from 0 to 180 °C: 1.1) heating at a rate of 10 °C/min; 1.2) isothermal for 5 minutes; 2.1) cooling at a rate of 10 °C/min; 2.2) isothermal for 5 minutes; 3) heating at a rate of 10 °C/min. Nitrogen gas was fluxed at 50 ml/min during all DSC scans. Solution pH measurements were done with a Broadley James Fermprobe that was attached to an Expandable ionAnalyzer 920. The pH probe was calibrated using Metler Toledo calibration solutions (pH 4.01, pH 10.01).

3.1.8 Error

Measurement errors are reported as the standard deviation of duplicate or triplicate data sets. No error propagation was completed. Instrumental error was not considered in the calculation of error.

3.2 Results and Discussion

3.2.1 Hydrogel Synthesis and Physical Characterization

Our group has previously described the synthesis of a DMEA + TAAEA hydrogel in toluene, using azobisisobutyronitrile (AIBN) as a radical initiator [2]. These conditions result in the precipitation of polymer from solution, leading to a hydrogel that has a non-uniform crosslink density. An image of this material is provided in Figure 3.1a. The regions of high monomer density (yellow) and high crosslink density (white) are observable.

a) b)

Figure 3.1. 30% Hydrogel Synthesized Using Different Solvents: a) Toluene; b) Water.

Avoiding precipitation required a switch of the reaction solvent from toluene to water. Water dissolves both monomers and the polymer; this miscibility allows the reactants to react uniformly throughout the hydrogel. An additional benefit of substituting toluene with water is that a teratogenic organic solvent is removed, lessening the environmental impact of the procedure. The revised process also required a switch from AIBN to a water soluble initiator, such as 2,2'-azobis(2-methylpropionamidine)dihydrochloride (V50). The formed hydrogel had a more uniform colour than the previous hydrogel (Figure 3.1b). Following this success, hydrogels of various crosslink densities were prepared using different mass ratios of DMEA:TAAEA (Table 3.1). These polymerizations provided high DMEA conversions. All of the hydrogels that are synthesized in this work are presented in Figure 3.2.

Table 3.1 Hydrogel Formulations.

Target Weight Fraction (wt% TAAEA)	Mass DMEA (g)	Mass TAAEA (g)	Mass V50 (g)	V_{Water} (ml)	DMEA Conversion (%)	Actual Weight Fraction (wt% TAAEA)	Glass Transition Temperature (°C)
3.5%	0.965 g	0.035 g	0.09 g	6 ml	88%	4.1%	109
4.0%	0.960 g	0.040 g	0.09 g	6 ml	85%	4.7%	116
5.0%	0.950 g	0.050 g	0.09 g	6 ml	87%	5.7%	118
10.0%	0.900 g	0.100 g	0.09 g	4 ml	95%	10.0%	123
30.0%	0.700 g	0.300 g	0.07 g	2 ml	98%	30.0%	138
50.0%	0.500 g	0.500 g	0.05 g	2 ml	99%	50.0%	Unobserved

a) b) c) d) e) f)

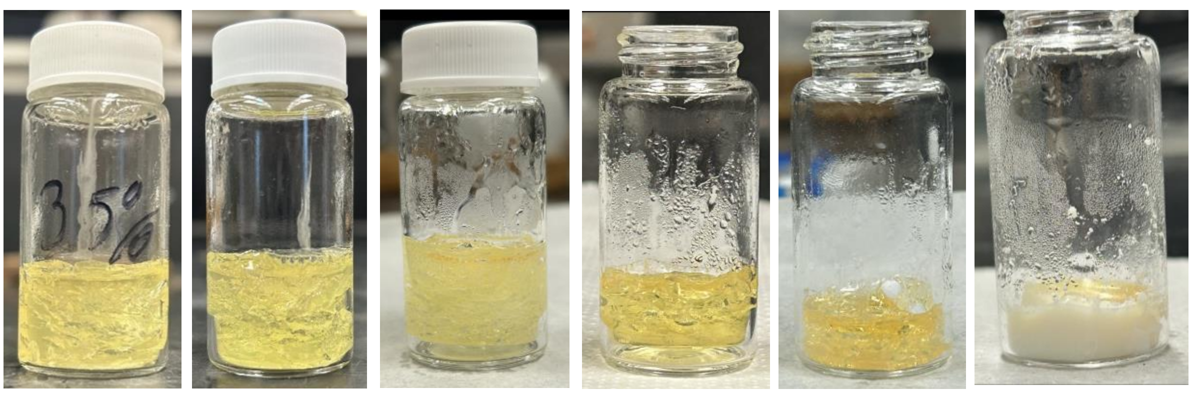

Figure 3.2. Hydrogels After Synthesis: a) 3.5%; b) 4%; c) 5%; d) 10%; e) 30%; f) 50%.

The glass transition temperature (T_g) of each hydrogel in its dry state was determined by differential scanning calorimetry. An upper limit of 180 °C on all DSC scans was imposed by the decomposition of PDMEA at 190 °C (Figure B.2). The tri-functional monomer content of the polymer had a pronounced effect on its chain segment mobility in the dry state; small quantities resulted in significant increases of the Tg from linear PDMEA (T_g = 65 °C) (Table 3.1). This finding is consistent with the reporting of Zarzyka et al., who found that increasing the crosslink density of PNIPA-based hydrogels raised their Tg and broadened their glass transitions [4]. The glass transitions of our hydrogels also broadened at higher CDs (Figure B.3). The 50% hydrogel did not produce a visible T_g under the analysis conditions due to excessive peak broadening.

The effect of crosslink density on hydrogel swelling is illustrated in Figure 3.3. To acquire the data of Figure 3.3, hydrogel was swelled in water (pH 7.0), aqueous SA solution (pH 3.0), or aqueous HCl solution (pH 3.0). The data reveals that there is an inverse relationship between swelling ratio and the material's TAAEA content. This relation is derived from the crosslinked network architecture of the hydrogel, which prevents its dissolution in water. The prevention of the hydrogel's dissolution by crosslinking causes its equilibrium swelling ratio to be governed by a balance of the entropy-driven process for solvating the polymer, and the entropy-driven elasticity of network chain segments. Higher crosslinking causes the polymer chains to be more severely restricted in solution. This additionally lowers the swelling ratio of the hydrogel. The swelling reaches a minimum in all solutions above a 30% TAAEA composition.

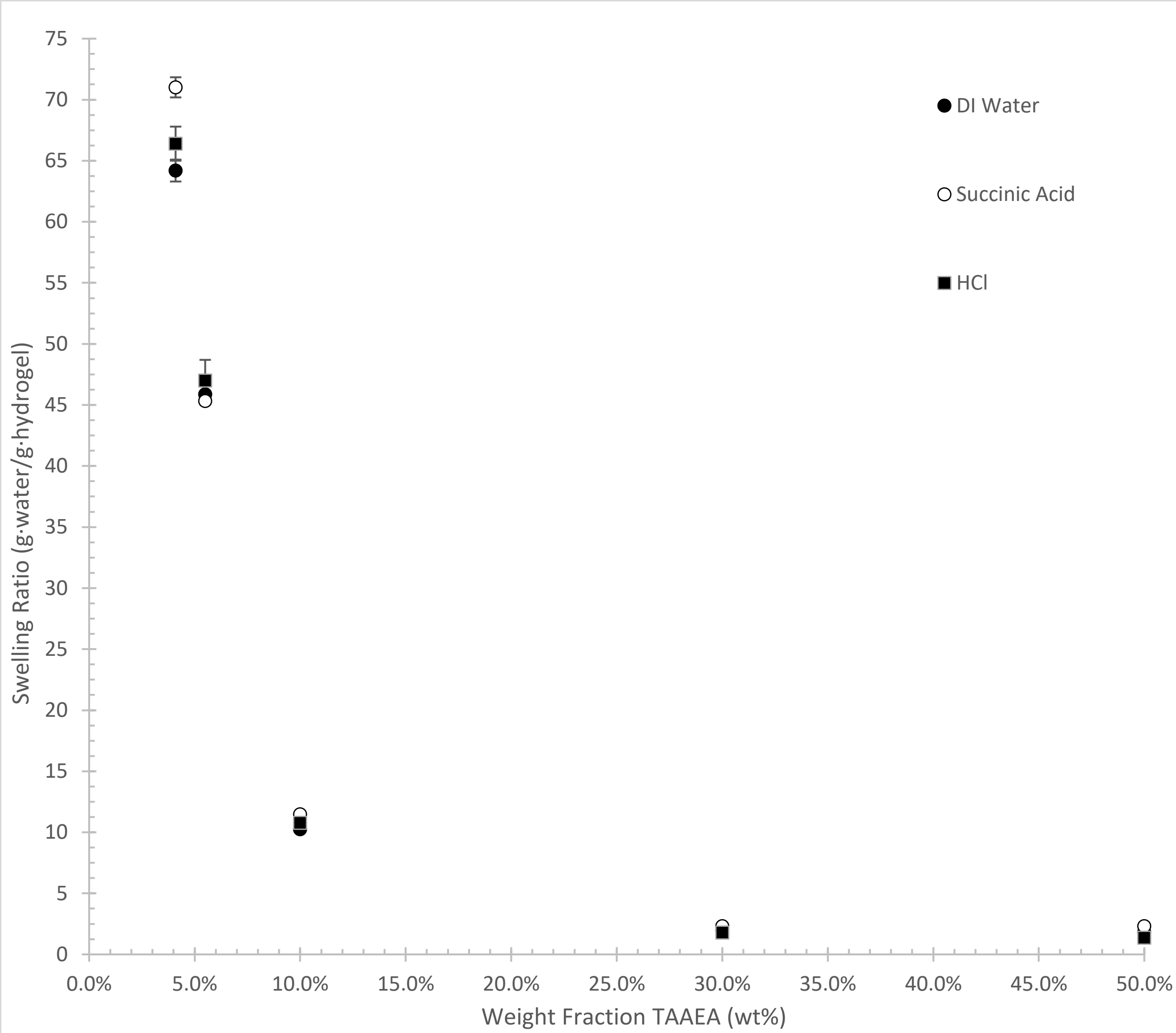

Figure 3.3 Swelling Ratio of the Hydrogels of Varying TAAEA Weight Fractions at a F = 0.01 in Water (pH 7.0), 2.5 g·SA/L Solution (pH 3.0) and HCl Solution (pH 3.0) (25 ºC).

The differences of the swelling ratios of the hydrogels amongst the three solutions are the most pronounced at low crosslink densities. The swelling of the 3.5% hydrogel is the smallest in pH 7.0 water (64.2 $\pm$ 2.7 g·water/g·hydrogel). This result is expected, since the neutral solution pH results in the lowest conversion of amine to the ammonium salt. This is followed by less swelling from the electrostatic repulsion of the ammonium salts. The swelling increases slightly in HCl solution to give a chloride salt that has a swelling ratio of 66.4 $\pm$ 1.4 g·water/g·hydrogel. The swelling ratio of the 3.5%

hydrogel is the highest in 2.5 g·SA/L solution; the succinate salt forms with a swelling ratio of 71.0 $\pm$ 3.1 g·water/g·hydrogel. It is unknown if the swelling differences of the 3.5% hydrogel within the different solutions of identical initial pH (pH 3.0) are from different conversion ratios to the ammonium salt, or different screening effects from the different anions. Both of these result in different electrostatic repulsions of the ammonium salts. All of the hydrogels swelled in water (pH 7.0) are presented in Figure 3.4.

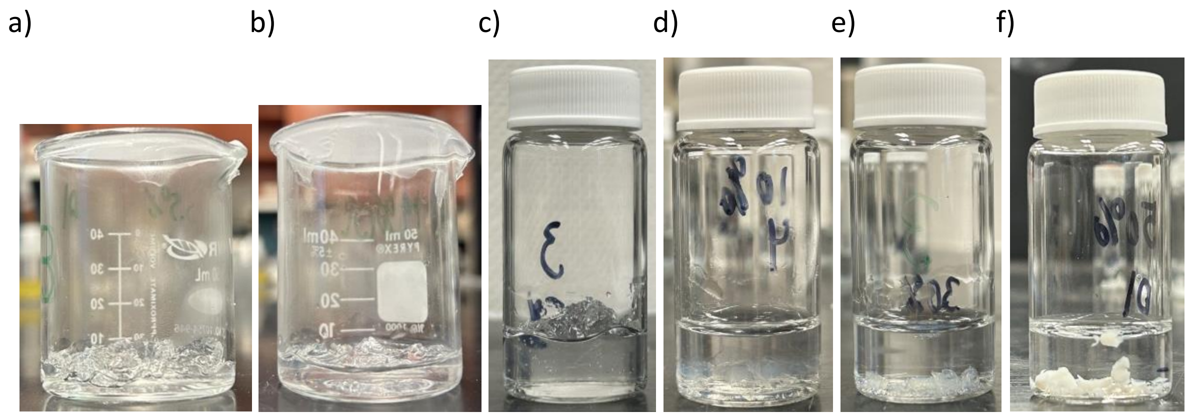

Figure 3.4. Hydrogels of Various TAAEA Weight Fractions (wt%) Swelled at Equilibrium in Water (pH 7.0) at a F = 0.01 (25 ^{o}C): a) 3.5%; b) 4% c) 5% d) 10%; e) 30%; f) 50%.

3.2.2 Crosslink Density and Basicity

The basicity of the tertiary amine within DMEP, linear PDMEA, and the hydrogels of various TAAEA weight fractions was studied to determine how its confinement in solution affected its reactivity with weak organic acid. Initial studies focused on the neutralization of BA (aq) solutions. This weak acid/weak base reaction proceeded very rapidly with DMEP (not shown), since the proton exchange to give an ammonium benzoate salt was instantaneous. The water-soluble polymer of PDMEA reacted quickly with BA upon dissolving in solution. The neutralization of BA occurred considerably more slowly when interphase mass transfer was influential [5]. The BA solution took 12 h to reach equilibrium with the solid-phase hydrogels due to mass transfer (Figure 3.5).

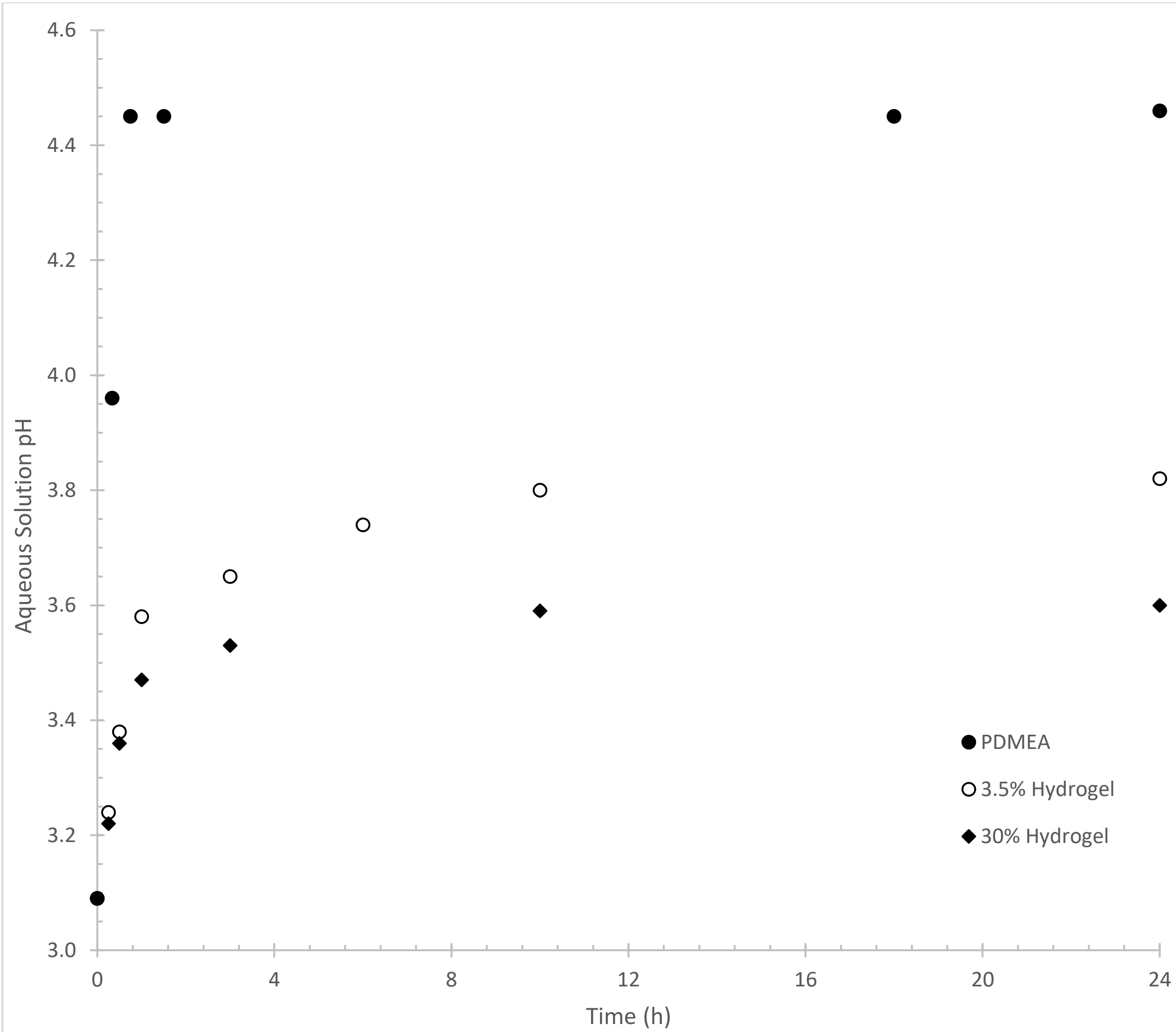

Figure 3.5. Chemisorption Dynamics of Benzoic Acid Using PDMEA and the 3.5% and 30% Hydrogels at Approximately 1.0 mole·amine/1.0 mole·BA (2.5 g·BA/L, 25 °C).

The data plotted in Figure 3.5 also reveals that the neutralization of BA reaches different extents with the different materials. The equilibrium pH of linear PDMEA was higher than that of the hydrogel materials. This result indicates that the basicity of the amine substantially reduces when it is crosslinked. This trend is supported with the data that is plotted in Figure 3.6. This data illustrates the equilibrium pH of the different materials at various amine loadings. These titration curves were acquired by incrementally adding base to a 2.5 g·BA/L solution. A cumulative ratio of 1.5 moles·amine/1.0 mole·BA was reached with all of the materials.

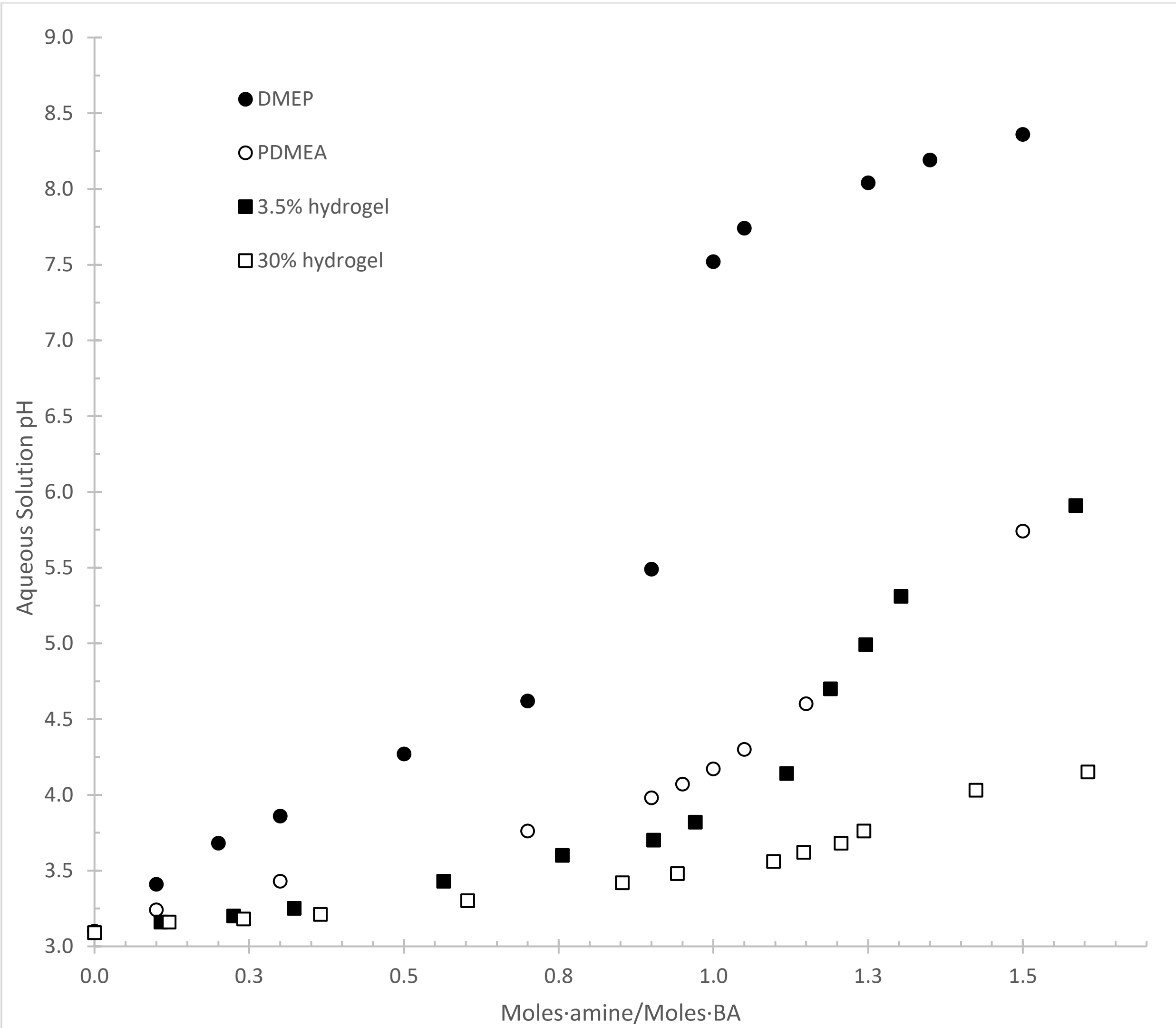

Figure 3.6. BA Solution Titrations with Various 3° Amine Containing Materials (2.5 g·BA/L, 25 °C).

Within Figure 3.6, the amine group basicity had the largest difference between DMEP and the other materials. The confinement that is imposed by covalently binding the amine to itself and the crosslinker raises the thermodynamic activity of the ammonium carboxylate salt. This rise reduces the total amount of ammonium carboxylate salt that is formed.

The performance of PDMEA and the 3.5% hydrogel are comparable throughout most of the titration. However, the highly crosslinked 30% hydrogel is considerably less basic than these materials. This hydrogel reaches an equilibrium pH of 4.2 at the highest polymer loading. This low pH is a result of the restriction of the polymer chain mobility and the associated high activity of the pendant functional groups. **The hypothesis that the basicity of our hydrogel is sensitive to crosslink density is proven.**

The thermodynamic capacities of the hydrogels for SA are listed in Table 3.2. These capacities were measured in 2.5 g·SA/L solution at a phase fraction of F = 0.01. This data shows that there is a decline in SA neutralization with increasing crosslink density; this result is consistent with the conclusions of the BA titration data.

Table 3.2 Sorption Capacities of Hydrogels of Various TAAEA Weight Fractions at 3.0 moles·amine/1.0 mole·SA (F = 0.01) in 2.5 g·SA/L Solution (25 ^{o}C).

TAAEA Weight Fraction (wt%)	Functional Group Content (mmoles·amine/g·hydrogel)	Average Capacity (g·SA/g·hydrogel)	pH
5%	6.8	0.249 ± 0.004	5.7
10%	6.7	0.247 ± 0.004	5.0
30%	5.9	0.217 ± 0.002	4.1
50%	5.1	0.177 ± 0.004	3.7

3.2.3 Strain Sensitivity of Hydrogel Basicity

The proven inverse relationship between basicity and functional group confinement led to the development of a novel process for isolating organic acids from dilute aqueous solution. This recovery uses pressure to displace aqueous solution from the hydrogels through a screen/membrane. The process involves: a) chemisorbing acid from aqueous solution using a hydrogel; b) physically isolating the saturated hydrogel; c) imposing strain-on the hydrogel to release a concentrated acid solution.

This researched pressure-swing recovery process is different than the conventional use of temperature or pH swings. The confinement that is imposed by strain is expected to destabilize the hydrogel's ammonium carboxylate functionality. This releases the organic acid, effectively recovering it from aqueous solution.

The swollen hydrogel acted as an incompressible fluid at the conditions of this study. An experiment was designed that supported the theory of the hydrogel's incompressibility. The hydrogel was uniformly pressurized with gas in an autoclave. This test failed to expel any liquid. Through iterations, it was found that: a pressure gradient was required to displace aqueous solution from the material; water had to be displaced to compress and apply strain to the hydrogel. We achieved the gradient using an aluminum syringe that was capable of compressing the hydrogel in the direction of the cylinder axis. The syringe was equipped with a water-permeable membrane whose effluent side remained at atmospheric pressure. This apparatus allowed aqueous solution to be discharged from the hydrogel if enough pressure was applied to overcome the hydrogel's swelling pressure [6], [7].

Although the relationship between swelling pressure and the swelling ratio of our hydrogels is not a principal interest of this research, the relationship is relevant to the organic acid recovery process under development. Arens et al. help explain this relationship through the development of an osmotic engine. This group reports that the various neutralizations of a poly(acrylic acid) hydrogel changes its swelling ratio, and subsequently varies the forces that develop against the external load of the osmotic engine. This group found that: a) higher forces develop at higher swelling pressures; b) swelling pressures increase at lower swelling ratios [8]. These results are important, since they support our observation that increased pressures are required to displace water at higher strains.

The crosslink density of a hydrogel is a key design consideration for a pressure-based acid recovery process. The crosslink density dictates a hydrogel's equilibrium swelling ratio and its basicity, as discussed prior. These considerations contribute to the swelling pressure of the hydrogel and the SA concentration of the released solution after the application of strain. When an excessively low crosslink density hydrogel is placed in aqueous solution, a space-filling gel is yielded since the material takes up high quantities of aqueous solution. The high-water composition of the hydrogel then results in a dilute solution being released when the hydrogel is pressed. On the other hand, an excessively high crosslink density hydrogel that is placed in aqueous solution becomes a marginally swollen hydrogel that requires high pressures to impose significant strains. Throughout data collection, it was found that hydrogels that required less pressure to impose significant strains allowed for less strenuous experiments and a more consistent data collection. A series of trial-and-error experiments had settled on a copolymer formulation containing 4 wt% TAEAA to present the pressure-swing process. When this 4% hydrogel was immersed in 2.5 g·SA/L solution at a F = 0.01 (3.0 moles·amine/1.0 mole·SA), the material absorbed about one-half of the solution to give a swelling ratio of 59.6 $\pm$ 1.7 g·water/g·hydrogel. Further optimization of the hydrogel and the separation conditions are expected to improve this SA recovery.

The strain-induced recovery of organic acid from this swollen hydrogel was tested by pressing hydrogel within the syringe to engineering strain targets (Δlength / original length) of 0.20, 0.40, 0.60 and 0.80. Since the hydrogel is incompressible at the pressures of this work, the swelling ratio decreases linearly with applied strain, and the volume of aqueous solution that displaces from the material is approximately equal to the change of the system volume. The data that is plotted in Figure 3.7 illustrates this trend. The plot shows a decline of the swelling ratio from 57.6 g·water/g·hydrogel in the unconfined state to 37.5 g·water/g·hydrogel at a strain of 0.40, and 20.4 g·water/g·hydrogel at a strain of 0.80.

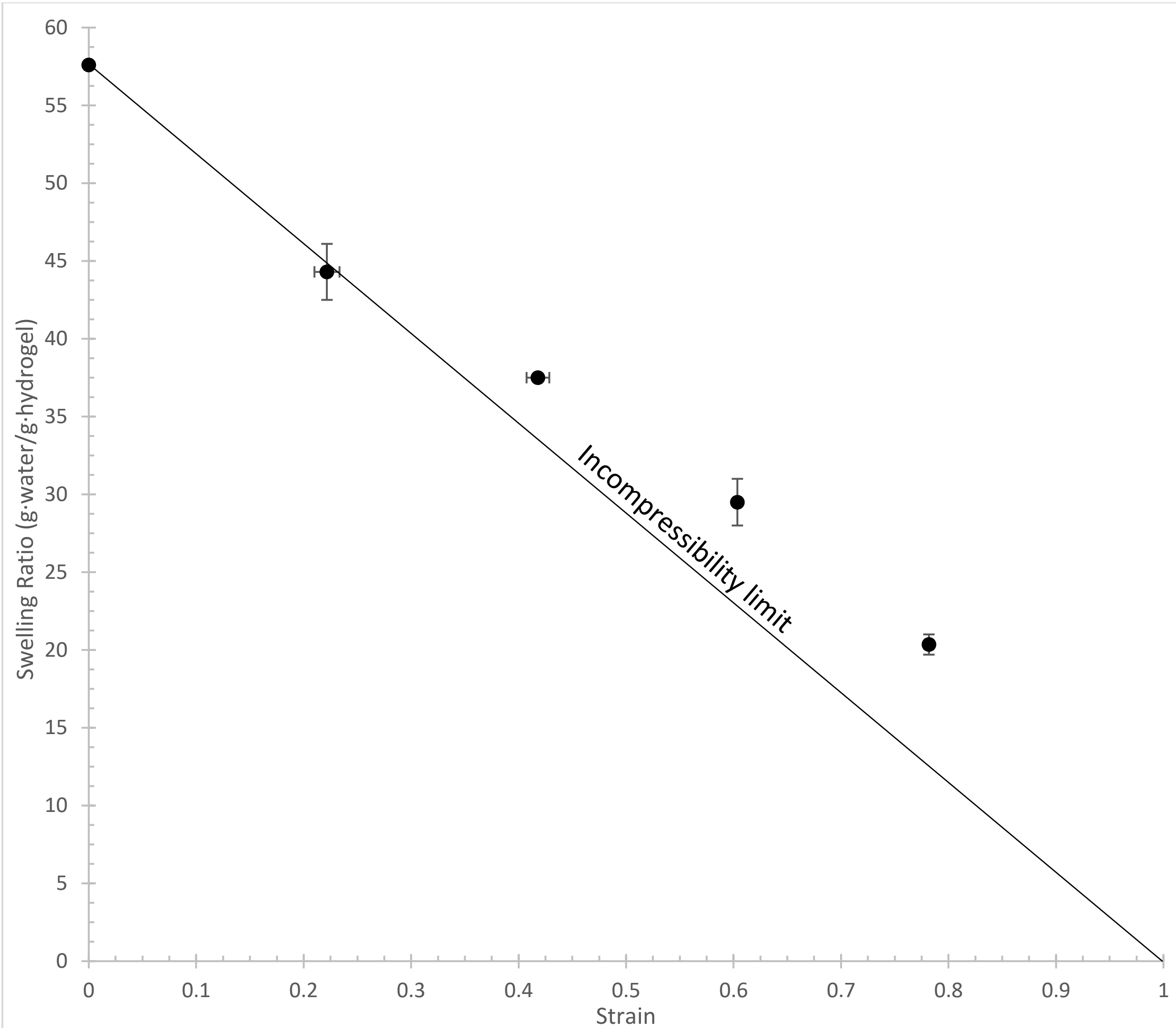

Figure 3.7. Swelling Ratio of the 4% Hydrogel at Various Strains (25 °C).

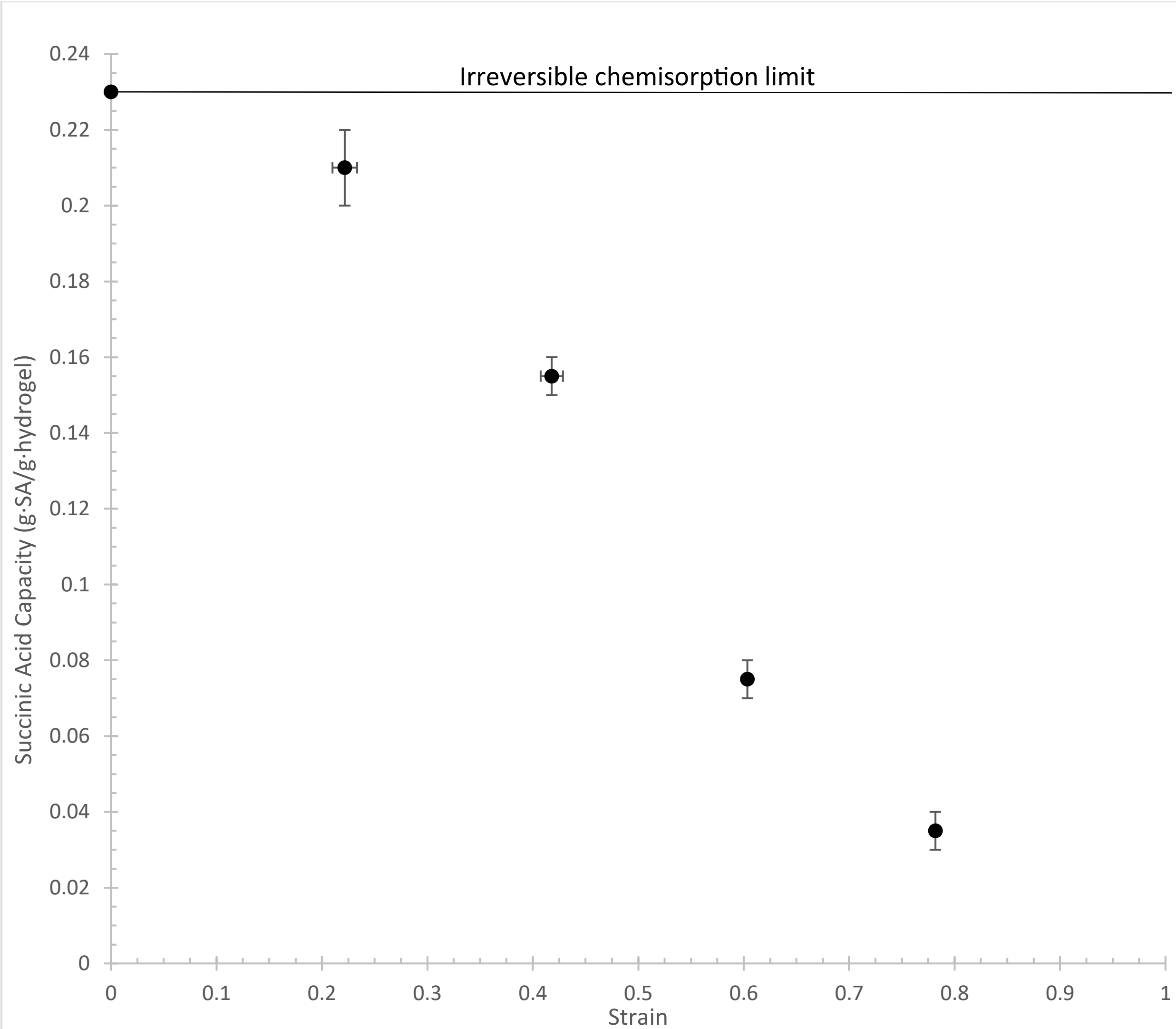

Figure 3.8. Succinic Acid Capacity of the 4% Hydrogel at Various Strains (25 ^{o}C).

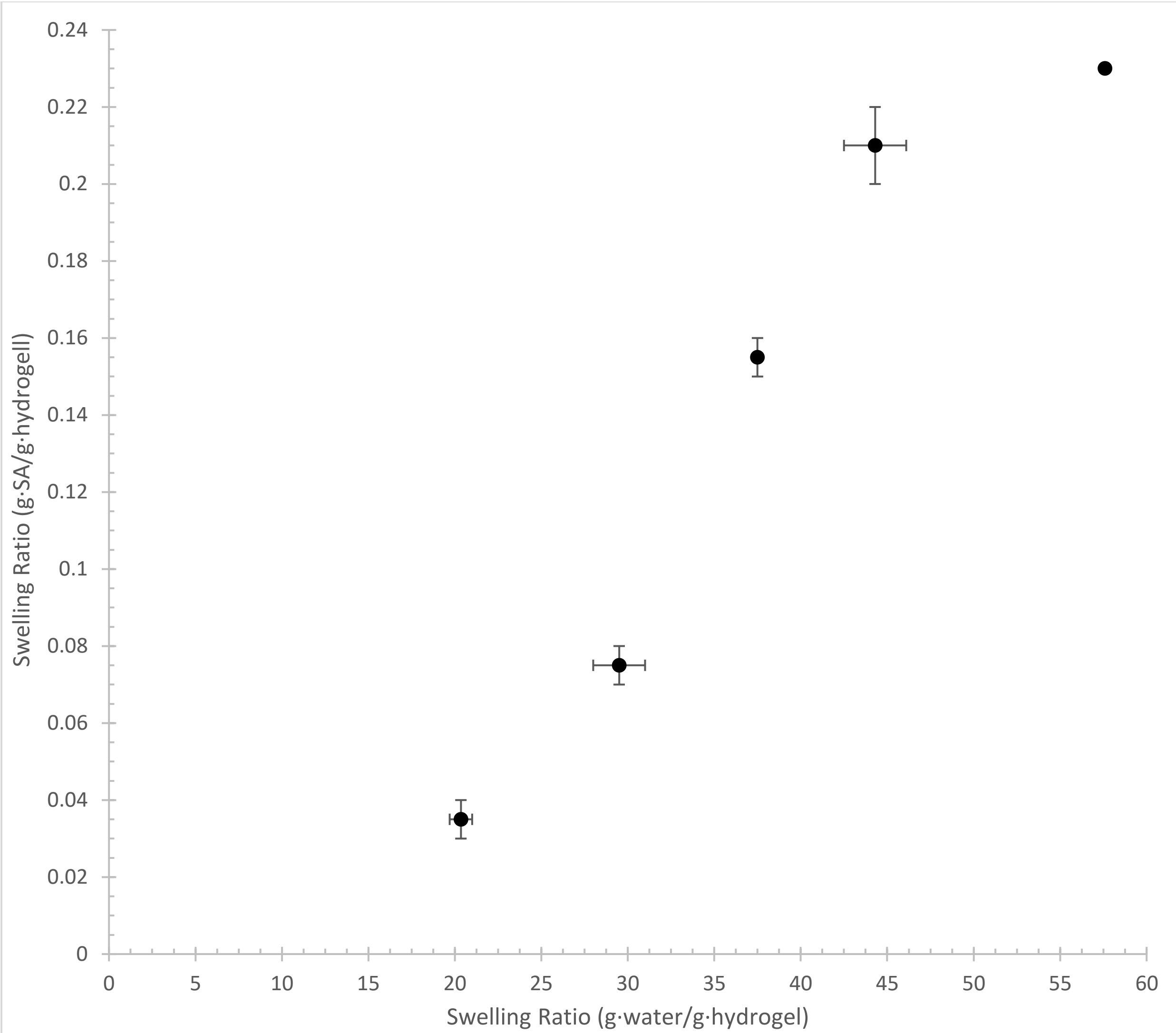

Figure 3.9. The Relation of Swelling Ratio to SA Capacity for the 4% Hydrogel (25 °C).

Another key performance variable of a pressure-swing process is the composition of the aqueous phase that is displaced from the hydrogel. If organic acid chemisorbs irreversibly, then an applied strain ejects pure water. This phenomenon would cause the acid concentration in the solid hydrogel phase to rise. On the other hand, if the organic acid is sorbed very weakly, then an applied strain releases solution with an SA concentration that is approximately the same as the initially absorbed solution. In this case the capacity of the hydrogel declines linearly with strain; the organic acid uptake is only accomplished through physisorption.

The SA capacity data that is presented in Figure 3.8 shows organic acid release behavior that is intermediate between irreversible chemisorption, and pure physisorption. The SA capacity declines from 0.23 g·SA/g·hydrogel in the unconfined state to a capacity of 0.22 g·SA/g·hydrogel at a strain of 0.2. The polymer retains much of its inherent basicity at this low level of functional group confinement.

Increasing the applied strain to 0.40 causes the SA capacity to decline to 0.15 g·SA/g·hydrogel. This capacity is significantly lower than the unconfined value. This finding is consistent with a strain-induced destabilization of the ammonium carboxylate salt. The confinement effect is much more pronounced at a strain of 0.60, which delivers a capacity of 0.07 g·SA/g·hydrogel. This capacity is less than a third of that of unconfined hydrogel. **Therefore, the hypothesis that the basicity of our hydrogel is strain sensitive is proven.**

The differences of the concentration of SA in the displaced aqueous phase between various strains are significant. Therefore, the known released concentrations between various strains can be used to optimize the recovery: dilute solutions that are released can be discarded or returned to a bioprocess, while concentrated solutions that are released can be retained. The SA solution that desorbs between the strains of 0.02 - 0.06 has a concentration of 9.2 g·SA/L, and a total SA recovery from the initial 2.5 g·SA/L solution of 51% (Table 3.3). The solution becomes slightly more concentrated between the strains of 0.04 – 0.06 at 10.1 g·SA/L. The total recovery lowers to 30% between these strains. **The hypothesis that the strain sensitive basicity of our hydrogel can be used to concentrate SA from dilute aqueous solution is proven.**

Table 3.3 Succinic Acid Desorption Solution Concentrations Between Various Strains (25 °C).

Strain Range (%)	$[SA]_{Desorption}$ (g/L)	Total SA Recovery (%)
0% – 20%	1.6 g/L	8%
20% – 60%	9.2 g/L	51%
40% – 60%	10.1 g/L	30%
60% – 80%	4.0 g/L	14%
0% – 80%	5.2 g/L	72%

The strain-based process for isolating and concentrating SA from dilute solution is energy efficient. The process also does not use or form strong bases or undesirable by-products, and produces the final product of SA + water. These attributes present significant advantages for the smart recovery in comparison to recoveries that are reported in literature, since they indicate that the smart recovery is more environmentally conscious and does not have a requirement of processing unwanted chemicals.

The use of the pH sensitivity of the hydrogel to recover SA was also considered. High pH collapses the hydrogel, neutralizes SA, and regenerates the amine. However, the [NaOH] that is needed to fully regenerate the hydrogel and concentrate SA would create a solution of pH > 12. This extreme pH is known to cause hydrolysis in acrylamide polymers, as demonstrated by Yasuda et al. This group reports that there is significant polyacrylamide hydrolysis in NaOH (aq) solutions of pH > 13 [9] at 50 °C. To concentrate SA using this pH recovery, the stability of our hydrogel in alkaline pH would have to be verified.

3.3 Conclusions

Weakly basic, amine-functionalized hydrogels of varying crosslink densities have been proven to recover succinic acid from dilute aqueous solution effectively. The basicity of the amine was proven to decline substantially in a polymer formulation, and continued to depress with crosslinking. The relationship between amine group confinement and basicity was applied to develop a smart recovery process. Imposing strain on the hydrogel increased the activity of the ammonium succinate salt, and reversed the reaction equilibrium to form amine + SA. Varying the strain ranges during the smart recovery optimized the SA concentration. Recovering solution between the strains of 0.20 – 0.60 provided a [SA] of 9.2 g/L, and resulted in a recovery of half of the SA from the aqueous solution. The recovery can be optimized further by tuning the strain range, or by using a hydrogel of higher crosslink density.

References

[1] Y. Chang and C. L. McCormick, "Water-Soluble Copolymers. 49. Effect of the Distribution of the Hydrophobic Cationic Monomer Dimethyldodecyl(2-acrylamidoethyl)ammonium Bromide on the Solution Behavior of Associating Acrylamide Copolymers," *Macromolecules*, vol. 26, no. 22, pp. 6121–6126, 1993, doi: 10.1021/MA00074A038.

[2] J. Alexiou, R. Biro, A. Tremblay, A. Daugulis, and J. S. Parent, "Base-functionalized polymeric chemisorbents for succinic acid recovery from aqueous solution," *React Funct Polym*, vol. 181, p. 105412, Dec. 2022, doi: 10.1016/J.REACTFUNCTPOLYM.2022.105412.

[3] Polymer gels, methods for their preparation and their use in electrophoretic applications, by G. Patras et al. (2000, Mar. 23). Patent AU760792B2 [Online]. Available: https://patents.google.com/patent/AU760792B2/en.

[4] I. Zarzyka, M. Pyda, and M. L. Di Lorenzo, "Influence of crosslinker and ionic comonomer concentration on glass transition and demixing/mixing transition of copolymers poly(N-isopropylacrylamide) and poly(sodium acrylate) hydrogels," *Colloid Polym Sci*, vol. 292, no. 2, pp. 485–492, Oct. 2014, doi: 10.1007/S00396-013-3092-9.

[5] J. T. Dafoe and A. J. Daugulis, “In situ product removal in fermentation systems: Improved process performance and rational extractant selection,” *Biotechnol Lett*, vol. 36, no. 3, pp. 443–460, Oct. 2014, doi: 10.1007/S10529-013-1380-6.

[6] K. D. Schulze *et al.*, “Polymer Osmotic Pressure in Hydrogel Contact Mechanics,” *Biotribology*, vol. 11, pp. 3–7, Sep. 2017, doi: 10.1016/J.BIOTRI.2017.03.004.

[7] S. Zhao, “Osmotic pressure versus swelling pressure: Comment on ‘bifunctional polymer hydrogel layers as forward osmosis draw agents for continuous production of fresh water using solar energy,’” *Environ Sci Technol*, vol. 48, no. 7, pp. 4212–4213, Apr. 2014, doi: 10.1021/ES5006994.

[8] L. Arens *et al.*, “FULL PAPER 1700112 (1 of 8) Osmotic Engine: Translating Osmotic Pressure into Macroscopic Mechanical Force via Poly(Acrylic Acid) Based Hydrogels,” 2017, doi: 10.1002/advs.201700112.

[9] K. Yasuda, K. Okajima, and K. Kamide, “Study on Alkaline Hydrolysis of Polyacrylamide by 13 C NMR,” *Polym J*, vol. 20, no. 12, pp. 1101–1107, 1988.

Chapter 4

Comparison of the Researched Recoveries to Literature Recoveries

4.1 Comparing PIL-HCO_3 with the 4% Hydrogel

The weakly basic polymeric chemisorbents of PIL-HCO_3 and the 4% hydrogel are both able to chemisorb SA from dilute aqueous solution with high yields (0.20 $\pm$ 0.01 g·SA/g·PIL; 0.23 g·SA/g·hydrogel). **These yields are competitive to other chemisorbents that are reported in literature (Table 4.1), proving the hypothesis.** The researched sorbents differ by the type of chemisorption reaction, the stability of the succinate salt and the method of regeneration. These comparisons are presented in Table 4.2.

Table 4.1 Succinic Acid Capacities of Base Functionalized Polymers.

Sorbent	Polymer Backbone	Basic Functional Group	Functional Group Content (mmoles/g)	$[SA]_0$ Test Condition (g/L)	Polymer Phase Fraction (F)	SA Capacity (g/g·polymer)	Reference
Hydrogel (4 wt% TAAEA)	Poly(dimethylaminooethylacrylamide)	3° Amine	6.9	2.5	0.01	0.23	This work
PIL-HCO_3	Poly(vinyldodecylimidazolium)	Bicarbonate	1.9	2.5	0.01	0.20	This work
PIL-OH	Poly(vinyldodecylimidazolium)	Hydroxide	1.9	2.5	0.01	0.20	[1]
Amberlite IRA - 910	Poly(vinylbenzyldimethylhydroxymethylammonium-co-divinylbenzene)	Hydroxide	4.0	2.5	0.01	0.25	[2][a]
Riellex HQP	Poly(vinylmethylpyridium)	Hydroxide	3.6	2.5	0.01	0.25	[2][a]
Dowex MWA - 1	Poly(vinylbenzyldimethylamine-co-divinylbenzene)	3° Amine	4.7	2.5	0.01	0.24	[2][a]
Reillex 425	Poly(vinylpyridine-co-divinylbenzene)	Pyridine	6.3	2.5	0.01	0.06	[2][a]

[a]The capacity was calculated for the reported conditions from the Langmuir isotherm values.

Table 4.2 Comparison of PIL-HCO_3 with the 4% Hydrogel for the Recovery of SA.

Sorbent	Salt	Method to Increase the FG Content	Basicity	Stability of the Succinate Salt	Water Uptake (Succinate Salt) (%)	Regeneration Options
PIL-HCO_3	4° ammonium succinate salt	Increase $[NaHCO_3]_0$ or lower F during synthesis	Psuedo-Irreversible (when sparged). Neutralizes to pH 7.0 at 2 moles·HCO_3/1 mole·SA (2.5 g·SA/L)	Desorbs by acidification or ion exchange	100% $\pm$ 2%	Traditional strong acid regeneration. Green H_2CO_3 or $NaHCO_3$ desorptions.
Hydrogel (4%)	3° ammonium succinate salt	Lower crosslink density (wt% TAAEA)	Reversible. Reaches pH 5.4 at 3 moles·amine/1 mole·SA (2.5 g·SA/L)	Reversible. Stability is dependent on the [SA] of the surrounding solution	5960% $\pm$ 170%	Traditional strong base regeneration. Smart recovery with strain.

Sorbent	Best Regeneration Technology Tested in this Thesis	Phase Fraction (F) or Strain Range (fr.)	$[SA]_{Desorption}$ (g/L) of the Technology	Total SA Recovery from 2.5 g/L Solution
PIL-HCO_3	Saturated $NaHCO_3$	0.19	23.5 ± 3.1	59%
Hydrogel	Smart recovery	0.00 – 0.80	5.2	72%
(4%)	with strain	0.20 – 0.60	9.2	51%
		0.40 – 0.60	10.1	30%

4.2 Comparison of the SA Recovery Methods to Traditional Organic Acid Recovery Methods

PIL-HCO_3 has an 89% extraction efficiency of SA in 2.5 g·SA/L solution at 1 mole·base/1 mole·SA; the 4% hydrogel has an 85% extraction efficiency of SA in 2.5 g·SA/L at 3 moles·base/1 mole·SA. The efficiencies of both sorbents are $\geq$ the 85% extraction efficiency of SA by $Ca(OH)_2$ [3]. **Therefore, the hypothesis that the researched extractions are competitive to the traditional SA extraction with alkaline salts is proven.**

Both of the researched recoveries regenerate the initial sorbent during desorption. The PIL uses cheap sodium bicarbonate during its recovery. The hydrogel uses cheap mechanical pressure during its recovery. These methods are qualitatively (environmentally and economically) favourable to the use of alkaline salts to recover SA (Scheme 4.1a), which burdens significant costs and environmental concerns due to the sourcing of strong base.

After initial chemisorptions in 2.5 g·SA/L solution at a F = 0.01, the researched sorbents recover SA with the following efficiencies: the 4% hydrogel has a 72% recovery efficiency from 2.5 g·SA/L solution between the strains of 0 – 0.80 with the smart recovery; PIL-HCO_3 has a 59% acid recovery efficiency from 2.5 g·SA/L solution at a F = 0.19 with the saturated $NaHCO_3$ (aq) recovery. These researched recoveries are competitive to other established technologies such as electrodialysis. The electrodialysis of SA from fermentation broth provides a SA yield of 60% -- this includes a complete purification and crystallization of SA [3]. Given that only ultrafiltration and crystallization are additionally required to use our smart recovery on fermentation broth (Scheme 4.1b), it is suspected that the researched efficiency of our smart recovery in this work would be similar to its industrial efficiency. This makes the smart recovery competitive to recovery with electrodialysis.

The recovery of SA with PIL-HCO_3 requires additional unit operations to separate the recovered succinate from the Na^+, HCO_3^- and Cl^- ions. These additional steps lower the 59% efficiency. A possible process to separate succinate from the other ions is the presented process in Scheme 4.1c, which uses a sequence of ion exchange resins. Within this process, the concentrated succinate solution passes through strongly acidic cationic-exchange resins. These resins remove the Na^+ and HCO_3^- ions from solution. The solution then passes through anionic exchange resins to remove Cl^- impurities.

One group published the efficacy of using strongly acidific cationic exchange resins to remove $NaHCO_3$ from solution. This group, Millar et al., report that using a lanxess S108H resin in $NaHCO_3$ solution removes a maximum of 62.2 g·Na^+/kg·resin. This resin decomposes HCO_3^- to CO_2 + H_2O from the exchange of Na^+ for H^+. The group also reports that 6 g of resin caused the pH of a $NaHCO_3$ (aq) solution to reduce from 8.5 to 4.4 [4]. The release of protons into solution due to the ion exchange should also acidify succinate, allowing SA to be separated from Cl^- with the anion exchange resins.

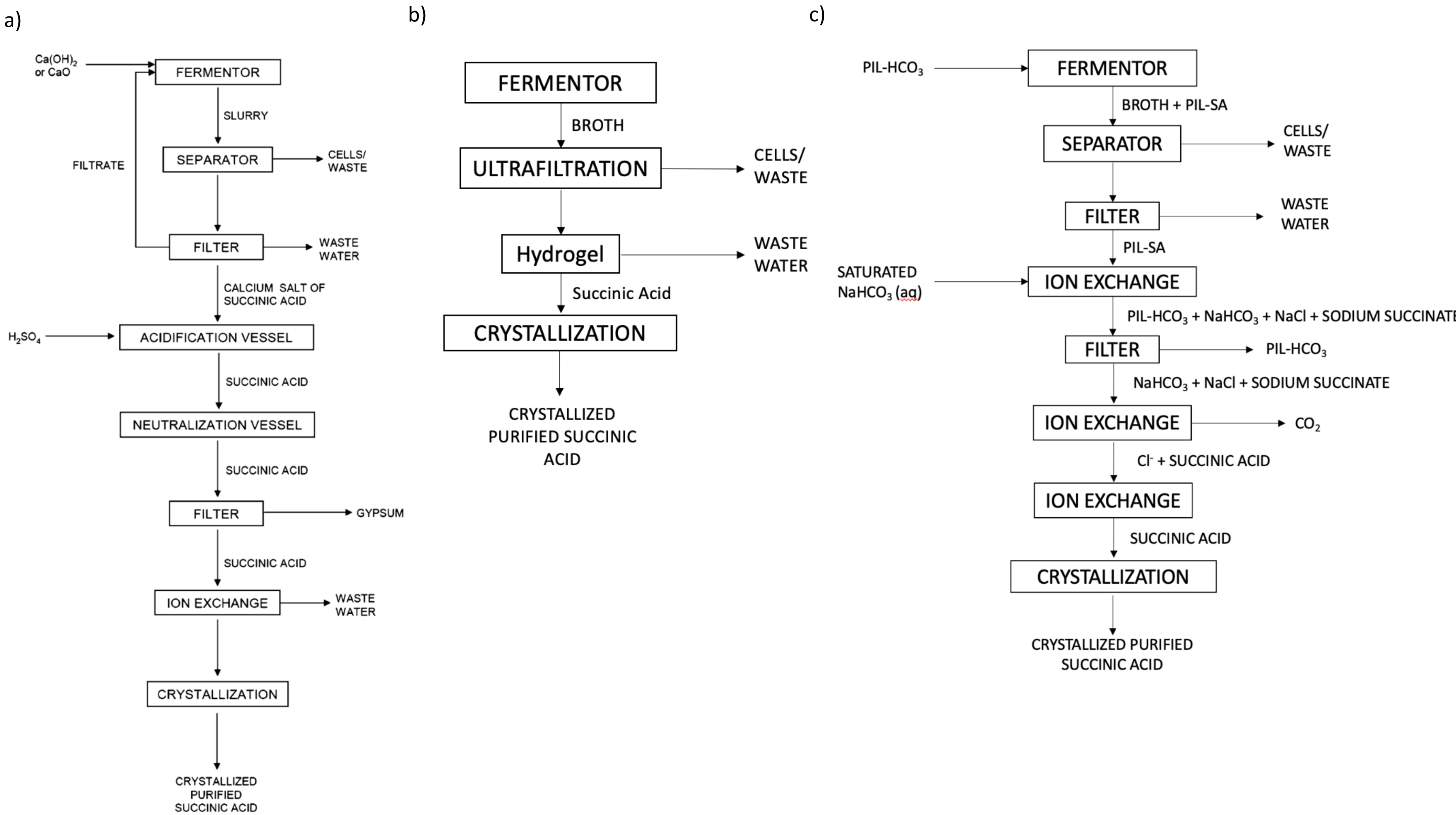

Scheme 4.1 Comparison of Traditional Acid Extraction with the Proposed Industrial SA Recovery Processes of PIL-HCO_3 with Saturated $NaHCO_3$ and the 4% Hydrogel with its Smart Recovery: a) Traditional Acid Recovery (© Tanja Kurzrock, reprinted with permission); b) 4% Hydrogel Smart Recovery; c) PIL-HCO_3 Saturated $NaHCO_3$ Recovery.

4.3 Comparison of the Researched Recoveries to the Recoveries of the Failed Ventures

4.3.1 Descriptions of the Venture Recoveries

The researched recoveries of this thesis have advantages and disadvantages in comparison to the technologies of the failed ventures that were mentioned in Chapter 1 [5]. A brief description of each venture technology is provided in this section. A comparison of the researched recoveries to the recoveries of the failed ventures is presented to describe characteristics of our recoveries that could contribute to a more successful venture.

Succinity used an alkaline salt recovery with $Mg(OH)_2$. During the fermentation, $Mg(OH)_2$ precipitated SA and maintained the broth pH (Scheme 4.2a). After precipitation, SA was recovered from MgSA with HCl. $MgCl_2$ was subsequently precipitated. $Mg(OH)_2$ was regenerated from the thermal cracking of $MgCl_2$ to MgO + HCl. MgO was further hydrated to $Mg(OH)_2$ [5].

Myriant implemented ammonia precipitation (Scheme 4.2b) which uses the weak base of ammonia. Ammonia precipitates SA and maintains the pH of the broth during fermentation. A significant disadvantage of this recovery is that ammonia can inhibit bacteria metabolism. SA is recovered from the ammonium succinate salt by H_2SO_4. This acidification produces the by-product of $(NH_4)_2SO_4$. $(NH_4)_2SO_4$ can be sold as a fertilizer, or can be thermally cracked into ammonia + ammonium bisulfate [5].

Reverdia implemented a low pH fermentation, which is a fermentation that is operated at pH < 3. This technology was designed to acidify all of the produced SA (Scheme 4.3a). This process is very simple. Unfortunately, having a low pH during fermentation creates low SA yields. To implement this technology, specific SA-producing bacteria strains and specialized process designs are essential for competitiveness [5].

BioAmber implemented a low pH fermentation with electrodialysis. This recovery combines low pH fermentation with an electrodialysis bipolar membrane (EBM). The EBM splits sodium succinate to

NaOH + SA. The fermentation broth pH is also partially controlled with NaOH. This recovery is presented in Scheme 4.3b [5].

4.3.2 Advantages and Disadvantages of the Researched Recoveries

One of the main disadvantages of our researched recoveries is that the *in-situ* stabilization of fermentation broth pH by either sorbent has not yet been verified. Since the ISPR of SA has not been proven effective with either sorbent, we have to apply a conservative argument that a strong base such as NaOH is required to stabilize the broth pH in both processes. Stabilizing the broth pH would increase the SA yield from fermentation, however, it would also lower the chemisorption efficiencies of the sorbents since the recoveries require acidified SA. Given the untested stabilizations, there is the possible issue of requiring low pH fermentations to efficiently chemisorb SA. These would lower the SA yields of our recoveries.

Although stabilizations of fermentation broth are not done in this thesis, insights of the results of stabilizations with the new sorbents can be gleaned from analyzing our research group's previous work; this work used earlier analogs of our researched sorbents. In our group's previous work, PIL-OH was able to stabilize a simulated fermentation broth at pH > 6 [1]. Given the same basicity of PIL-HCO_3 to PIL-OH, the only limiting factor that would prevent an identical stabilization would be a lowered chemisorption rate due to the potential sparging requirement for the chemisorption of SA with PIL-HCO_3.

The previous 30% hydrogel was unable to stabilize a simulated fermentation broth at pH > 3.8, and could only raise the pH of 2.5 g·SA/L solution with 3 moles·base/1 mole·SA from pH 3.0 to 4.6 [1]. The higher basicity of the newly researched 4% hydrogel has the potential to stabilize the solution at a higher pH.

Proving the *in-situ* stabilization of fermentation broth with our sorbents would confirm that our recoveries are highly competitive recoveries to those of the ventures. The recoveries would provide high

SA yields from fermentation and effectively concentrate SA with high yields. This would be performed without the use of strong acids, strong bases, or single-use reactants. The recoveries would also simultaneously regenerate the sorbents during desorption and purify SA with cheap and simple methods (ion exchange and mechanical pressure). It is important to note that the recoveries also do not require the additional processing or disposal of complicated by-products.

It should be recognized that all of the technologies that are analyzed in this thesis are not inherently selective for SA; they chemisorb any organic acid that is dissolved in a fermentation broth. To solve this problem, microbiologists have designed bacteria that have a high selectivity for the metabolism of SA. One designed bacteria, *Basfia succiniproducens*, which is the bacteria that Succinity implemented to improve their low pH bioproduction, had its formic acid metabolism eliminated, its lactic acid production reduced and its pyruvic acid production increased. The SA yield of this bacteria improved from 0.75 moles·SA/1.00 mole·glucose in its wild form to 1.08 moles·SA/1.00 mole·glucose in the described engineered form [6].

Other technologies have also been used to isolate SA after fermentation. One of these technologies is nanofiltration. The difilitration of simulated broth is proven to remove 99.9%, 99.2% and 97.0% of the ions of formate, acetate and lactate from aqueous solution after 150 h, while keeping 62% of the initial SA [7].

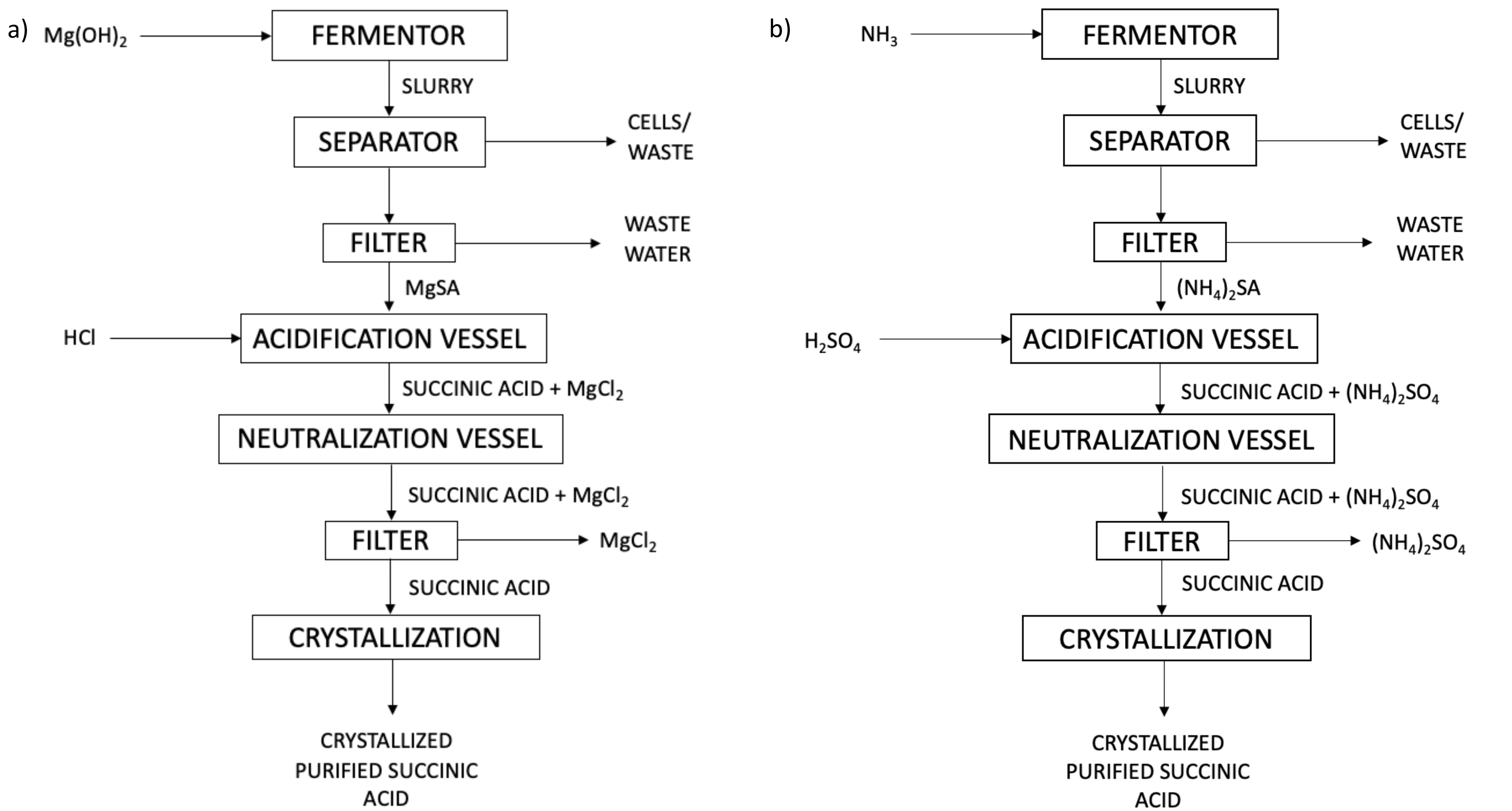

Scheme 4.2 Processes of the Venture Technologies: a) $Mg(OH)_2$ Precipitation; b) Ammonia Precipitation.

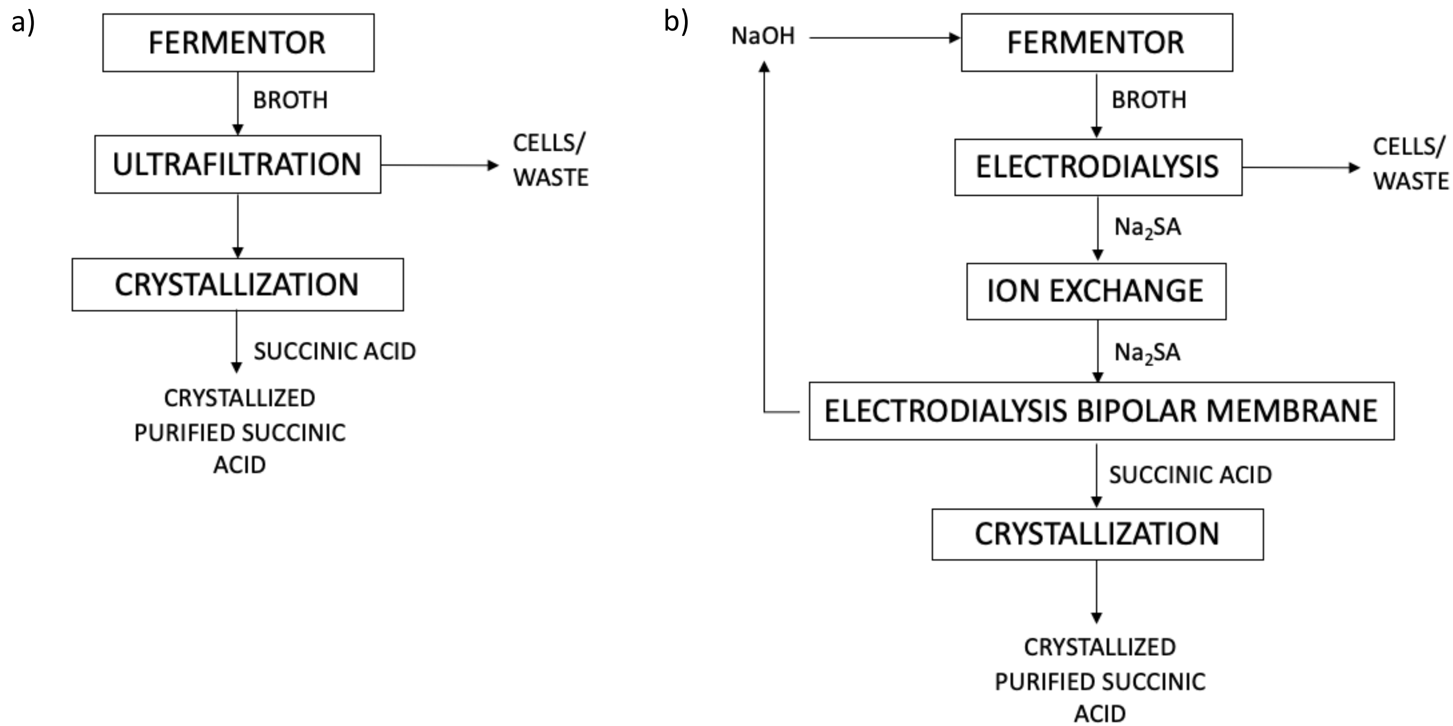

Scheme 4.3 Processes of the Venture Technologies: a) Low pH Fermentation; b) Electrodialysis.

References

[1] J. Alexiou, R. Biro, A. Tremblay, A. Daugulis, and J. S. Parent, "Base-functionalized polymeric chemisorbents for succinic acid recovery from aqueous solution," *React Funct Polym*, vol. 181, p. 105412, Dec. 2022, doi: 10.1016/J.REACTFUNCTPOLYM.2022.105412.

[2] L. A. Tung, "Recovery of carboxylic acids at pH greater than pKa," University of California at Berkeley, 1993.

[3] T. Kurzrock and D. Weuster-Botz, "Recovery of succinic acid from fermentation broth," *Biotechnol Lett*, vol. 32, no. 3, pp. 331–339, Feb. 2010, doi: 10.1007/S10529-009-0163-6.

[4] G. J. Millar, S. J. Couperthwaite, and S. Papworth, "Ion exchange of sodium chloride and sodium bicarbonate solutions using strong acid cation resins in relation to coal seam water treatment," *Journal of Water Process Engineering*, vol. 11, pp. 60–67, Jun. 2016, doi: 10.1016/J.JWPE.2016.03.003.

[5] M. L. A. Jansen and W. M. van Gulik, "Towards large scale fermentative production of succinic acid," *Curr Opin Biotechnol*, vol. 30, pp. 190–197, Dec. 2014, doi: 10.1016/J.COPBIO.2014.07.003.

[6] J. H. Ahn, Y. S. Jang, and S. Y. Lee, "Production of succinic acid by metabolically engineered microorganisms," *Curr Opin Biotechnol*, vol. 42, pp. 54–66, Dec. 2016, doi: 10.1016/J.COPBIO.2016.02.034.

[7] S. H. Kang and Y. K. Chang, "Removal of organic acid salts from simulated fermentation broth containing succinate by nanofiltration," *J Memb Sci*, vol. 246, no. 1, pp. 49–57, Jan. 2005, doi: 10.1016/J.MEMSCI.2004.08.014.

Copyrights

Scheme 4.1a reprinted with permission from T. Kurzrock and D. Weuster-Botz, "Recovery of succinic acid from fermentation broth," *Biotechnol Lett*, vol. 32, no. 3, pp. 331–339, Feb. 2010, doi: 10.1007/S10529-009-0163-6. Copyright 2010 Springer. Copyright 2010 Springer.

Chapter 5

Thesis Conclusions

5.1 Assessing Hypotheses

5.1.1 Confirmed Hypotheses

Most of the hypotheses that were examined in this thesis were confirmed. These include:

- PIL-HCO_3 is competitive with PIL-OH for chemisorbing SA.
- the PIL can recover SA from dilute aqueous solution using green methods. Saturated H_2CO_3 and $NaHCO_3$ solutions both desorb SA from PIL-SA. Recovery by saturated $NaHCO_3$ is highly effective.
- confining DMEP by polymerization lowers its basicity for SA and BA. Crosslinking the polymer and increasing its crosslink density further lowers its basicity.
- the hydrogel has strain sensitive basicity.
- the strain-sensitive basicity of the hydrogel can be used to effectively recover SA from dilute aqueous solution.
- the SA capacity of both sorbents are competitive to polymeric chemisorbents that are reported in literature.
- the recoveries with the researched sorbents are competitive with traditional SA recovery by alkaline salt.

5.1.2 Unconfirmed Hypotheses

Some hypotheses were unconfirmed in this work, and require confirmation by future experiments or analyses. These are:

- SA desorption with saturated H_2CO_3 solution is not efficient at a partial CO_2 pressure of 59 bar. Higher partial pressures are suspected to improve the desorption.

5.2 Final Conclusions and Future Work

The researched sorbents of this thesis effectively chemisorb SA from dilute aqueous solution. Their capacities are competitive to our group's previously tested chemisorbents, and other chemisorbents that are published in literature. The weakly basic functionality of the sorbents allows for mild regeneration conditions with green methods. Regenerating the PIL with saturated $NaHCO_3$ and the hydrogel with its strain-sensitivity effectively concentrates SA and regenerates both sorbents' weakly basic functionalities. The SA desorption concentrations of the recoveries can be maximized by: a) increasing the F of desorption of the PIL; b) optimizing the strain range of the hydrogel. The assessed recoveries are competitive with traditional organic acid recoveries with alkaline salt, and other technologies such as electrodialysis. The recoveries are also competitive with the technologies that were used in the ventures of SA bioproduction during the 2010s.

Given the assessments of this thesis, it is recognized that there is a potential for the researched recoveries to create a more successful venture than the venture technologies. The suggested additional tests of Chapter 4 should be done to verify the competitiveness of the researched recoveries. If the tests prove that the ISPR of SA is efficient with the researched recoveries, the bioproduction of SA has the potential to be a viable venture.

Appendices

Appendix A Literature Information

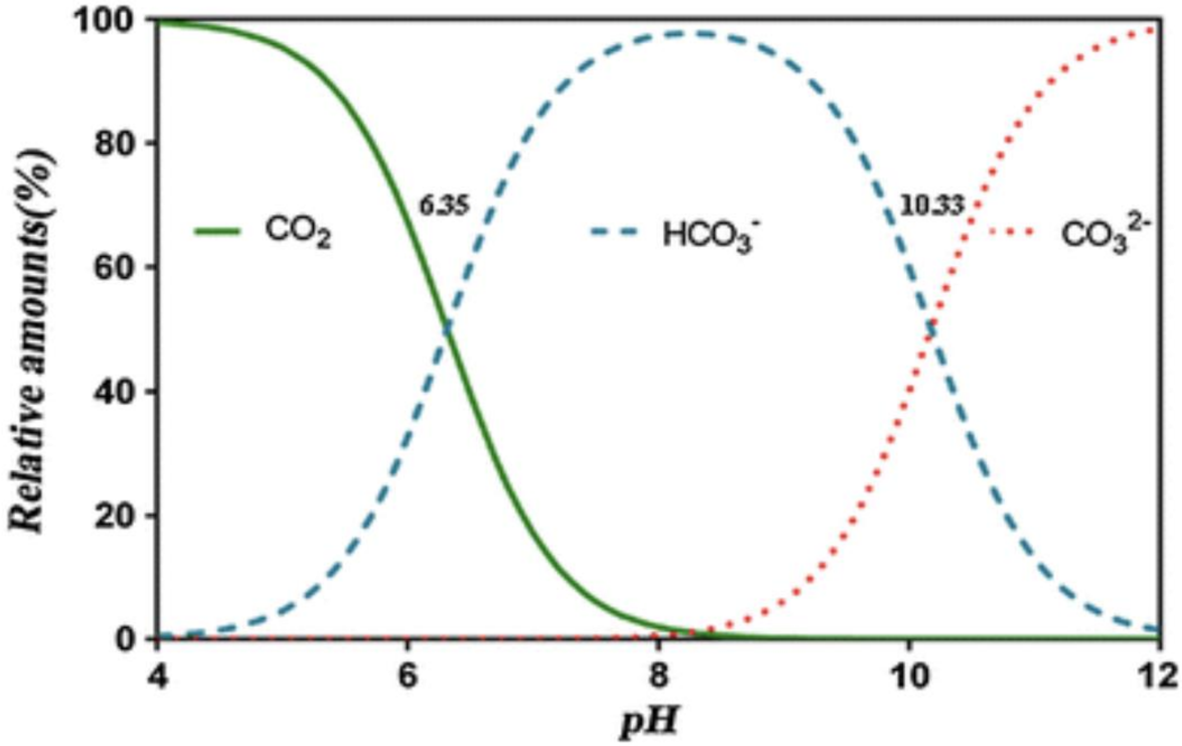

Figure A.1. CO_2 Equilibrium in Water at RT (© Mohammad Ghobadi, reprinted with permission) [1].

Table A.1 SA Producing Bacteria (© Ke-Ke Cheng, adapted with permission) [2].

Strains	Wild or engineered	Substrates	Conditions	Concentration (g/L)	Productivity (gL/h)	Yield (g/g)
A. Succinogenes 130Z	Wild	Sake lees	Anaeorobic, batch	48	0.94	0.75
		Whey	Anaeorobic, batch	21.5	0.44	0.57
A. Succinogenes CGMCC 2650	Wild	Corn Straw	Anaeorobic, batch	15.8	0.62	1.23
A. Succinogenes CGMCC 1593	Wild	Cane Molasses	Anaeorobic, batch	50.6	0.84	0.80
A. Succinogenes CGMCC 1593	Wild	Glucose	Anaeorobic, batch	60.2	1.30	0.75
A.Succiniprodu-cens ATCC53488	Wild	Glucose	Anaerobic, continuous with cell recyling	83	10.4	0.88
A.Succiniproduc-ens ATCC29305	Wild	Glucose	Anaerobic, continuous with cell recyling	14.3	3.3	0.71
E.coli KJ060	Engineered	Glucose	Anaeorobic, batch	86.5	0.9	0.93
E. coli KJ122	Engineered	Glucose	Anaeorobic, batch	83	0.88	0.90

Appendix B Figures

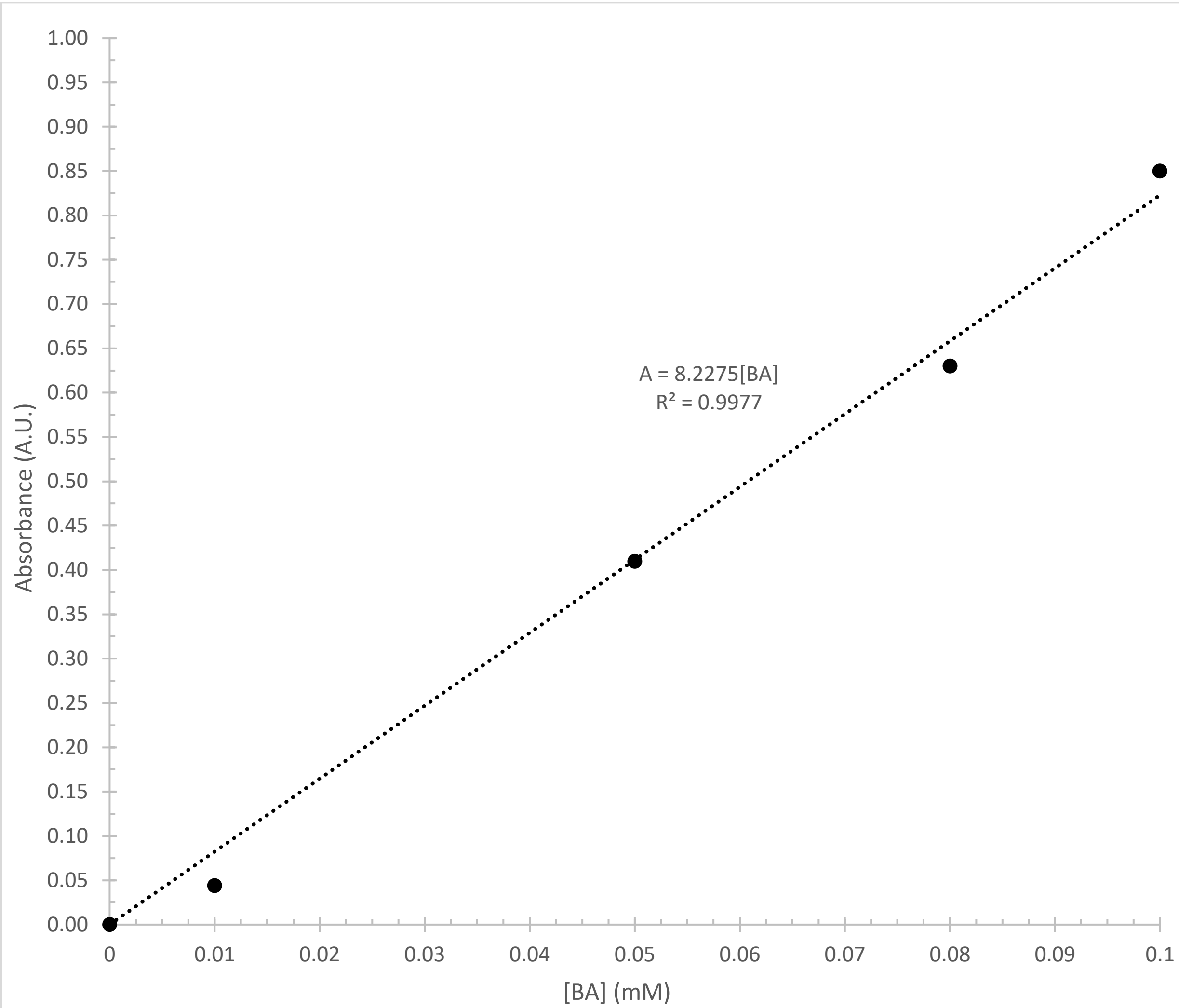

Figure B.1 UV-Vis Calibration of Benzoic Acid (λ = 225 nm) Between 0 – 0.1 mM at 20 ^{o}C (Slope = 8.2275).

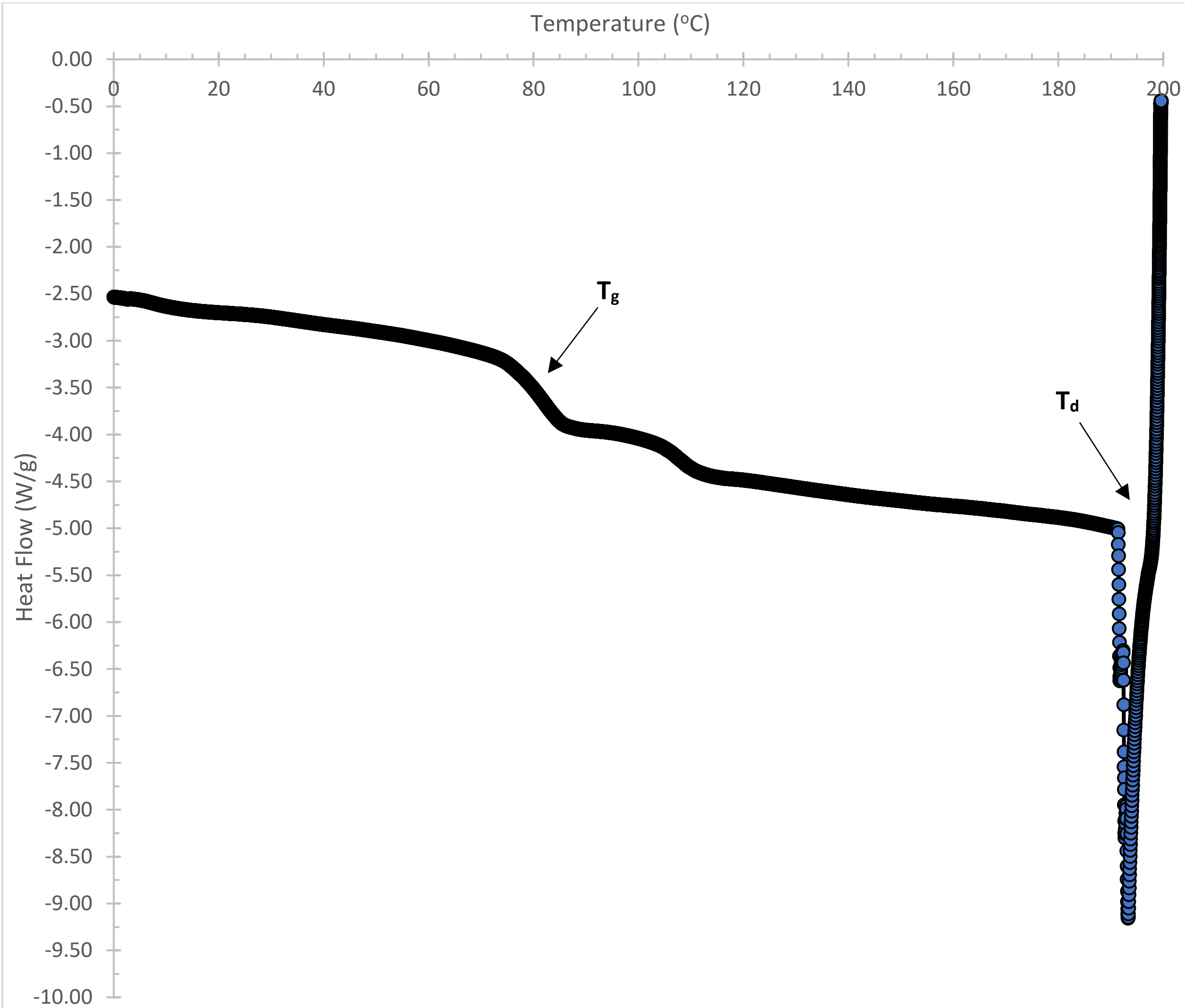

Figure B.2 The Degradation of Linear PDMEA During Dynamic Scanning Calorimetry Scans Between 0 – 200 °C (3rd cycle).

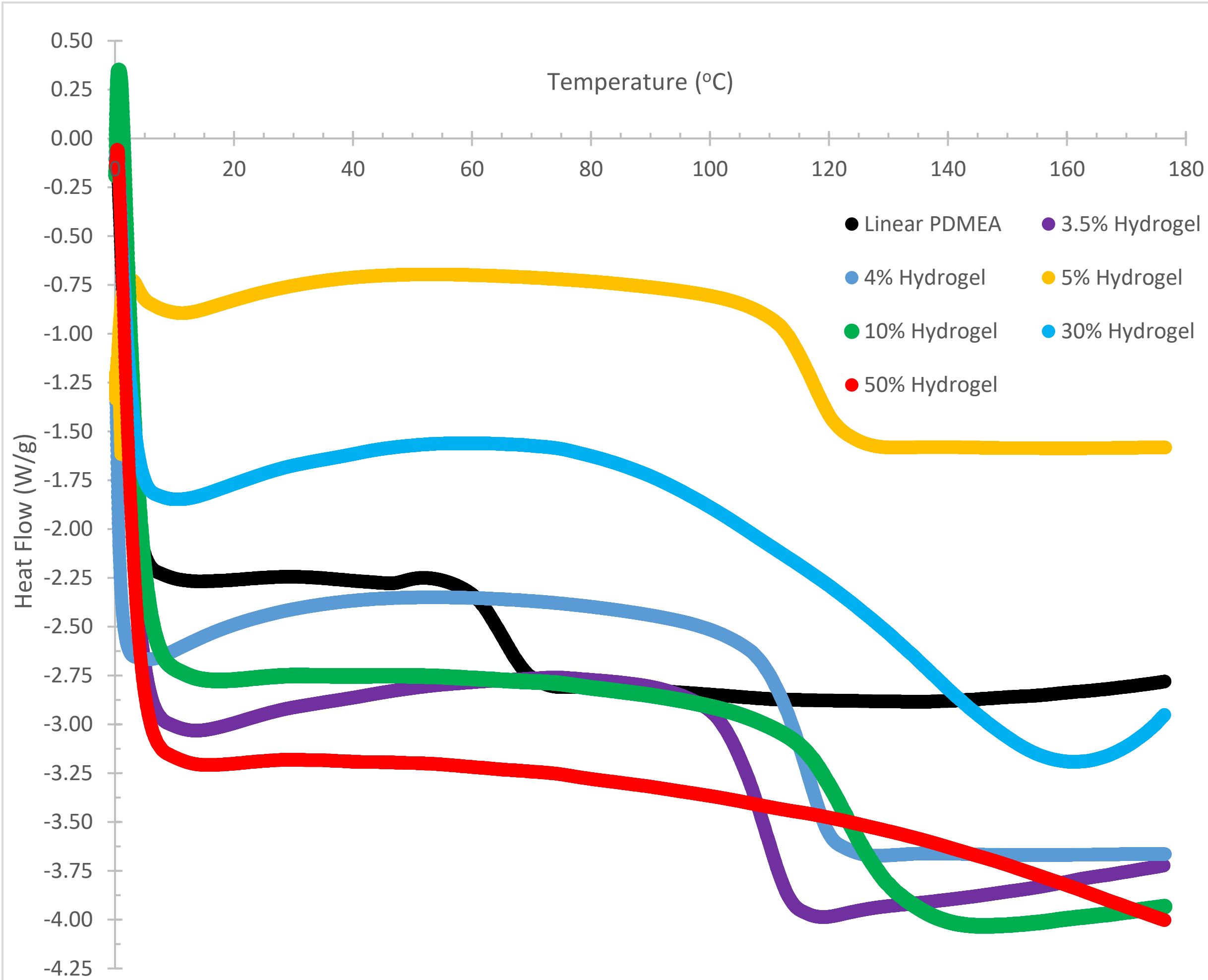

Figure B.3 Dynamic Scanning Calorimetry Plots of the Various Hydrogels Between 0 - 180 °C (3rd cycle).

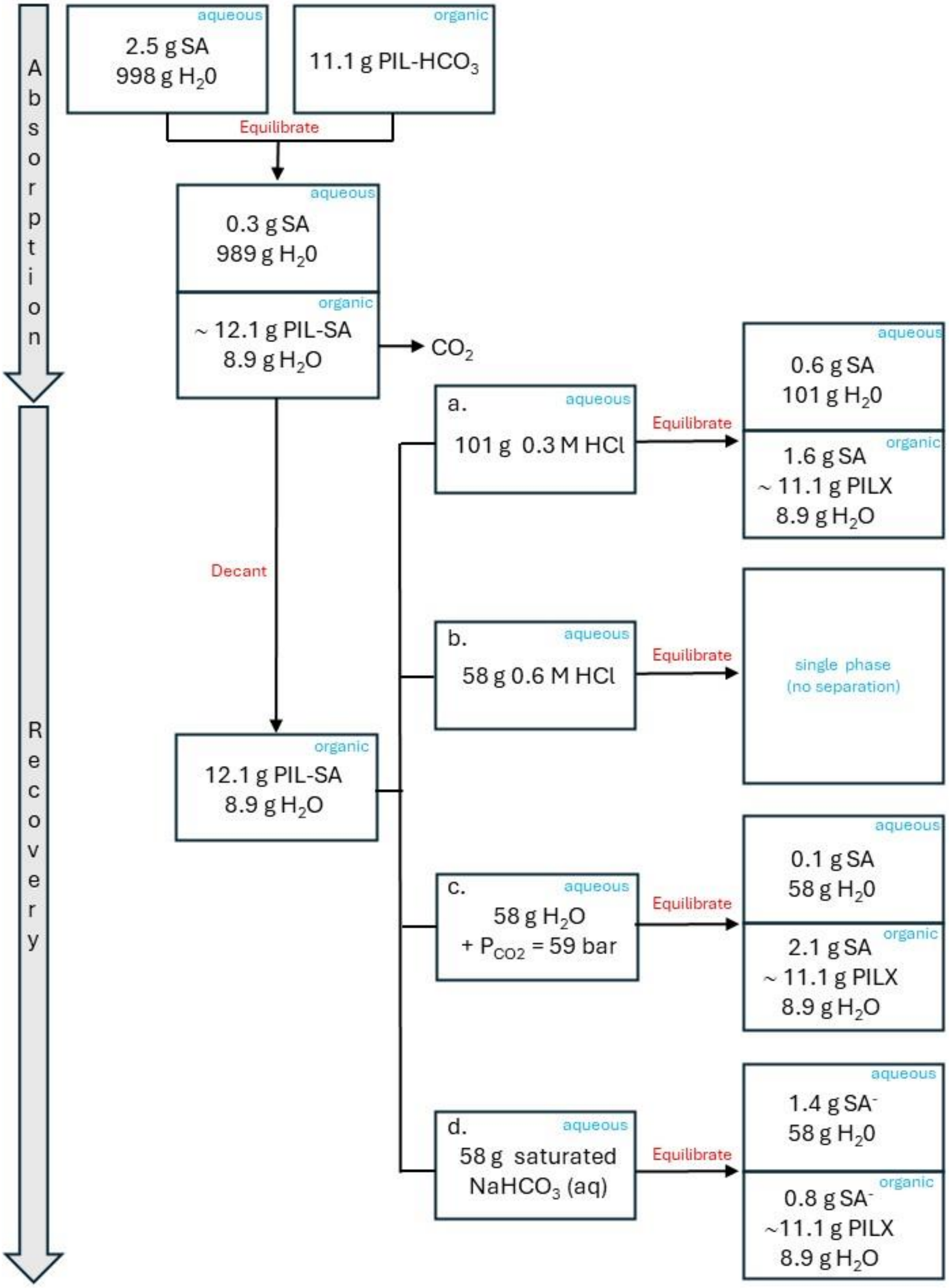

Scheme B.1 Recoveries of Succinic Acid with PIL-HCO_3.

Appendix C Data

Note: The data is included in the order of appearance in this thesis.

Table C.1 Absorption of SA and BA using PIL-Cl: BA Measured Using UV-Vis at a λ = 225 nm; SA Measured with ^{1}H NMR with a Citric Acid Reference of 41 mg (20 ^{o}C).

Acid	Phase Fraction (F)	Moles·Cl^- /mole·acid	$[Acid]_f$ (g·acid/L)	Capacity (g·acid/g·polymer)	Acid Removal (%)
Succinic Acid	0.011	1.7	1.8	0.06	28%
Succinic Acid	0.044	7.0	0.9	0.04	66%
Benzoic Acid	0.002	0.3	1.6	0.43	37%
Benzoic Acid	0.005	0.8	0.9	0.30	65%
Benzoic Acid	0.009	1.4	0.5	0.24	82%
Benzoic Acid	0.011	1.7	0.3	0.20	87%

Table C.2 Raw Data of the Ion Exchange Equilibrium of Cl^- to HCO_3^- in PIL-Cl that is Suspended in $NaHCO_3$ (aq) at Various Concentrations (0.05 M – Saturated; F = 0.01; 20 °C).

Trial	[$NaHCO_3$] (M)	Moles·HCO_3^- /mole·Cl^-	V_{NaOH} (Reference) (ml)	V_{NaOH} (Titration) (ml)	Conversion (%)
1	0.05	1.5	111	77	51%
2	0.05	1.5	111	71	58%
3	0.05	1.5	111	72	58%
1	0.10	3.0	111	68	64%
2	0.10	3.0	111	66	67%
3	0.10	3.0	111	64	71%
1	0.25	7.4	100	50	74%
2	0.25	7.5	100	50	75%
3	0.25	7.5	100	48	78%
1	0.50	14.9	101	46	82%
2	0.50	14.8	101	48	78%
3	0.50	14.9	101	48	79%
1	Saturated	30.2	108	47	92%
2	Saturated	29.9	108	48	90%
3	Saturated	29.6	108	46	92%

Table C.3 Summary of the Ion Exchange Equilibrium of Cl^- to HCO_3^- in PIL-Cl that is Suspended in 5 ml of $NaHCO_3$ (aq) at Various Concentrations (0.05 M – Saturated; F = 0.01; 20 °C).

$[NaHCO_3]$ (M)	Moles·HCO_3^- /mole·Cl^-	Conversion (%)	σ	pH_0 (A.U.)	pH_f (A.U.)
0.05	1.5	56%	3%	8.2	8.5
0.10	3	67%	3%	8.3	8.6
0.25	7.4	75%	2%	8.4	8.9
0.50	14.9	80%	2%	8.4	8.7
Saturated	29.9	91%	1%	8.3	8.6

Table C.4 Ion Exchange of Cl^- to HCO_3^- in PIL-Cl that is Suspended in 150 ml of $NaHCO_3$ (aq) for 48 h (0.50 M; F = 0.007; 20 °C).

Trial	V_{NaOH} (Reference) (ml)	V_{NaOH} (Titration) (ml)	Conversion (%)
1	222	142	60%
2	210	129	61%
3	210	130	60%
Average	-	-	60% $\pm$ 0%

Table C.5 Ion Exchange of Cl^- to HCO_3^- in PIL-Cl that is Suspended in CO_2 Saturated Aqueous Solution for 24 h (P = 59 bar; F = 0.007; 20 °C).

Trial	V_{NaOH} (Reference) (ml)	V_{NaOH} (Titration) (ml)	Conversion (%)
1	238	226	9%
2	259	245	10%
3	259	242	13%
Average	-	-	11% $\pm$ 2%

Table C.6 Raw Data of the Equilibrium Water Uptake (%) by the Various PIL Salts (F = 0.01, 20 °C).

PIL Salt	Trial	mWet (g)	Water Uptake (%)
PIL-Cl	1	0.19	85%
	2	0.20	97%
	3	0.19	88%
PIL-HCO_3	1	0.17	73%
	2	0.17	72%
	3	0.18	82%
PIL-SA	1	0.20	100%
	2	0.20	98%
	3	0.20	102%

Table C.7 Raw Data of the Titrations of SA and BA to 2.5 moles·HCO_3^-/1.0 mole·SA and 1.5 moles·HCO_3^-/1.0 mole·BA by PIL-HCO_3 (2.5 g·acid/L, 20 °C).

Moles·HCO_3^- /mole·acid	Phase Fraction (F)	Aqueous Solution pH (Succinic Acid)	Aqueous Solution pH (Benzoic Acid)
0.00	0.000	3.04	3.10
0.10	0.001	3.07	3.14
0.20	0.002	3.12	3.20
0.30	0.003	3.20	3.30
0.50	0.006	3.32	3.57
0.70	0.008	3.46	4.05
0.80	0.009	-	4.97
0.90	0.010	3.68	6.21
1.00	0.011	-	6.97
1.15	0.013	-	7.08
1.30	0.014	4.30	-
1.50	0.017	-	7.17
1.70	0.019	5.30	-
1.80	0.020	5.82	-
1.85	0.021	6.32	-
1.90	0.021	6.79	-
1.95	0.022	7.05	-
2.00	0.022	7.17	-
2.05	0.023	7.23	-

Moles·HCO_3^- /mole·acid	Phase Fraction (F)	Aqueous Solution pH (Succinic Acid)	Aqueous Solution pH (Benzoic Acid)
2.15	0.024	7.26	-
2.50	0.028	7.26	-

Table C.8 Raw Data of the Recovery of SA by Various Recovery Technologies; Measured with ^{1}H NMR with a Citric Acid Reference (41 mg) (20 °C).

Technology	Trial	Phase Fraction (F)	^{1}H NMR Integration	[SA] (g/L)	Acid Desorbed (%) (physisorption not accounted)
HCl	1	0.11	1.72	10.8	55%
HCl	1	0.19	No Separation	No Separation	No Separation
Saturated $NaHCO_3$	1	0.19	3.46	21.8	62%
	2		3.32	20.9	59%
	3		4.43	27.9	79%
Saturated H_2CO_3 (P_{CO_2}= 860 psi)	1	0.19	0.40	2.5	7%
	2		0.29	1.8	5%
	3		0.26	1.7	5%

Table C.9 Raw Data of the Equilibrium Swelling Ratio (g·water/g·hydrogel) of the 3.5% Hydrogel in DI Water (pH 7.0), Aqueous 2.5 g·SA/L Solution (pH 3.0) and Aqueous HCl Solution (pH 3.0) (F = 0.01, 25 °C).

Solution	Trial	M_{wet} (g)	Swelling Ratio (g·water/g·hydrogel)	Solution Equilibrium pH
DI Water	1	3.14	60.5	8.3
	2	3.36	64.9	8.4
	3	3.41	67.1	8.4
SA	1	3.46	74.2	5.6
	2	3.36	72.0	5.7
	3	3.05	66.8	5.2
HCl	1	3.46	68.2	8.3
	2	3.36	66.2	8.6
	3	3.29	64.8	8.4

Table C.10 Raw Data of the Equilibrium Swelling Ratio (g·water/g·hydrogel) of the 5% Hydrogel in DI Water (pH 7.0), Aqueous 2.5 g·SA/L Solution (pH 3.0) and Aqueous HCl Solution (pH 3.0) (F = 0.01, 25 ^{o}C).

Solution	Trial	M_{wet} (g)	Swelling Ratio (g·water/g·hydrogel)	Solution Equilibrium pH
DI Water	1	2.40	47.1	7.6
	2	2.35	45.1	7.9
	3	2.32	45.4	8.3
SA	1	2.17	46.2	6.0
	2	2.17	44.2	5.4
	3	2.19	45.5	5.7
HCl	1	2.34	45.8	-
	2	2.39	45.8	7.8
	3	2.52	49.4	7.4

Table C.11 Raw Data of the Equilibrium Swelling Ratio (g·water/g·hydrogel) of the 10% Hydrogel in DI Water (pH 7.0), Aqueous 2.5 g·SA/L Solution (pH 3.0) and Aqueous HCl Solution (pH 3.0) (F = 0.01, 25 °C).

Solution	Trial	M_{wet} (g)	Swelling Ratio (g·water/g·hydrogel)	Solution Equilibrium pH
DI Water	1	0.56	10.1	7.4
	2	0.60	10.8	7.7
	3	0.54	9.9	7.5
SA	1	0.62	11.7	5.0
	2	0.60	11.5	5.0
	3	0.59	11.2	5.1
HCl	1	0.58	10.4	7.6
	2	0.57	10.5	7.2
	3	0.61	11.4	7.2

Table C.12 Raw Data of the Equilibrium Swelling Ratio (g·water/g·hydrogel) of the 30% Hydrogel in DI Water (pH 7.0), Aqueous 2.5 g·SA/L Solution (pH 3.0) and Aqueous HCl Solution (pH 3.0) (F = 0.01, 25 ^{o}C).

Solution	Trial	M_{wet} (g)	Swelling Ratio (g·water/g·hydrogel)	Solution Equilibrium pH
DI Water	1	0.16	2.1	7.0
	2	0.15	2.0	7.3
	3	0.14	1.8	7.2
SA	1	0.16	2.0	4.1
	2	0.20	2.7	4.0
	3	0.18	2.3	4.3
HCl	1	0.14	1.8	6.2
	2	0.14	1.8	6.2
	3	0.14	1.7	6.2

Table C.13 Raw Data of the Equilibrium Swelling Ratio (g·water/g·hydrogel) of the 50% Hydrogel in DI Water (pH 7.0), Aqueous 2.5 g·SA/L Solution (pH 3.0) and Aqueous HCl Solution (pH 3.0) (F = 0.01, 25 ^{o}C).

Solution	Trial	M_{wet} (g)	Swelling Ratio (g·water/g·hydrogel)	Solution Equilibrium pH
DI Water	1	0.14	1.8	7.2
	2	0.14	1.8	-
	3	0.14	1.8	7.2
SA	1	0.20	2.2	3.7
	2	0.20	2.3	3.8
	3	0.21	2.4	3.6
HCl	1	0.13	1.5	6.0
	2	0.13	1.6	6.2
	3	0.10	1.0	5.9

Table C.14 Summary of the Equilibrium Swelling Ratios (g·water/g·hydrogel) of the Various Hydrogels in DI Water (pH 7.0), Aqueous 2.5 g·SA/L Solution (pH 3.0) and Aqueous HCl Solution (pH 3.0) (F = 0.01, 25 °C).

Weight Fraction of TAAEA (wt%)	Solution	Average Swelling Ratio (g·water/g·hydrogel)	σ (g·water/g·hydrogel)	Aqueous Solution pH
3.5%	DI	64.2	2.7	8.4
	SA	71.0	3.1	5.6
	HCl	66.4	1.4	8.4
5%	DI	45.9	0.9	7.9
	SA	45.3	0.8	5.7
	HCl	47.0	1.4	7.8
10%	DI	10.3	0.4	7.5
	SA	11.5	0.2	5.0
	HCl	10.8	0.5	7.2
30%	DI	2.0	0.1	7.2
	SA	2.3	0.3	4.1
	HCl	1.8	0.1	6.2
50%	DI	1.8	0.01	7.2
	SA	2.3	0.3	3.7
	HCl	1.4	0.3	6.0

Table C.15 Chemisorption Dynamics of BA by PDMEA and the 3.5% and 30% Hydrogels at Approximately 1 mole·amine/1 mole·BA (2.5 g·acid/L, 25 ^{o}C).

Time (h)	Aqueous Solution pH (PDMEA)	Aqueous Solution pH (3.5% Hydrogel)	Aqueous Solution pH (30% Hydrogel)
0.00	3.1	3.1	3.1
0.25	-	3.2	3.2
0.33	4.0	-	-
0.50	-	3.4	3.4
0.75	4.5	-	-
1.00	-	3.6	3.5
1.50	4.5	-	-
3.00	-	3.7	3.5
6.00	-	-	-
10.00	-	3.8	3.6
18.00	4.5	-	-
24.00	4.5	3.8	3.6

Table C.16 Raw Data of the Titrations of BA with DMEP to 1.5 moles·amine/1.0 mole·BA (2.5 g·BA/L, 25 °C).

Moles·amine/ mole·BA	Aqueous Solution pH
0.00	3.1
0.10	3.4
0.20	3.7
0.30	3.9
0.50	4.3
0.70	4.6
0.90	5.5
1.00	7.5
1.05	7.7
1.25	8.0
1.35	8.2
1.50	8.4

Table C.17 Raw Data of the Titrations of BA with PDMEA to 1.5 moles·amine/1.0 mole·BA (2.5 g·BA/L, 25 ^{o}C).

Moles·amine/ mole·BA	Aqueous Solution pH
0.00	3.1
0.10	3.2
0.30	3.4
0.70	3.8
0.90	4.0
0.95	4.1
1.00	4.2
1.05	4.3
1.15	4.6
1.50	5.7

Table C.18 Raw Data of the Titrations of BA with the 3.5% Hydrogel to Approximately 1.5 moles·amine/1.0 mole·BA (2.5 g·BA/L, 25 ^oC).

Moles·HCO_3^-/ mole·acid	Aqueous Solution pH (30% Hydrogel)
0.00	3.1
0.11	3.2
0.23	3.2
0.32	3.3
0.56	3.4
0.76	3.6
0.90	3.7
0.97	3.8
1.12	4.1
1.19	4.7
1.25	5.0
1.30	5.3
1.59	5.9

Table C.19 Raw Data of the Titrations of BA with the 30% Hydrogel to Approximately 1.5 moles·amine/1.0 mole·BA (2.5 g·BA/L, 25 °C).

Moles·HCO_3^-/ moles·acid	Aqueous Solution pH (30% Hydrogel)
0.00	3.1
0.12	3.2
0.24	3.2
0.36	3.2
0.60	3.30
0.85	3.4
0.94	3.5
1.10	3.6
1.15	3.6
1.21	3.7
1.24	3.8
1.42	4.0
1.61	4.2

Table C.20 Succinic Acid Capacities of the Various Hydrogels at 3.0 moles·amine/1.0 mole·SA (2.5 g·SA/L; F = 0.01; 25 °C); Measured with ^{1}H NMR with a Citric Acid Reference (41 mg).

Weight Fraction of TAAEA (wt%)	Trial	m·hydrogel (g)	^{1}H NMR Integration	Capacity (g·SA/g·hydrogel)	Aqueous Solution pH
5%	1	0.05	0.020	0.253	6.0
	2	0.05	0.019	0.244	5.4
	3	0.05	0.019	0.249	5.7
10%	1	0.05	0.007	0.251	5.0
	2	0.05	0.012	0.249	5.0
	3	0.05	0.021	0.2442	5.1
30%	1	0.05	0.018	0.217	4.1
	2	0.05	0.014	0.220	4.0
	3	0.06	0.017	0.214	4.3
50%	1	0.06	0.049	0.171	3.7
	2	0.06	0.042	0.180	3.8
	3	0.06	0.036	0.180	3.6

Table C.21 Swelling Ratios of the Fully Swollen 3.5% and 4% Hydrogels within the 25 ml Experiments at Approximately 3.0 moles·amine/1.0 mole·SA (F = 0.01, 25°C).

Weight Fraction of TAAEA (wt%)	Trial	m·hydrogel$_{dry}$ (g)	m·hydrogel$_{wet}$ (g)	Swelling Ratio (g·water/g·hydrogel)	pH of Extraction Solution
3.5%	1	0.27	20.6	76.0	6.7
4%	1	0.23	13.7	57.6	5.3

Table C.22 Back Titrations of the Fully Swollen 3.5% and 4% Hydrogels within the 25 ml Experiments at Approximately 3.0 moles·amine/1.0 mole·SA (F = 0.01), using 15 mM NaOH in 15 mM HCl (25 °C).

Weight Fraction of TAAEA (wt%)	Trial	V_{ref} of NaOH (ml)	$V_{titration}$ of NaOH (ml)	pH_f of Titration Solution	Capacity (g·SA/g·hydrogel)
3.5%	1	49.0 (pH 7.0 ≈ pH 10.0)	55.8	10.0	0.23
4%	1	43.6 (pH 7.0), 48.6 (10.5)	53.4	10.50	0.23

Table C.23 Strain measurements of the 4% Hydrogel.

Target ε (%)	Trial	H_{Ref}	H_0	H_ε	Actual ε (%)
20	1	15.9	18.9	18.2	23
	2	-	-	-	21
40	1	16.5	19.2	18.1	41
	2	16.0	18.8	17.6	43
60	1	16.4	19.4	17.6	60
	2	16.5	19.3	17.6	61
80	1	16.5	19.2	17.1	78
	2	16.4	19.2	17.0	79

Table C.24 Back Titrations of the Strained 4% Hydrogel After Sorption with 3.0 moles·amine/1.0 mole·SA in 2.5 g·SA/L (F = 0.01), using 15 mM NaOH in 15 mM HCl (25 °C).

ε (%)	Trial	V_{ref} of NaOH (ml)	$V_{titration}$ of NaOH (ml)	m_{ε} (g)	Swelling Ratio (g·water/g·hydrogel)	Capacity (g·SA/g·hydrogel)
20	1	43.6 (pH 7.0), 44.8 (pH 10.0)	49.4	0.75	42.5	0.22
	2	-	-	-	46.1	0.20
40	1	42.4 (pH 7.0), 43.8 (pH 10.0)	46.8	0.65	37.5	0.15
	2	39.2 (pH 7.0), 44.6 (pH 10.5)	47.8	0.62	37.5	0.16
60	1	43.6 (pH 7.0), 44.8 (pH 10.0)	46.4	0.54	31.0	0.08
	2	43.6 (pH 7.0), 44.8 (pH 10.0)	46.2	0.50	28.0	0.07
80	1	39.2 (pH 7.0), 40.6 (pH 10.0)	41.4	0.35	21.0	0.04
	2	39.2 (pH 7.0), 40.6 (pH 10.0)	41.2	0.33	19.7	0.03

References

[1] M. H. Ghobadi, M. Firuzi, and E. Asghari-Kaljahi, “Relationships between geological formations and groundwater chemistry and their effects on the concrete lining of tunnels (case study: Tabriz metro line 2),” *Environ Earth Sci*, vol. 75, no. 12, pp. 1–14, Jun. 2016, doi: 10.1007/S12665-016-5785-0.

[2] K. K. Cheng, X. B. Zhao, J. Zeng, and J. A. Zhang, “Biotechnological production of succinic acid: Current state and perspectives,” *Biofuels, Bioproducts and Biorefining*, vol. 6, no. 3, pp. 302–318, May 2012, doi: 10.1002/BBB.1327.

Copyrights

Figure A.1 reprinted from M. H. Ghobadi, M. Firuzi, and E. Asghari-Kaljahi, “Relationships between geological formations and groundwater chemistry and their effects on the concrete lining of tunnels (case study: Tabriz metro line 2),” *Environ Earth Sci*, vol. 75, no. 12, pp. 1–14, Jun. 2016, doi: 10.1007/S12665-016-5785-0. Copyright 2016 Springer.

Table A.1 adapted from K. K. Cheng, X. B. Zhao, J. Zeng, and J. A. Zhang, “Biotechnological production of succinic acid: Current state and perspectives,” *Biofuels, Bioproducts and Biorefining*, vol. 6, no. 3, pp. 302–318, May 2012, doi: 10.1002/BBB.1327. Copyright 2012 Society of Chemical Industry and John Wiley & Sons, Ltd.

License

This work is licensed under a Creative Commons Attribution-NonCommercial 4.0 International License.

License: http://creativecommons.org/licenses/by-nc/4.0/